CHALMERS
UNIVERSITY OF TECHNOLOGY

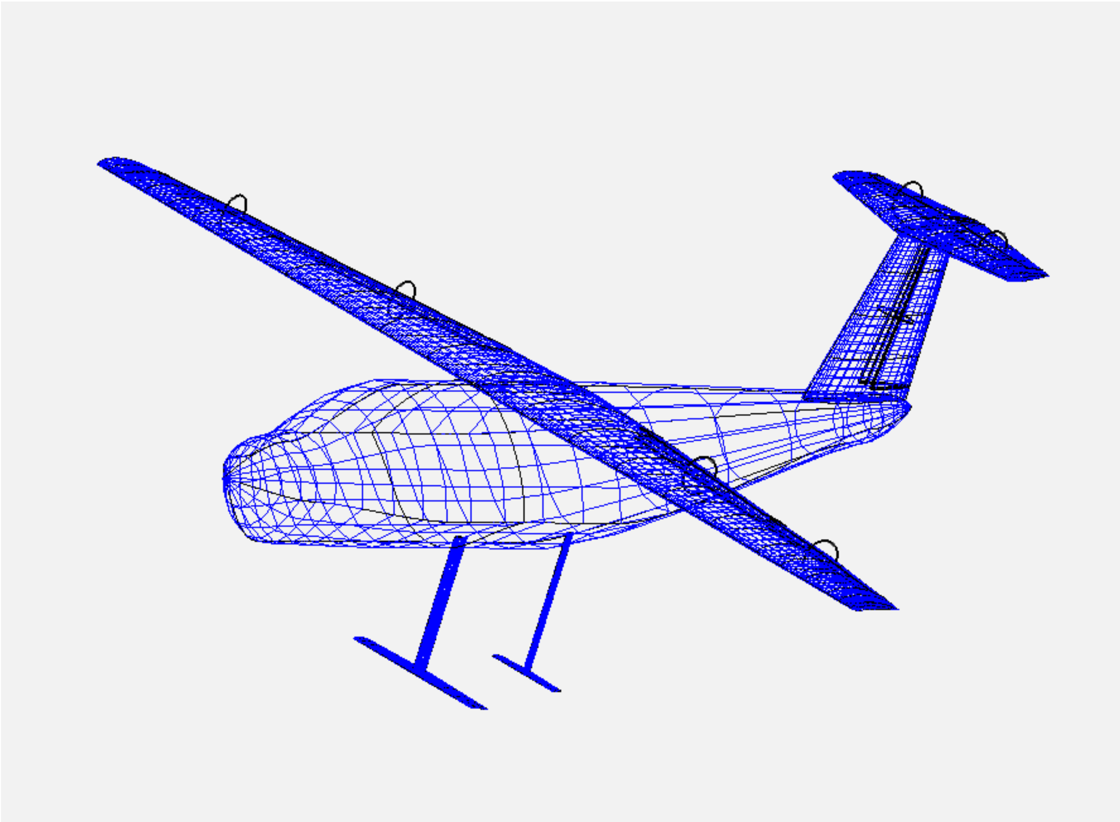

Conceptual Design of a Hydrofoil Seaplane

A Study on the Feasibility of Hydrofoil-Assisted Takeoff

Master's thesis in Mobility Engineering - Aerospace track

FELIX DJÄRV

DEPARTMENT OF MECHANICS AND MARITIME SCIENCES
CHALMERS UNIVERSITY OF TECHNOLOGY
Gothenburg, Sweden 2026
www.chalmers.se

Master's thesis 2026

Conceptual Design of an Hydrofoil Seaplane

A Study on the Feasibility of Hydrofoil-Assisted Takeoff

FELIX DJÄRV

CHALMERS
UNIVERSITY OF TECHNOLOGY

Department of Mechanics and Maritime Sciences
Division of Fluid Mechanics
Chalmers University of Technology
Gothenburg, Sweden 2026

Conceptual Design of a Hydrofoil Seaplane
A Study on the Feasibility of Hydrofoil-Assisted Takeoff
FELIX DJÄRV

Supervisor: Xin Zhao, Mechanics and Maritime Sciences
Examiner: Carlos Xisto, Mechanics and Maritime Sciences

Master's Thesis 2026
Department of Mechanics and Maritime Sciences
Division of Fluid Mechanics
Chalmers University of Technology
SE-412 96 Gothenburg
Telephone +46 31 772 1000

Cover: OpenVSP model of an conceptual design of an electric hydrofoil aircraft.

Typeset in LaTeX
Printed by Chalmers Reproservice
Gothenburg, Sweden 2026

Conceptual Design of a Hydrofoil Seaplane
A Study on the Feasibility of Hydrofoil-Assisted Takeoff
FELIX DJÄRV
DEPARTMENT OF MECHANICS AND MARITIME SCIENCES
Chalmers University of Technology

Abstract

This thesis studies the possibility of using a fixed hydrofoil to reduce the takeoff distance for an electric seaplane. A conceptual design of what this type of aircraft could look like is done, based on the requirements from Hydroaerospace. The conceptual design mostly follows Raymers methods and includes weight estimation, size calculations and modeling in OpenVSP. Then the aircrafts takeoff performance is estimated through one of Raymers methods but modified for the hydrofoil case. The results based on the calculations show that the takeoff distance is not shorter when using the Hydrofoil. However, this comes from the fact that the hydrofoil is not controllable and in reality the takeoff distance should be shorter. It is also shown that the idea of using the aerodynamic surfaces of the aircraft to control the hydrofoil is not an option, since the force difference is too large. Overall, the study shows that a fixed or uncontrollable hydrofoil is not a viable option.

Keywords: conceptual aircraft design, aerodynamics, airfoil, hydrofoil, aircraft performance, electric aircraft, seaplane, flying boat.

Acknowledgments

I would like to express my sincere gratitude to my supervisor for the guidance, feedback, and support throughout this thesis. Your input has been essential in shaping the direction and quality of the work. I would also like to thank my examiner for valuable comments and suggestions that have contributed to improving the report. Finally, I would like to thank my parents for their continuous support and encouragement during my thesis and throughout my studies.

Felix Djärv, Gothenburg, Month Year

List of Acronyms

Below is the list of acronyms that have been used throughout this thesis listed in alphabetical order:

AAM	Advanced Air Mobility
A/C	Aircraft
AR	Aspect Ratio
BWF	Battery Weight Fraction
CG	Center of Gravity
eCTOL	Electric Conventional Take-off and Landing
eVTOL	Electric Vertical Take-off and Landing
EWF	Emtpy Weight Fraction
FM	Foiling Mode
HF	Hydro Foil
HT	Horizontal Tail
OF	Only Float
OpenVSP	Open Vehicle Sketch Pad
RC	Radio Controlled
SMP	Sizing Matrix Plot
TOP	Takeoff Parameter
UAM	Urban Air Mobility
VT	Vertical Tail
VTOL	Vertical Takeoff and Landing

Nomenclature

Below is the nomenclature of parameters and variables that have been used throughout this thesis.

Parameters and Variables

AR	Aspect ratio
C_D	Drag coefficient
C_{D_0}	Zero-lift (parasitic) drag coefficient
C_{D_f}	Drag coefficient of the fuselage
C_{D_i}	Induced drag coefficient
C_{D_t}	Drag coefficient of the tail
C_{D_w}	Drag coefficient of the wing
$C_{D_{a/c}}$	Aircraft drag coefficient
$C_{D_{hf}}$	Hydrofoil drag coefficient
$C_{D_{vt}}$	Drag coefficient of the vertical tail
C_L	Lift coefficient
C_{L_t}	Lift coefficient of the tail (relative to main wing)
C_{L_w}	Lift coefficient of the wing
C_{L_α}	Lift curve slope
$C_{L_{hf}}$	Lift coefficient of the hydrofoil (with wing reference area)
$\hat{C}_{L_t}$	Lift coefficient of the tail (with its own reference values)
$\hat{C}_{L_{hf}}$	Lift coefficient of the hydrofoil (local reference area)
C_{m_G}	Pitching moment coefficient about CG
$C_{m_{AC}}$	Pitching moment coefficient about aerodynamic center
C_{mAChf}	Hydrofoil pitching moment coefficient about its AC
$C_{mG\alpha}$	Derivative of pitching moment coefficient w.r.t. α
$C_{fmG\alpha}$	Fuselage contribution to $C_{mG\alpha}$

D	Total drag force
D^f	Drag from the fuselage
D^t	Drag from the tail
D^w	Drag from the wing
D^{vt}	Drag from the vertical tail
K_A	Aerodynamic constant (in takeoff calculation)
$K_{A_{FM}}$	Constant dependent on hydrofoil drag coefficient
K_T	Constant dependent on static thrust
L	Total lift force
L^t	Lift from the tail
L^w	Lift from the wing
L^{hf}	Lift from the hydrofoil
$L_{a/c}$	Lift from the aircraft
L/D	Lift-to-drag ratio
M	Total pitching moment
M^f	Pitching moment from the fuselage
M^t	Pitching moment from the tail
M^w	Pitching moment from the wing
Re	Reynolds number
S	Reference area
S^{ht}	Horizontal tail area
S^{vt}	Vertical tail area
S^w	Wing area
S_{35}, S_{45}	Takeoff distances at 35, 45 m/s respectively
T	Thrust force
T/W	Thrust-to-weight ratio
V	Velocity
V_f	Final velocity
V_i	Initial velocity
V_{TO}	Takeoff velocity
W	Weight
b	Wingspan
e	Oswald efficiency factor
g	Gravitational acceleration

k	Induced drag factor, $k = \frac{1}{\pi e AR}$
k_d	Scaling factor (weight scaling)
k_{hf}	Hydrofoil moment arm ratio
k_t	Tail moment arm ratio
q	Dynamic pressure, $q = \frac{1}{2}\rho V^2$
μ	Dynamic viscosity
ρ	Density
σ^{hf}	Reference area ratio for the hydrofoil, $\frac{S_{hf}}{S_w}$
σ^t	Reference area ratio for the tail, $\frac{S_t}{S_w}$
ξ_{AC}	Position of aerodynamic center (non-dimensional)
ξ_{AChf}	Position of hydrofoil aerodynamic center
ξ_G	Position of center of gravity (non-dimensional)
η^{hf}	Dynamic pressure ratio for the hydrofoil
η^t	Dynamic pressure ratio for the tail, $\frac{q_t}{q_w}$
ϵ_α	Downwash gradient
$\hat{S}_{total}$	Total takeoff distance
a^t	Lift curve slope of the tail
a^w	Lift curve slope of the wing
a^{hf}	Lift curve slope of the hydrofoil
α	Angle of attack

Contents

List of Figures

List of Tables

1
Introduction

Seaplanes have historically been very common in air travel. Today they are just a fraction of what they used to be. With new companies diving back into this field of aeronautics and combining it with newer technologies, what could a future seaplane look like?

1.1 Purpose and Boundaries

The purpose of the project is to develop a preliminary design of a modern electric seaplane that uses a hydrofoil for waterborne operations. The project is done together with the company Hydroaerospace, and will follow their requirements.

1.1.1 Hydroaerospace

Electric aviation is deemed to be the future of aeronautics, and there have been large steps forward in this area during the last couple of years. With a lot of up and coming projects such as Urban Air Mobility (UAM), Advanced Air Mobility (AAM), eVTOL (Electric Vertical Take-Off and Landing), and eCTOL (Electric Conventional Take-Off and Landing)[3]. Seplanes and flyingboats were the most common from the early days of flying right up until the second world war. Today they are still in use, although only in highly specific areas like Vancouver and the Maldives.

There are projects today focusing on electric seaplanes, and they do bring some great benefits over conventional landbased aircrafts. The most obvious one being that you do not need a runway and surrounding infrastructure for takeoff and landing. However, there are still some big drawbacks to seaplanes.

- **Wave sensitivity.** Rough water increases take-off distance and limits safe operating conditions.
- **High drag.** Pontoons and hulls create significant drag, increasing takeoff distance.
- **Maneuverability constraints.** Water handling—especially crosswind taxiing—can be challenging and hazardous.
- **Infrastructure footprint.** Large hulls and wide wingspans complicate docking in harbors.

Hydrofoils seems to offer a solution to some of these problems by lifting the fuselage of the airplane out of the water. The main benefits include

- **Potentially shorter take-off runs.** Reduced drag should lower the distance to get airborne.
- **Improved energy efficiency.** Lower drag translates directly into longer range or reduced battery mass.
- **Wave-tolerant operations.** Foils cut through the waves, enabling operations in rougher waters.
- **Minimal wake.** Reduced displacement minimizes wash, allowing high-speed taxi in sensitive harbors.

Hydroaerospace has the idea to combine both an electric seaplane togheter with a hydrofoil which would help mitigate some of the issues facing conventional seaplanes today. They have made a simple concept as a starting point based on one of Airbus concept airplanes, and a racing boat with hydrofoils.

Figure 1.1: Airbus electric aircraft concept and airbus racing boat with hydrofoils [3]

Combining and scaling these two into

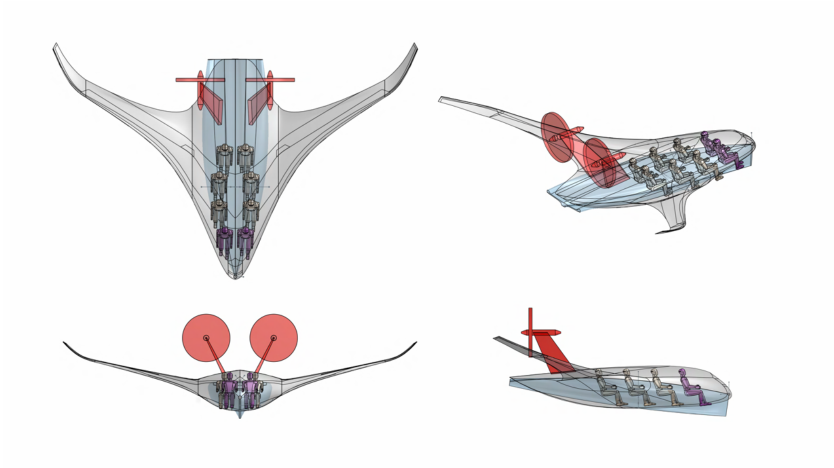

Figure 1.2: Initial idea for hydroaerospace concept [3]

After some adjustments

Figure 1.3: Different views of Hydroaerospace concept [3]

Figure 1.4: Top view of Hydroaerospace concept [3]

So far Hydroaerospace has performed tests with a midsize radio controlled plane(rcplane) which they put a hydrofoil on. The tests gave a positive result with a shorter takeoff distance being achieved compared to the rcplane not using the hydrofoil.

Table 1.1: Specifications and Design Boundaries from Hydroaerospace

Design Specifications
80 m/s cruise speed
Range: 100 nm ≈ 185 km
Wingspan: 14 m
6 passengers
2 crew members
Hydrofoil
Stabilizing the hydrofoil with the aircraft tail

Design Boundaries
Targeted at short and regional trips for commercial use.
Must allow easy docking for efficient passenger and cargo loading/unloading.
Must be capable of taking off and landing within a reasonable distance.

1.2 Thesis Question

The research question is: Can a fixed hydrofoil seaplane achieve a shorter takeoff distance compared to a conventional seaplane?
In order to answer this research question, the following objectives are addressed:

- To develop a conceptual design of a hydrofoil-assisted electric seaplane, including the overall configuration, component sizing, and key design parameters such as weight, wing loading, and thrust-to-weight ratio.
- To evaluate the aerodynamic and hydrodynamic performance of the aircraft during takeoff.
- To assess whether the aircraft can maintain stability and controllability in foiling mode using only aerodynamic control surfaces.
- To compare the takeoff performance of the hydrofoil configuration with that of a conventional seaplane.

2
Theory

2.1 General Equations for Lift, Drag and Pitch Moment With Corresponding Derivations and Notations

This section goes over the general equations for lift, drag and pitch moment and how they are notated in this report. These notations and derivations comes from Professor Riboldis book [7], and are used extensively in the methodology chapter.

2.1.1 Lift Equations

The total lift of an airplane is the total lift from all lifting surfaces added together, typically only the wing(L^w) and the horizontal tail(L^t).

$$L = L^w + L^t$$

With the general lift equation

$$L = qSC_L$$

With q being the dynamic pressure

$$q = \frac{1}{2}\rho V^2$$

Both the wing and tail have their own respective reference area(S), dynamic pressure(q) and lift coefficient(C_L).

$$L_w = q^w S^w C_{L_w}, \quad L_t = q^t S^t \hat{C}_{L_t}$$

Where the $\hat{C}_{L_t}$ is the tails own non altered lift coefficient. Since the wing and tail uses different reference values, they can not be added directly to each other. Dividing both contributions with the reference values of the main wing we get

$$C_L = C_{L_w} + \eta^t \sigma^t C_{L_t}$$

Where η^t is the dynamic pressure ratio for the tail $\frac{q^t}{q^w}$ and σ^t is the reference area ratio $\frac{S^t}{S^w}$. C_L^t without the "hat" is the lift coefficient for the tail with the main wing as the reference area.

2.1.1.1 Derivation of lift coefficient with respect to the angle of attack

Deriving the lift coefficient with respect to alpha, $\frac{\delta C_L}{\delta\alpha} = C_{L\alpha}$. From Proffesors Riboldis book[7]

$$C_{L\alpha} = a^w + \eta\sigma^t a^t(1-\epsilon_\alpha)$$

Where a^w and a^t are the lift curve slope for the wing and the tail and ϵ_α being the change in the downwash angle with respect to α.

2.1.2 Drag Coefficient

The drag follows a similar derivation as the lift, where the total drag is the sum of all contributions. Typically the wing(D^w), horizontal tail(D^t), vertical tail(D^{vt}) and fuselage(D^f)

$$D = D^w + D^t + D^{vt} + D^f$$

Where each drag component uses its own dynamic pressure, reference area and drag coefficient(C_D).

$$D_w = q^w S^w C_{D_w}, \quad D_t = q^t S^t \hat{C}_{D_t}, \quad D_{vt} = q^{vt} S^{vt} \hat{C}_{D_{vt}}, \quad D_f = q^f S^f C_{D_f}$$

Dividing all contributions with the reference values of the main wing we get

$$C_D = C_{D_w} + q^t S^t C_{D_t} + q^{vt} S^{vt} C_{D_{vt}} + C_{D_f}$$

The drag coefficient can be split up into two contributions. The parasitic drag C_{D_0} and the induced drag C_{D_i}, where C_{D_i} is dependent on the C_L, Aspect Ratio (AR) and the Oswald efficiency factor(e).

$$C_D = C_{D_0} + kC_L^2$$

$$k = \frac{1}{\pi e AR}$$

2.1.3 Pitch Moment Coefficient

The pitching moment is dependent on contributions from the wing(M^w), tail(M^t) and fuselage(M^f).

$$M = M^w + M^t + M^f$$

Following similar derivations as for the lift and drag, from Riboldis book[7], the following equation for the pitching moment coefficient is obtained as:

$$C^a_{mG} = C_{mAC^w} + C_{L_w}(\xi_{AC^w} - \xi_G) + \eta^t\sigma^t(k^t C_{mAC^t} + C_{L_t}(\xi_{AC^t} - \xi_G)) + C^f_{mG}$$

Where C_{mAC^w} is the pitching moment coefficient of the aerodynamic center of the wing, ξ_{AC^w} and ξ_G are the non-dimensionalized positions of the aerodynamic center of the wing and the center of gravity, and C^f_{mG} is the pitching moment coefficient of the fuselage. The tail follows a similar notation, with the added k^t which is the ratio between the moment arm of the wing and the moment arm of the horizontal tail for the pitching moment.

2.1.3.1 Derivation of pitching moment coefficient with respect to the angle of attack

To asses the stability around the pitch axis, the pitching moment coefficient(equation 2.1.3) is derived with respect to the angle of attack(α). This gives

$$C^a_{mG\alpha} = a^w(\xi_{AC^w} - \xi_G) + \eta^t\sigma^t a^t(\xi_{AC^t} - \xi_G) + C^f_{mG\alpha}$$

Equation 2.1.3.1 shows how the pitching moment varies with α. For the aircraft to be statically stable the slope must be negative.

2.2 Hydrofoil Contribution

For the hydrofoil contributions, similar descriptions and notations are used where the superscript "^{hf}" stands for the hydrofoil related variables.

$$C_L = C_{L_w} + \eta^t\sigma^t C_{L_t} + \eta^{hf}\sigma^{hf}C_{L_{hf}}$$
$$C_D = C_{D_w} + \eta^t\sigma^t C_{D_t} + \eta^{vt}\sigma^{vt}C_{D_{vt}} + \eta^{hf}\sigma^{hf}C_{D_{hf}} + C_{D_f}$$
$$C^a_{mG} = C^w_{mAC^w} + C^w_L(\xi_{AC^w} - \xi_G) + \eta^t\sigma^t(k^t C^t_{mAC^t} + C^t_L(\xi_{AC^t} - \xi_G)) +$$
$$\eta^{hf}\sigma^{hf}(k^{hf}C^{hf}_{m\ AC^{hf}} + C^{hf}_L(\xi_{AC^{hf}} - \xi_G)) + C^f_{mG}$$

$$C^a_{mG\alpha} = a^w(\xi_{AC^w} - \xi_G) + \eta^t\sigma^t a^t(\xi_{AC^t} - \xi_G) + \eta^{hf}\sigma^{hf}a^{hf}(\xi_{AC^{hf}} - \xi_G) + C^f_{mG\alpha}$$

3
Methods

The conceptual design of the hydrofoil aircraft will be done based on the suggestions and guidelines from Raymers book [6], as well as some theory and notations based on Riboldis book [7] and slides [8]

3.1 Initial Design

To get an estimation for the total weight of the aircraft, Raymers approach was followed [6, Ch. 3].

3.1.1 Initial Weight Estimation and Breakdown

$$W = \frac{W_c + W_p}{1 - \frac{W_b}{W} - \frac{W_e}{W}}$$

From the requirements the weight for the crew(W_c) and the weight for the payload(W_p)(in this case passengers) can be found. Typically a fuel fraction would be used but since the aircraft is electric it has to be substituted with a battery weight fraction(BWF = $\frac{W_b}{W}$). The battery weight fraction is calculated from the formula [6, Ch. 20, p.757]:

$$BWF = \frac{Rg}{\frac{L}{D}\eta E}$$

Where R is the range, g is gravity, eta is the efficiency and E is the specific energy of the batteries.

For the empty weight fraction of the aircraft(EWF = $\frac{W_e}{W}$), the graph on existing empty weight data from Raymers book is used.

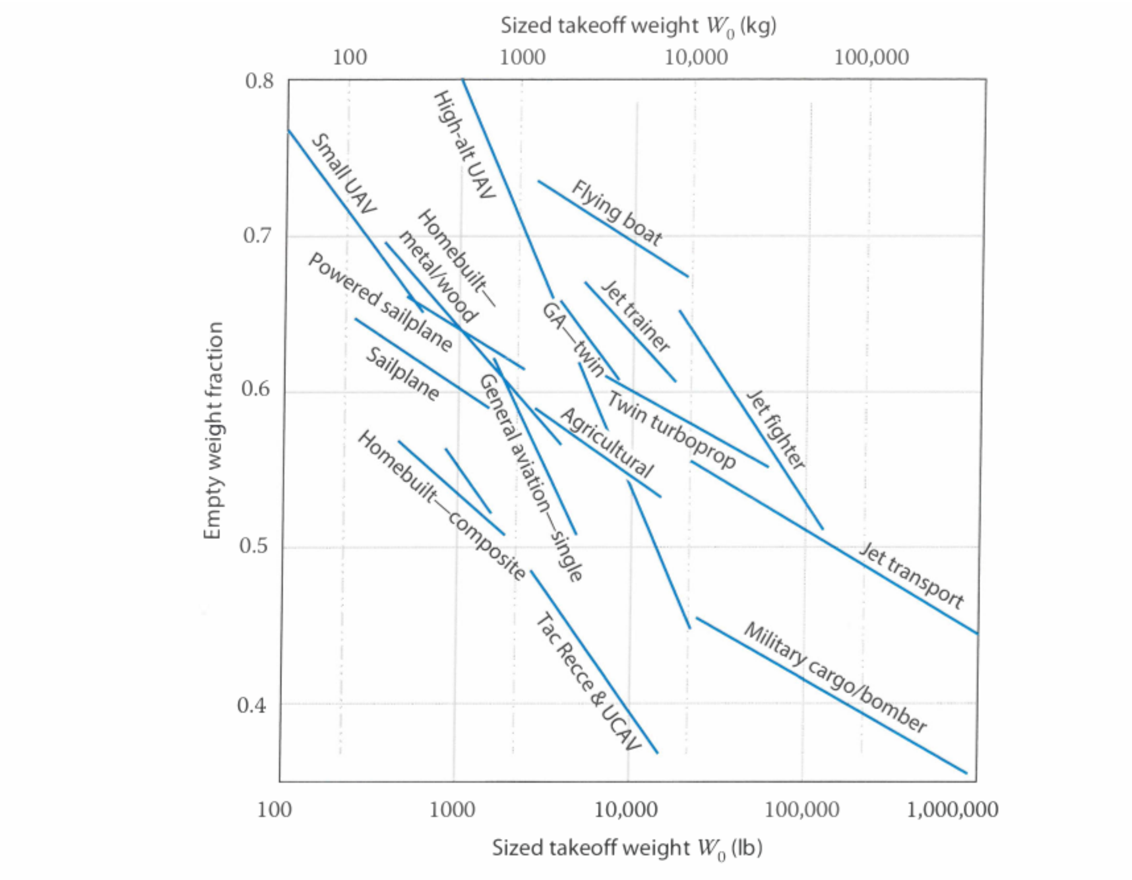

Figure 3.1: Raymers empty weight estimation plot

3.1.2 Sizing Matrix Plot (SMP)

The initial sizing is done using a sizing matrix plot (SMP), where the thrust-to-weight (T/W) ratio is plotted against the wing loading (W/S). Four performance constraints are included in the same graph to determine a suitable design point for the aircraft[8].

3.1.3 Landing Constraint

The landing constraint is found by starting from the formula for lift:

$$L = \frac{1}{2}\rho V_{stall}^2 S C_{L_{max}}$$

For flight, the lift must be equal to the Weight

$$W = \frac{1}{2}\rho V_{stall}^2 S C_{L_{max}}$$

Finally

$$\frac{W}{S} = \frac{1}{2}\rho V_{stall}^2 C_{L_{max}}$$

3.1.4 Takeoff Constraint

The takeoff constraint is found through an energy based approximation.

$$T * d_{takeoff} = \frac{1}{2} m V_{TO}^2$$

$$T * d_{takeoff} = \frac{1}{2} \frac{W}{g} V_{TO}^2$$

$$T * d_{takeoff} = \frac{1}{2} \frac{W}{g} \frac{W}{\frac{1}{2} \rho S C_{L_{TO}}}$$

Which gives

$$\frac{T}{W} = \frac{1}{g \rho d_{takeoff} C_{L_{TO}}} \frac{W}{S}$$

A takeoff parameter(TOP) is introduced to account for factors not captured by this simple energy model.

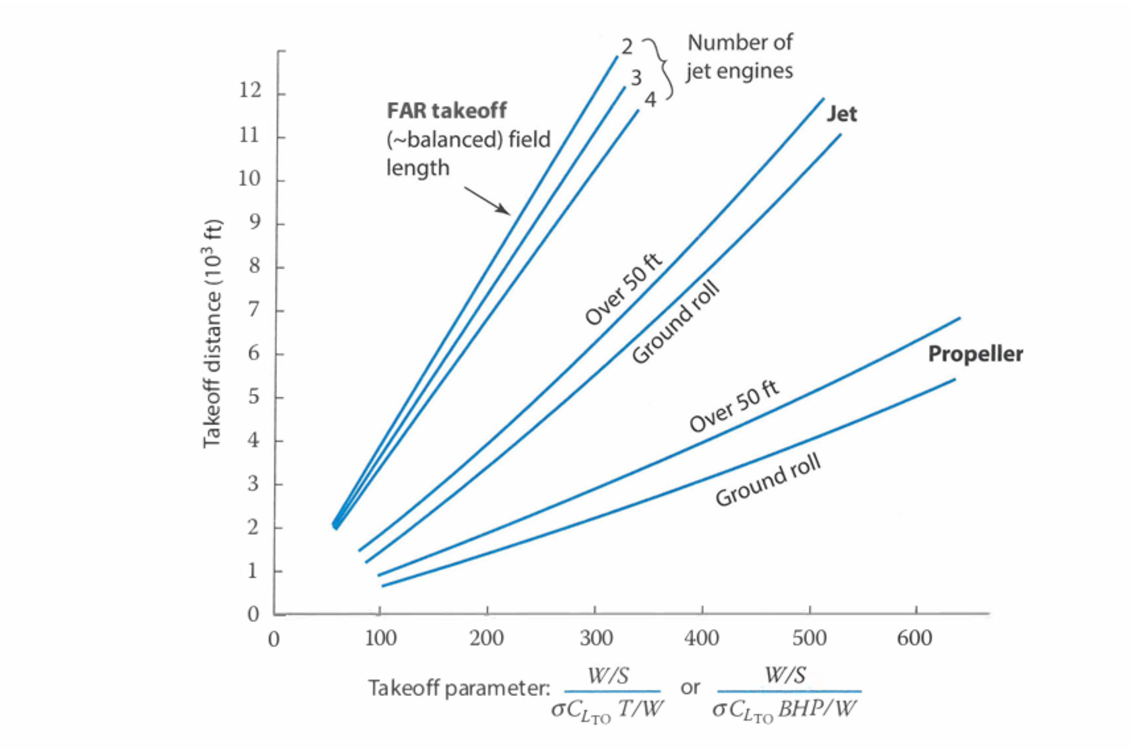

Figure 3.2: Takeoff Parameter Graph

$$\frac{T}{W} = \frac{1}{TOP g \frac{\rho_{TO}}{\rho} C_{L_{TO}}} \frac{W}{S}$$

3.1.5 Climb Constraint

This constraint is found from the equation:

$$T - D = W * sin(\gamma)$$

$$\frac{T-D}{W} = sin(\gamma)$$
$$\frac{T-D}{W} = sin(\gamma)$$
$$\frac{T}{W} = sin(\gamma) + \frac{1}{\frac{L}{D}}$$

3.1.6 Cruise Constraint

The cruise constraint is found from the formula for the drag coefficient(C_D):

$$C_D = C_{D_0} + C_{D_i}$$

$$C_D = C_{D_0} + kC_L^2$$
$$\frac{D}{\frac{1}{2}\rho SV_{cruise}^2} = C_{D_0} + k(\frac{W}{\frac{1}{2}\rho SV_{cruise}^2})^2$$
$$D = \frac{1}{2}\rho SV_{cruise}^2 C_{D_0} + k\frac{W^2}{\frac{1}{2}\rho SV_{cruise}^2}$$
$$\frac{D}{W} = \frac{1}{2}\rho V_{cruise}^2 C_{Do}\frac{S}{W} + \frac{k}{\frac{1}{2}\rho V_{cruise}^2}\frac{W}{S}$$
$$\frac{T}{W} = \frac{1}{2}\rho V_{cruise}^2 C_{D_0}\frac{S}{W} + \frac{k}{\frac{1}{2}\rho V_{cruise}^2}\frac{W}{S}$$
$$k = \frac{1}{\pi ARe}$$

To find the lift-over drag, both the induced drag (C_{D_i}) and the parasitic drag(C_{D_0}) needs to be estimated. The induced drag is dependent on the lift coefficient(C_L), aspect ratio(AR) and the Oswalls efficiency factor (e), which are all dependent on the design of the wing. The parasitic drag however is harder to estimate, since it is dependent on how the actual aircraft looks. This early in the design phase, such a variable is hard to estimate. To find a good approximation value, regression data from existing flying boats are used. In the graph, the fraction C_{D0}/W is plotted logarithmically against the total weight of the aircraft.

Putting all of these equations together and plotting them in the SMP, a suitable wingloading and thrust-to-weight ratio is found. When choosing the desired values, as high of a wingloading as possible and as low of a thrust to weight ratio as possible is typically chosen.

3.1.7 Aerodynamic Surfaces Design

3.1.7.1 Main wing design

The required wing area is calculated by dividing the total weight of the aircraft with the chosen wingloading:

$$S = \frac{W}{\frac{W}{S}}$$

For the ailerons, Raymers suggestions [6, Ch. 6, p.161] are followed giving a span from 50 % to 90 % of the wingspan, with the aileron chord being approximately 15–25 % of the local wing chord. For the flaps, the same chord as for the ailerons is used. The flaps also extends from about 10 % to 50 % of the wingspan. Taking all of this into consideration, a simple wing model was created in OpenVSP with no sweep and a simple taper to reduce the induced drag.

For the tail sizing, Raymers method was utilized [6, Ch. 6, p.158].

3.1.7.2 Vertical tail design

$$S_{vt} = \frac{S * b * C_{vt}}{L_{vt}}$$

Where C_{vt} is a coefficient dependent on the actual type of aircraft. As an estimate, this aircraft will be considered as a flying boat and $C_{vt} = 0.06$ is chosen, and S, b and L_{vt} all comes from the design of the wing and size of the fuselage. The rudder provides yaw control for the aircraft. It extends vertically from the top of the fuselage to around 90 % of the vertical tail height. The rudder chord is designed to be approximately 25–50 % of the local tail chord.

3.1.7.3 Horizontal tail design

$$S_{ht} = \frac{S * c * C_{ht}}{L_{ht}}$$

Again here the C_{ht} coefficiant is taken from Raymers book and chosen as $C_{ht} = 0.7$, and S, c and L_{ht} all comes from the design of the wing and size of the fuselage. The elevator controls the pitch motion of the aircraft. It extends from the fuselage out to about 90 % of the horizontal tail span, with the elevator chord being approximately 25–50 % of the local tail chord.

3.1.7.4 Fuselage design

The aircraft developed in this project is, by design, a seaplane and must therefore possess sufficient buoyancy and hydrodynamic characteristics to safely float and operate on water. To estimate the fuselage geometry, the design was based on an established NACA flying boat hull configuration. Specifically, the NACA Model 101[5]. The NACA model is rescaled to match the needed displacement volume of the aircraft. The needed displacement volume is calculated from:

$$V_{requierd} = \frac{W}{\rho_{water}} * 1.2$$

3.1.8 OpenVSP Simulations

Finally, the design is simulated and refined in OpenVSP to ensure aerodynamic stability and consistency with the theoretical parameters. Key performance variables such as C_L, $\frac{L}{D}$, and C_m are analyzed to evaluate the behavior of the aircraft. The simulation is performed in three stages: first, the airplane is evaluated without the hydrofoil to ensure baseline stability; second, the hydrofoil is evaluated independently; and finally, the entire configuration is simulated to confirm overall stability and performance.

C_m vs α

For the design to be statically stable, the curve must slope downward. This enables the aircraft to return to level flight without any control input from the pilot or a flight control system. The moment coefficient should also be zero at the desired angle of attack.

C_L vs α

The required lift coefficient(C_L) must be met at the desired angle of attack, where the moment coefficient is zero. To achieve this, the incidence angles of the main wing and the horizontal tail are adjusted until the right value is obtained.

$\frac{L}{D}$ vs α

The lift-over-drag value is should be at its highest(or close to highest) where the moment coefficient is zero.

3.1.8.1 Crew, Passengers and Battery volume estimation and placement

To estimate the battery weight and volume an assumed battery performance is obtained from [9]. To calculate the battery weight the BWF is multiped with the total weight of the aircraft, and from the battery weight the battery volume can also be obtained.

$$BWF * W = W_b$$

The battery is then modeled in OpenVSP and adjusted until it fit within the aircraft without getting in the way of the passengers and pilots.

3.1.9 Hydrofoil Design

The design of the hydrofoil follows the same process as for the wing, but instead of creating a full SMP only one constraint is used. From this equation the hydrofoil area is then calculated

$$\frac{W}{S_{hf}} = \frac{1}{2}\rho_{water} V_{FM}^2 C_{L_{hf}}$$

$$S_{hf} = W / \frac{W}{S_{hf}}$$

Typically a hydrofoil, just like an aircraft wing, will have a stabilizing tail. However, from Hydroaerospaces specifications the hydrofoil needs to be stabilized with just the aircraft aerodynamic surfaces. To find out if this is even possible, the hydrofoil was stabilized with an ordinary hydrofoil tail first.

3.1.10 Weight Estimation of Parts

After completing the final aircraft design, the weight for each component was calculated using the empirical equations presented in Raymers book[6, Ch. 15, p.575]. The parameters used in these equations were primarily derived from the project's design phase. Any new parameters incorporated have been selected based on Raymers guidlines.

3.1.10.1 Wing Weight

$$W_{\text{wing}} = 0.0051(W_{\text{dg}}N_z)^{0.557}S_w^{0.649}A^{0.5}\left(\frac{t}{c}\right)^{-0.4}(1+\lambda_w)^{0.1}\cos(\Lambda_w)^{-1.0}S_{\text{csw}}^{0.1} \tag{3.1}$$

3.1.10.2 Horizontal Tail Weight

$$W_{\text{ht}} = 0.0379K_{\text{uht}}\left(1+\frac{F_w}{B_h}\right)^{-0.25}W_{\text{dg}}^{0.639}N_z^{0.1}S_{\text{ht}}^{0.75}L_t^{-1}K_y^{0.704}\cos(\Lambda_{\text{ht}})^{-1}A_{\text{ht}}^{0.166}\left(1+\frac{S_e}{S_{\text{ht}}}\right)^{0.1} \tag{3.2}$$

3.1.10.3 Vertical Tail Weight

$$W_{\text{vt}} = 0.0026\left(1+\frac{H_t}{H_v}\right)^{0.225}W_{\text{dg}}^{0.556}N_z^{0.536}L_t^{-0.5}S_{\text{vt}}^{0.5}K_z^{0.875}\cos(\Lambda_{\text{vt}})^{-1}A_v^{0.35}\left(\frac{t}{c_{\text{root}}}\right)^{-0.5} \tag{3.3}$$

3.1.10.4 Fuselage Weight

$$W_{\text{fuselage}} = 0.3280\,K_{\text{door}}\,K_{\text{Lg}}\,(W_{\text{dg}}N_z)^{0.5}\,L_f^{0.25}\,S_{\text{f}}^{0.302}\,(1+K_{\text{ws}})^{0.04}\left(\frac{L}{D}\right)^{0.10} \tag{3.4}$$

3.1.10.5 Electric motor sizing and weight estimation

The size and weight was estimated by combining the specific power(kw/kg) and the volumetric energy density (kw/L) and basing them of a BMW electric motor and inverter[11].

At first, the needed power was calculated from the thrust-to-weight ratio.

$$T = \frac{T}{W} \cdot W \cdot g$$

To find the power in cruise, the thrust is multiplied with the cruise velocity and then divided by the motor efficiency[2].

$$P = \frac{T \cdot V}{\eta}$$

To estimate the size and weight of the electric motor for the aircraft, an existing BMW motor is used as a reference.

Table 3.1: Power, Volume, and Weight Specifications for 2016 BMW i3 Electric Motor and Inverter

Component	Power (kW)	Volume (L)	Weight (kg)
Electric Motor	125	13.6	42
Inverter	123	6.77	8.81

A scaling factor between this motor and the BMW electric motor is calculated by creating a power ratio (K_{motor}). From this, the weight and volume can be calculated for the electric motor. For the inverter size and weight, the same method was used, and a scaling factor between this inverter and the BMW inverter is calculated by creating a power ratio($K_{inverter}$) From this, the weight and volume can be calculated for the inverter.

3.2 Takeoff Performance Modeling Methodology and Calculations

For a traditional seaplane or flying boat, the takeoff distance is generally longer than for a land based aircraft. The main idea for using the hydrofoil is that it will give the aircraft a shorter takeoff distance by lifting the airplane above the water surface, neglecting the hydrodynamic drag from the fuselage. To analyze the takeoff distance in more detail, Raymers takeoff calculation method is used and broken down into three different configurations for the a/c[6]. The three different configurations are

Table 3.2: Different a/c takeoff configurations

Configuration	Notation
Foiling Mode	FM
Float Mode	Float
Only Float	OF

Before diving deeper into the different configurations, the general takeoff distance formula will be introduced.

3.2.1 General Acceleration Equation

The basic equation of motion during the takeoff is:

$$a = \frac{g}{W}\left[T - D - \mu(W - L)\right] \tag{3.5}$$

where:
- a $[m/s^2]$ is the acceleration
- T [N] is thrust
- D [N] is total drag (Both aerodynamical and hydrodynamical)
- μ is the friction coefficient (For water $\mu = 0.1$)
- W [N] is the aircraft weight
- L [N] is total lift (Both aerodynamical and hydrodynamical)
- g $[m/s^2]$ is gravitational acceleration

3.2.2 Takeoff Distance Integration

By rewriting and integrating Eq. 3.5 from an initial velocity V_i to a final takeoff velocity V_f, the takeoff distance is calculated as:

$$\hat{S} = \frac{1}{2gK_A}\ln\left(\frac{K_T + K_A V_f^2}{K_T + K_A V_i^2}\right) \tag{3.6}$$

where:
- K_A is the aerodynamic and hydrodynamic drag constant
- K_T is a net thrust parameter accounting for friction losses (if necessary)

With this equation the takeoff distance can be calculated for the different configurations, where FM is when the a/c uses its hydrofoil. This configuration is of course in pair with the float mode, which is when the a/c does not have enough velocity for its hydrofoil to generate enough lift to lift the a/c up above the water. Finally, the OF-mode is for comparison and includes the same a/c, but it does not have a hydrofoil. Meaning that it will takeoff like a normal seaplane instead.

3.3 Takeoff Distance Modeling in Different Modes

As described earlier, the takeoff performance can be separated into three different modes. To accurately model the takeoff run, it is important to distinguish between these modes:
- **Float Mode:** The aircraft moves along the water surface supported by its buoyancy from its hull.
- **Foiling Mode (FM):** The aircraft transitions to hydrofoils, lifting the aircraft hull above the water.
- **Only Float:** The same aircraft but without the hydrofoil, so it will takeoff like a normal seaplane.

Each mode is characterized by different drag, lift and friction components, affecting the acceleration and takeoff distance.

3.3.1 Float Mode:

For the float mode, the drag and lift comes from both the a/c and hydrofoil. In its thrust constant ($K_{T_{float}}$), the friction from the water is also included.

$$a = \frac{g}{W}\left[T - (D_{a/c} + D_{hf}) - \mu(W - (L_{a/c} + L_{hf}))\right] \tag{3.7}$$

$$K_{A_{float}} = \frac{\rho_{\text{air}}}{2W/S^w}(\mu(C_{L_{TO}} + \eta^{hf}\sigma^{hf}C_{L_{hf}}) - (C_{D_{TO}} + \eta^{hf}\sigma^{hf}C_{D_{hf}})) \tag{3.8}$$

$$K_{T_{float}} = \frac{T}{W} - \mu \tag{3.9}$$

3.3.2 Foiling Mode (FM):

For the float mode, the drag and lift comes from both the a/c and hydrofoil. In its thrust constant ($K_{T_{FM}}$) the friction is not included, since the a/c is riding above the water surface.

$$a = \frac{g}{W}\left[T - (D_{a/c} + D_{hf})\right] \tag{3.10}$$

$$K_{A_{FM}} = \frac{\rho_{\text{air}}}{2W/S^w}\left(-\left(C_{D_{TO}} + \eta^{hf}\sigma^{hf}C_{D_{hf}}\right)\right) \tag{3.11}$$

$$K_{T_{FM}} = \frac{T}{W} \tag{3.12}$$

3.3.3 Only Float:

For the OF mode, the drag and lift comes from only the a/c. In its thrust constant ($K_{T_{OF}}$), the friction from the water is also included.

$$a = \frac{g}{W}\left[T - D_{a/c} - \mu(W - L_{a/c})\right] \tag{3.13}$$

$$K_{A_{OF}} = \frac{\rho_{\text{air}}}{2W/S^w}(\mu C_{L_{TO}} - C_{D_{TO}}) \tag{3.14}$$

$$K_{T_{OF}} = \frac{T}{W} - \mu \tag{3.15}$$

Since the three configurations are mostly similar in its variables, the dependent variables are compared to get an overview of what is independently affecting the performance of each mode.

Table 3.3: Comparison of Key Variables for Takeoff Modes

Parameter	**Float Mode**	**Foiling Mode (FM)**	**Only Float**
Friction Coefficient μ	Yes	No	Yes
Thrust-to-Weight T/W	Yes	Yes	Yes
Hydrofoil Drag $C_{D_{hf}}$	Yes	Yes	No
Hydrofoil Lift-to-Drag $(L/D)_{hf}$	Yes	No	No

For the aircraft with the hydrofoil the total takeoff distance is calculated by summing the distances of each mode:

$$S_{\text{total}} = S_{\text{float}} + S_{\text{FM}} \tag{3.16}$$

For the *Only Float* case, only S_{OF} is considered.

3.3.4 Takeoff performance evaluation

To evaluate the takeoff performance the acceleration for the aircraft with the hydrofoil will be plotted against the velocity and compared to the aircraft without the hydrofoil. The $\frac{T}{W}$ and $\frac{L}{D}$ will also be analyzed in order to evaluate if their values are reasonable.

3.3.4.1 $\frac{T}{W}$ Analysis

The required $\frac{T}{W}$ for the FM can be calculated by

$$\frac{T}{W} = \frac{D}{W}$$

$$\frac{T}{W} = -K_{A_{FM}} V^2$$

The $K_{A_{FM}}$ value is dependent on the drag coefficient $C_{D_{hf}}$ which in itself is dependent on the Reynolds number. The $\frac{L}{D}$ is plotted against the Reynolds number to find a span for the hydrofoils $\frac{L}{D}$ during takeoff. The Reynolds number is defined as:

$$Re = \frac{\rho V L}{\mu} \tag{3.17}$$

The needed $\frac{T}{W}$ is then calculated with the best $\frac{L}{D}$ to determine the required $\frac{T}{W}$ value.

3.3.4.2 $\frac{L}{D}$ Analysis

Looking instead at the required $\frac{L}{D}$ for the hydrofoil to satisfy the $\frac{T}{W}$, it can be calculated by:

$$K_{A,fm} = -\frac{\frac{T}{W}}{V^2}$$

3.3.4.3 Accounting for a/c lift

As the aircraft accelerates, the lift on the airplane wing will increase and the lift on the hydrofoil should decrease. This will change if the FM mode velocity changes, since the lift from the a/c changes when the velocity changes. To calculate the hydrofoil lift, the lift from the aircraft is subtracted from the total lift:

$$L_{hf} = L - L_{a/c}$$

$$\hat{C}_{L_{hf}} = \frac{L_{hf}}{0.5 * \rho_{water} * S_{hf} * (V_{FM}^2)}$$

The lift coefficient is then normalized with the a/c area

$$C_{L_{hf}} = \hat{C}_{L_{hf}} * \sigma^{hf}$$

Assuming that the $\frac{L}{D}$ is the same as for the original hydrofoil. V_{FM}^2 is then changed to see if any velocity would change the results.

3.3.5 New hydrofoil design

To see if it would be possible to design something in OpenVSP that would actually fulfill the calculations, a new hydrofoil size was calculated from the $\frac{T}{W}$, and a maximum desired drag value can be found. From this a drag coefficient and a surface sizing can be found

$$0.5 * \rho_{air} * V_{TO}^2 * S^w * (C_{D_{a/c}} + C_{D_{hf}} * 816.33)$$

$$C_{D_{a/c}} + C_{D_{hf}} * 816.33$$

$$C_{D_{hf}} = \frac{D - C_{D_{a/c}}}{816.33}$$

3.4 Weight Sensitivity Study

The weight is one of the driving factors in the design of an aircraft. It will affect everything from wing size, fuselage size, tail size, etc. The weight depends on a few variables.

$$W = \frac{W_c + W_p}{1 - BWF - EWF}$$

Since this is an electric aircraft, one of the most important variables is the battery weight, which depends on a few variables such as range(R), efficiency(η), specific energy density(E) and the lift over drag of the aircraft($\frac{L}{D}$).

$$BWF = \frac{Rg}{\frac{L}{D}\eta E}$$

3.5 Down Scaled Design for Testing

Hydroaerospace wants to build and test the design to validate the results. They wanted the maximum weight to be 25 kg to meet legal limits. To scale the design, a ratio was created between the drone weight and the aircraft weight.

$$k_d = \sqrt{\frac{25}{W_{a/c}}}$$

Multiply the old wingloading of 49.2 psf by the scaling factor.

$$k_d * \frac{W}{S}_{old} = \frac{W}{S}_{new}$$

From this the new wing area is calculated again.

$$S = \frac{W}{\frac{W}{S}}$$

The proportions are made to be as similar as possible. To determine the new fuselage length, the old wing width to fuselage length ratio is calculated, and then the drone fuselage length is calculated from that.

$$\frac{L_{fus}}{b_{a/c}} = \frac{L_{drone}}{b_{drone}}$$

For the vertical and horizontal tail sizing, they are also found by multiplying K_d with their original surface areas.

$$S_{vt} = k_d * S_{vt_{OA}}$$

$$S_{ht} = k_d * S_{ht_{OA}}$$

The needed displacement volume is again calculated.

$$V_{requierd} = \frac{W}{\rho_{water}} * 1.2$$

The fuselage is then adjusted to obtain a close value to the desired displacement volume.
The hydrofoils are also downscaled to match the downscaled aircrafts size.

4

Results

4.1 Initial Design

4.1.1 Initial Weight Estimation and Breakdown

$$W_c = 2 * 85 = 140kg$$

$$W_p = 6 * 92 = 480kg$$

Considering the expected improvement for batteries during the coming decades, a value of E = 500 $\frac{kWh}{kg}$ is choosen instead[9]. An efficiency value of 75 percent is chosen based on [4]. The range is just the specified range from hydroaerospace.

$$BWF = \frac{Rg}{\frac{L}{D}\eta E} = \frac{185 * g}{14.5 * 0.75 * 500} = 0.3338$$

Just choosing a value for flying boats in figure 3.1 would cause some problems with the formula. The problem is that the denominator of the total weight equation cannot be less than zero. Just basing the empty weight fraction of this plot would give a value that is not complaint with the equation(or an extremely high weight). To obtain a reasonable value for the total weight, a value of EWF = 0.6 is chosen. Substituting all of these formulas into the original equation, a value of $W = 9.3607 * 10^3 kg$ is obtained.

4.1.2 Sizing Matrix Plot (SMP)

Landing Constraint

Variable	**Value**
ρ	1.225 kg/m^3
V_{stall}	45 m/s
$C_{L_{max}}$	1.9

Takeoff Constraint

Variable	**Value**
g	9.8 m/s^2
TOP	240 psf
ρ_0	1.225
ρ	1.225
$C_{L_{TO}}$	1.3

Climb Constraint

Variable	**Value**
γ	1°–2°
L/D	9.9–15.4

Cruise Constraint

Variable	**Value**
ρ	0.736
V_{cruise}	80 m/s
C_{D_0}	0.022
e	0.85

The values used in the constraint analysis were chosen based on typical values for aircraft. For the landing constraint, a value of $C_{L_{max}} = 1.9$ was selected. This was considered a reasonable value for a wing with high-lift devices. For the takeoff constraint, $C_{L_{TO}} = 1.3$ was used to represent takeoff conditions with flaps deployed. The set takeoff distance is 600 m. 600 m $\approx$ 2000 ft. Looking at where the "over 50 ft" line for propellers reaches a value of 2000 ft, a TOP value of 240 is obtained. Standard sea-level conditions were assumed for the air density.

In the climb constraint, climb angles between 1° and 2° were used, which represent typical performance requirements [8]. The L/D ratio was varied between 9.9 and 15.4 to account for different flight conditions. For the cruise constraint, a cruise velocity of 80 m/s was selected based on the design requirements. The zero-lift drag coefficient was estimated as $C_{D_0} = 0.022$ using the regression plot in Fig 4.1. An Oswald factor of $e = 0.85$ was also used as an initial guess.

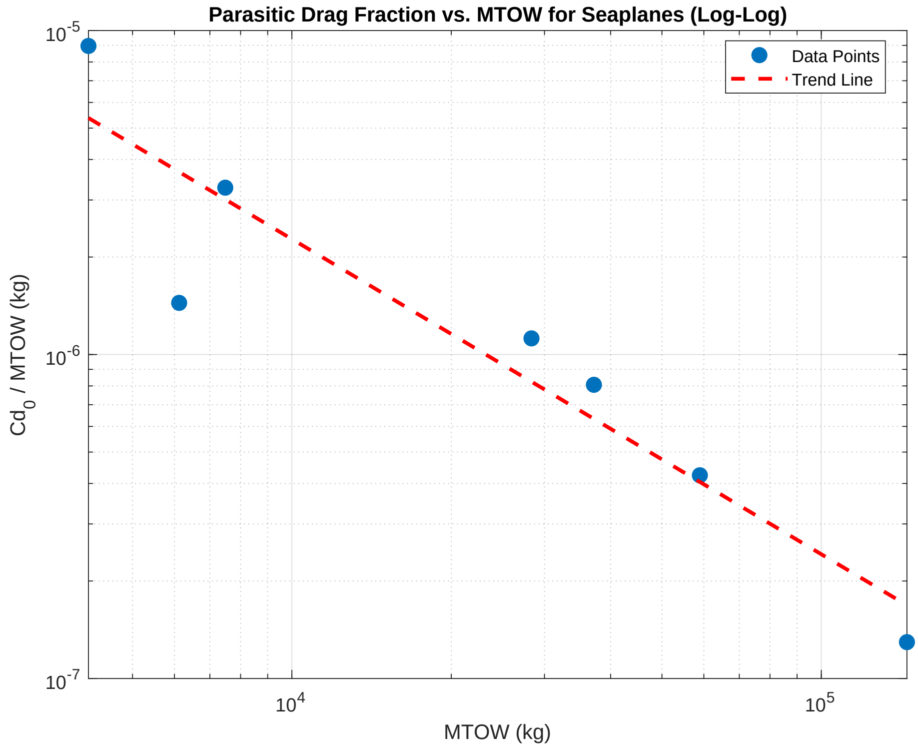

Figure 4.1: Regression plot used to estimate C_{D_0}.

Putting all of these equations together and plotting them in the SMP, a suitable wingloading and thrust-to-weight ratio is found.

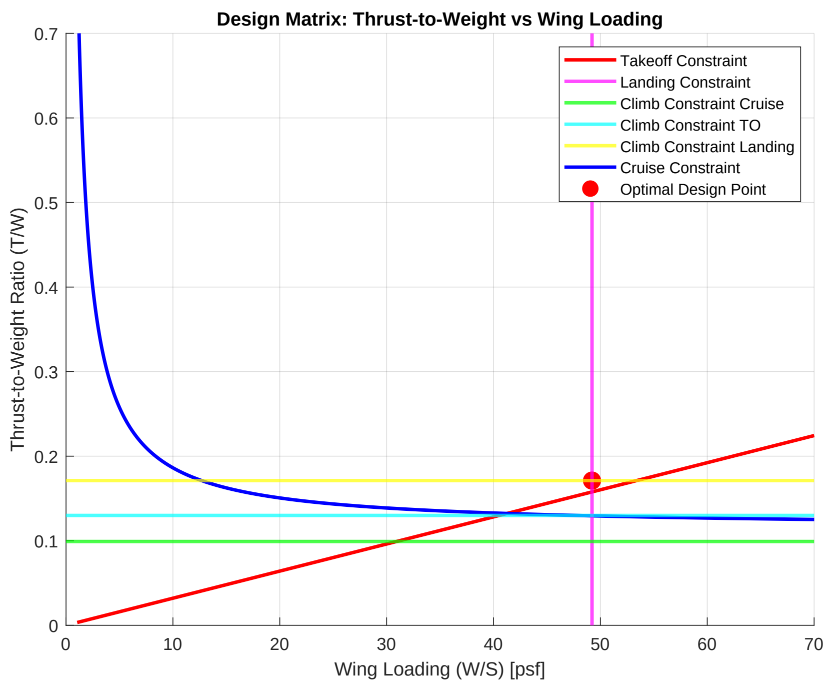

Figure 4.2: Sizing matrix plot

From the plot a wingloading of about 49.2 (psf) and a thrust to weight of 0.18 are chosen.

4.1.3 Aerodynamic Surfaces Design For 1st Iteration

4.1.3.1 Main wing design

The wing area was determined based on the selected wing loading from the SMP in Fig 4.2. Using the chosen design point, the resulting wing area is approximately $S = 38.95\ \text{m}^2$, which was rounded to 39 m^2 for the final design.

Table 4.1: Main wing geometric data and OpenVSP model

Parameter	**Value**
Span [m]	15
Area [m^2]	39
Aspect ratio	5.76
Wing loading [kg/m^2]	267.4
Tip chord [m]	1.35
Root chord [m]	3.39
Sweep [deg]	0
Incidence [deg]	4
Airfoil	NACA 5413
Dihedral [deg]	0
MAC [m]	2.76
Ailerons	
Chord fraction	0.25
Span [m]	2.625
Flaps	
Chord fraction	0.25
Span [m]	3

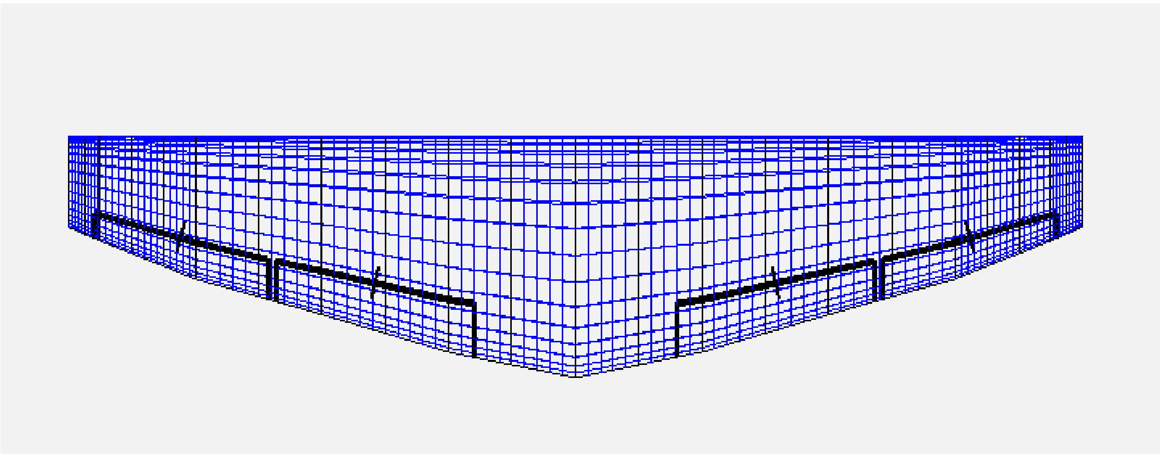

Figure 4.3: OpenVSP model of the main wing

4.1.3.2 Vertical tail design

The vertical tail area was calculated using the values shown in Table 4.2.

Table 4.2: Vertical tail calculation data

Parameter	Symbol	Value
Wing area	S	39 m^2
Wingspan	b	15 m
Vertical tail coefficient	C_{vt}	0.06
Vertical tail moment arm	L_{vt}	6 m

$S_{vt} = 5.84m^2$.

Table 4.3: Vertical Tail Geometric Data and Model

Parameter	Value
Span [m]	3.1
Area [m^2]	5.89
Aspect ratio	1.63
Tip chord [m]	1.31
Root chord [m]	2.19
Sweep [deg]	20
Airfoil	NACA 0015
Rudder	
Area [m^2]	2.24
Fraction of VT chord	0.46

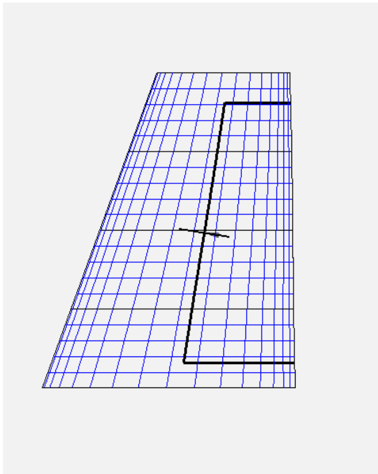

Figure 4.4: OpenVSP model of the vertical tail

4.1.3.3 Horizontal tail design

The horizontal tail area was calculated using the values shown in Table 4.4.

Table 4.4: Horizontal tail calculation data

Parameter	Symbol	Value
Wing area	S	39 m^2
Chord	b	2.34 m
Horizontal tail coefficient	C_{vt}	0.7
Horizontal tail moment arm	L_{vt}	6.7 m

$S_{ht} = 9.52m^2$.

Table 4.5: Horizontal Tail Geometric Data and Model

Parameter	Value
Span [m]	5.09
Area [m^2]	9.6
Aspect ratio	2.70
Tip chord [m]	1.26
Root chord [m]	2.52
Sweep [deg]	15
Incidence [deg]	-2
Airfoil	NACA 0012
Elevator Area [m^2]	2.9
Fraction of HT chord	0.36

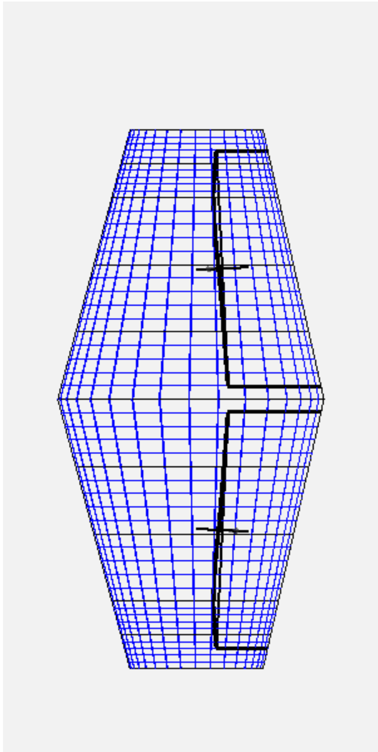

Figure 4.5: OpenVSP model of the horizontal tail

4.1.3.4 Fuselage design

The needed displacement volume was calculated based on the aircraft weight. The fuselage parameters were then adjusted until the required volume was obtained.

$$V_{requierd} = 11.24m^3$$

Table 4.6: Fuselage and Hull Geometric Data

Parameter	Value
Fuselage Length [m]	12.8
Maximum Diameter [m]	2
Hull Dimensions:	
Beam [m]	1.98
Forebody Length [m]	5.79
Afterbody Length [m]	5.79
Tail Extension [m]	0.98
Waterline Length [m]	11.58
Draft [m]	0.64
Estimated Displacement Volume [m^3]	11.54

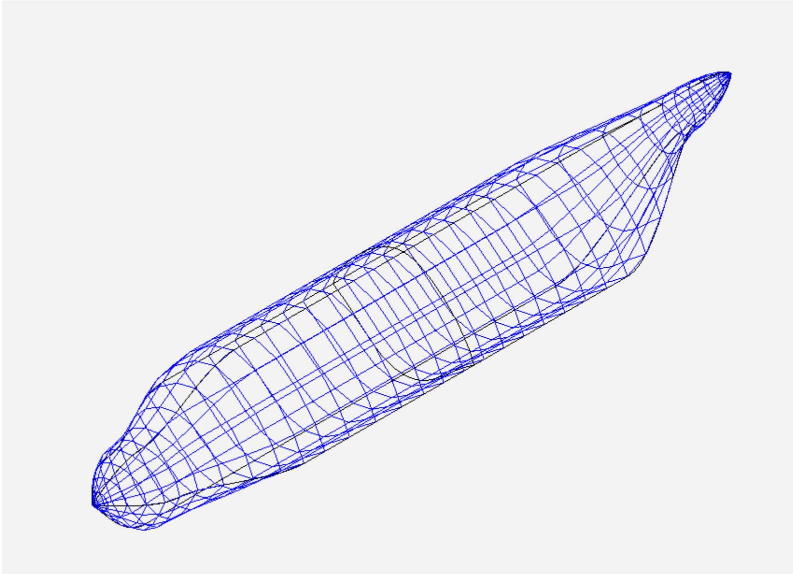

Figure 4.6: OpenVSP model of the fuselage

All of the parts together

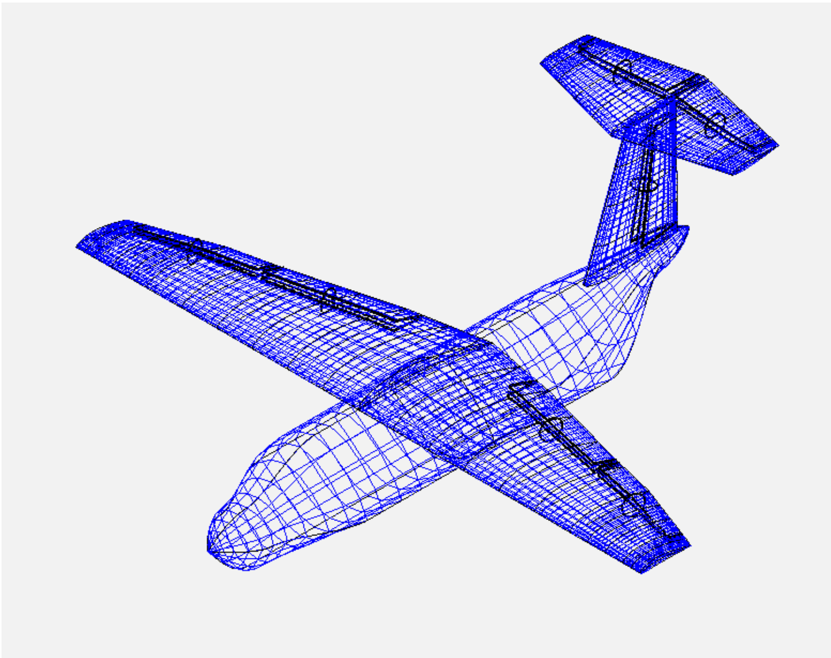

Figure 4.7: OpenVSP model of the aircraft

The aircraft was simulated in OpenVSP under cruise conditions to evaluate its aerodynamic characteristics.

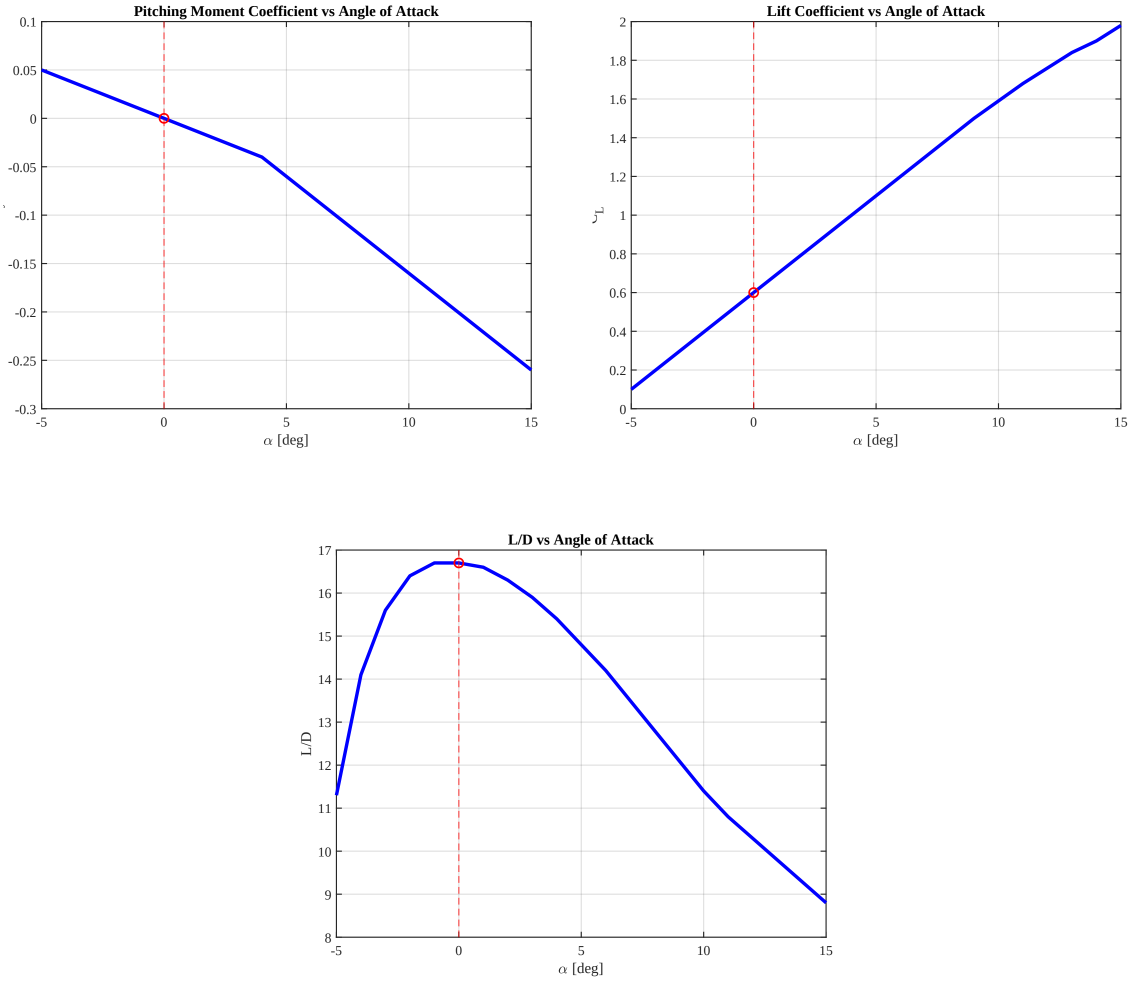

Figure 4.8: Aerodynamic coefficients for the aircraft configuration in cruise. Top left: C_m as a function of α. Top right: C_L as a function of α. Bottom: $\frac{L}{D}$ as a function of α.

The results in Fig. 4.8 show that the aircraft is statically stable, as indicated by the negative slope of the pitching moment curve. The pitching moment coefficient reaches zero at $\alpha = 0°$, indicating that the aircraft is trimmed at the expected cruise condition. The lift coefficient at this angle of attack is $C_L = 0.6$, which satisfies the required lift condition for cruise. The lift-to-drag ratio is slightly above 16 at $\alpha = 0°$, which is higher than the initial design estimate. This indicates that the aircraft has a higher aerodynamic efficiency than initially assumed. Overall, the results show that the initial aircraft configuration satisfies the stability, lift, and efficiency requirements in cruise.

More plots and pictures are available in Appendix.

4.1.3.5 Crew, Passengers and Battery volume estimation and placement

An assumed battery performance of $500\frac{Wh}{kg}$ and $400\frac{Wh}{L}$ [9].

$$\frac{500}{400} = 1.25\frac{L}{kg}$$

The battery weight fraction is 33.38 % of the total weight of the aircraft.

$$BWF * W = 3124.6kg$$

$$3124.6 * 1.25 = 3906L = 3.906m^3$$

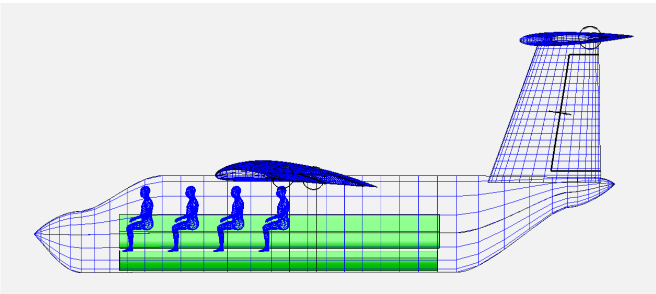

Figure 4.9: Side view of how the crew, passengers and the batteries could be placed

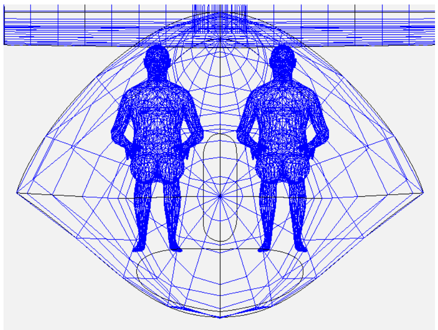

Figure 4.10: Front view of how the crew, passengers and the batteries could be placed

4.1.4 Electric motor sizing estimation

The needed power was calculated from the thrust-to-weight ratio.

$$\frac{T}{W} = 0.18$$

Which gives the required power

$$P = \frac{11221 \cdot 80}{0.82} = 1095.2 \text{ kW}$$

From this the motor and inverter weight and volume are estimated as:

$$W_{motor} = 368.0 \text{ kg}$$

$$V_{motor} = 119.16 \text{ L}$$

and

$$W_{Inverter} = 78.4 \text{ kg}$$

$$V_{Inverter} = 60.26 \text{ L}$$

Since the aircraft will have two motors the weight and volume of each electric motor and inverter will be halved.

4.1.5 Hydrofoil Design

A lift coefficient of 0.6 is chosen and the velocity for when the aircraft enters the foiling mode is set at 15 m/s (V_{fm} = 15 m/s). This gives:

$$\frac{W}{S_{hf}} = 1.4 * 10^3 kg/m^2$$

From this a surface area of $S_{hf} = 1.36\ m^2$ is obtained.

Table 4.7: Hydrofoil Geometric Data

Parameter	**Value**
Span [m]	2.8
Area [m^2]	1.36
Aspect ratio	5.74
Tip chord [m]	0.43
Root chord [m]	5.4
Sweep [deg]	0
Incidence [deg]	4.6
Airfoil	NACA 4412

4.2 Second iteration

The initial design was very heavy and had a lot of excess space for the 2 crew + 6 passengers. Also, from the simulations in OpenVSP the lift-over-drag was higher than the initial guess. To make the design smaller and lighter, L/D was increased to see if it would have any significant effects. After a few iterations, a new value of $L/D = 18$ was chosen and the new size and weight of the airplane were calculated from that.

4.2.1 Second Weight Estimation and Breakdown

Going back to the initial weight estimation breakdown, it can be seen that most of the things are exactly the same as for the first design.

$$W_c = 2 * 85 = 140kg$$

$$W_p = 6 * 92 = 480kg$$

The change only affects the BWF term since it includes the range in its equation, and with a $L/D = 18$

$$BWF = \frac{185 * g}{18 * 0.75 * 500} = 0.2689$$

The empty weight fraction(EWF) is still the same as for the first iteration. Combining these gives a new weight of $W = 5.5058 * 10^3$ kg. So changing the L/D from 14.5 to 18 gave a decrease in the total weight, where the BWF also decreases from 33.4 % to 26.9 %. The new weight is $\frac{5.5058}{9.3607} = 58.8\%$, of the original.

4.2.2 Second Sizing Matrix Plot

For the SMP the same constraints as for the first iteration were used, giving

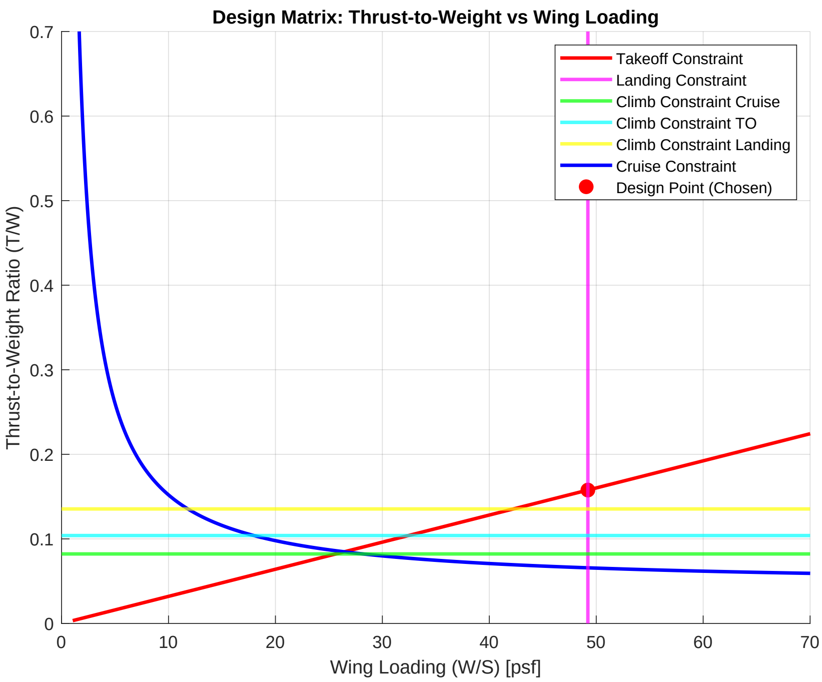

Figure 4.11: Second Iteration Sizing matrix plot

When choosing the desired values, as high of a wingloading as possible and as low of a thrust to weight ratio as possible are typically chosen. From the plot a wingloading of about 49.2 (psf) and a thrust to weight of 0.16 are chosen.

4.2.3 Second Iteration Lifting Surfaces Design

4.2.3.1 Main wing design

Just like previously the main wing area is calculated:

$$S = 22.9123m^2$$

From Hydroaerospace specifications the wingspan needs to be 14 m, but the previous iteration used 15 m to not make the AR too small. However, for this smaller main wing area, a 14 m wingspan gives a reasonable AR as well. Taking all of this into account, a new wing model was created in OpenVSP.

Table 4.8: Main Wing Geometric and Aerodynamic Data

Parameter	**Value**
Span [m]	14
Area [m^2]	23
Aspect ratio	8.4
Tip chord [m]	0.86
Root chord [m]	2.29
Average Taper	0.915
Sweep [deg]	0
Incidence [deg]	3.3
Airfoil	NACA 4412
Dihedral [deg]	0
MAC [m]	1.77
Ailerons	
Chord fraction	0.25
Span [m]	2.45
Flaps	
Chord fraction	0.25
Span [m]	2.8

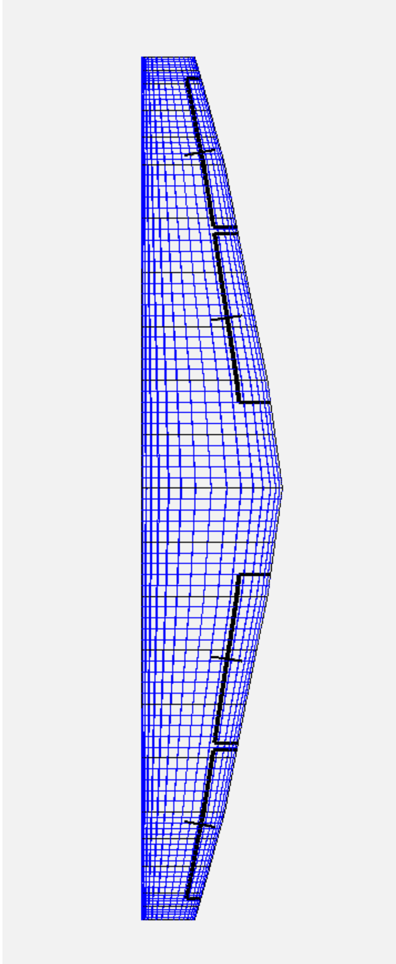

Figure 4.12: OpenVSP model of the main wing

4.2.3.2 Vertical tail design

The vertical tail size is again calculated giving $S_{vt} = 3.2m^2$

Table 4.9: Vertical Tail Calculation Data

Parameter	Value
S [m^2]	23
b [m]	14
C_{vt}	0.06
L_{vt} [m]	6

Table 4.10: Vertical Tail Geometric Data

Parameter	Value
Span [m]	2.3
Area [m^2]	3.3
Aspect ratio	1.63
Tip chord [m]	0.98
Root chord [m]	1.86
Taper	0.85
Sweep [deg]	20
Airfoil	NACA 0015
MAC [m]	1.47
Rudder	
Area [m^2]	0.835
Chord fraction	0.46

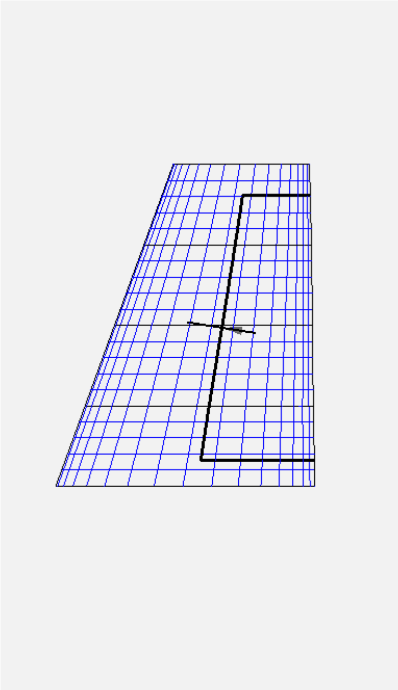

Figure 4.13: OpenVSP model of the vertical tail

4.2.3.3 Horizontal tail design

$C_{ht} = 0.7$, this gives $S_{ht} = 3.7m^2$

Table 4.11: Horizontal tail data and OpenVSP model

Calculation Data	
Parameter	**Value**
S [m^2]	23
c [m]	1.5
C_{ht}	0.7
L_{ht} [m]	6.7

Geometric Data	
Parameter	**Value**
Span [m]	3.2
Area [m^2]	3.7
Aspect ratio	2.76
Tip chord [m]	0.77
Root chord [m]	1.54
Sweep [deg]	15
Incidence [deg]	-2.7
Airfoil	NACA 0015
Elevator	
Area [m^2]	0.8
Chord fraction	0.36

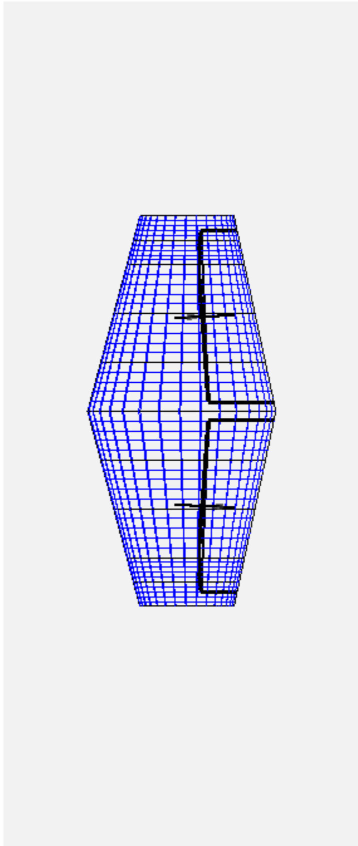

Table 4.12: OpenVSP model of the horizontal tail

4.2.3.4 Fuselage design

Since the new weight is substantially less than the old weight. The required displacement volume also changes. The new required displacement volume was calculated in the same way as the first design.

$$V_{requierd} = 6.6m^3$$

The change to the fuselage was tried to be as minimal as possible, meaning that the height, width, length and depth was kept the same. The major change comes in the form of an earlier start for the tailboom.

Table 4.13: Fuselage and Hull Geometric Data

Parameter	**Value**
Fuselage Length [m]	12
Maximum Diameter [m]	2
Hull Dimensions:	
Beam [m]	1.98
Forebody Length [m]	4.57
Afterbody Length [m]	1.22
Tail Extension [m]	0.98
Waterline Length [m]	5.79
Draft [m]	0.73
Estimated Displacement Volume [m^3]	6.6

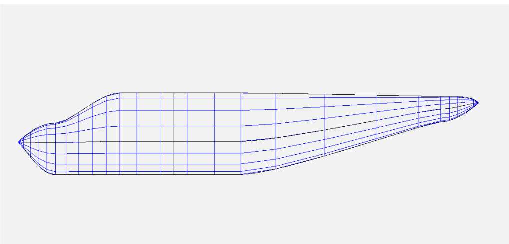

(a) Side view

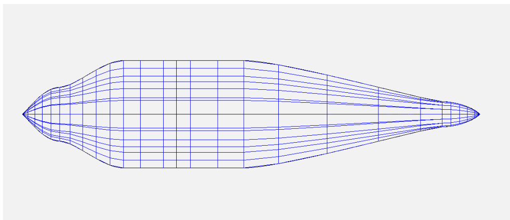

(b) Top view

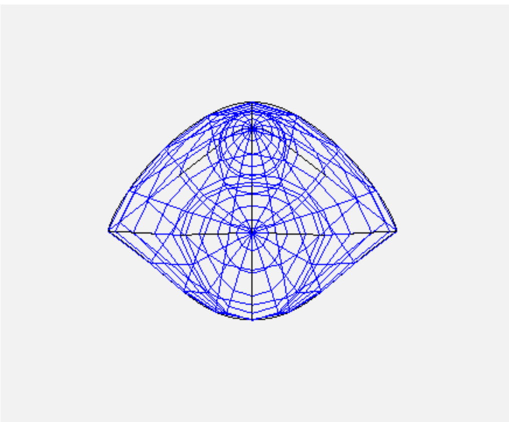

(c) Front view

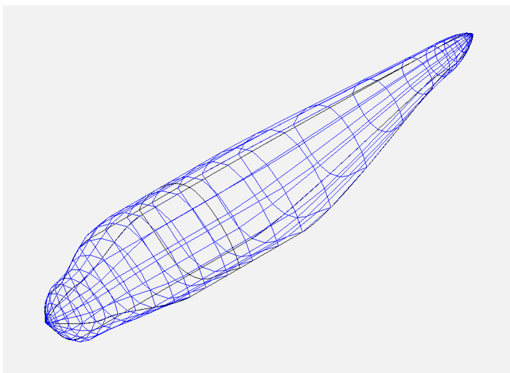

(d) Isometric view

Figure 4.14: OpenVSP models of the fuselage in different views.

All of the components together

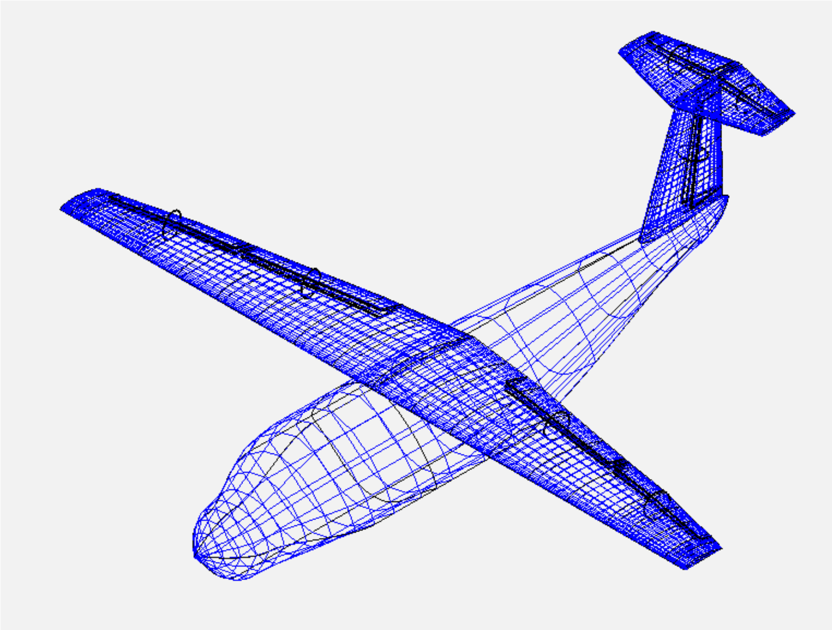

Figure 4.15: OpenVSP model of the aircraft

4.2.3.5 Crew, Passengers and Battery volume estimation and placement

An assumed battery performance of $500\frac{Wh}{kg}$ and $400\frac{Wh}{L}$.

$$\frac{500}{400} = 1.25\frac{L}{kg}$$

The battery weight fraction is 26.89 % of the total weight of the aircraft.

$$W_b * W = 1480.5kg$$

$$1480.5 * 1.25 = 1850.6L = 1.8506m^3$$

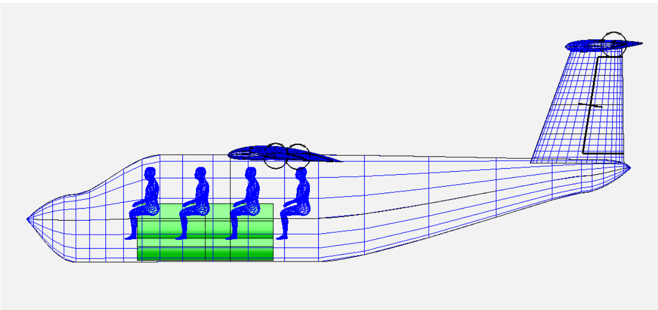

Figure 4.16: Side view of how the crew, passengers and the batteries could be placed

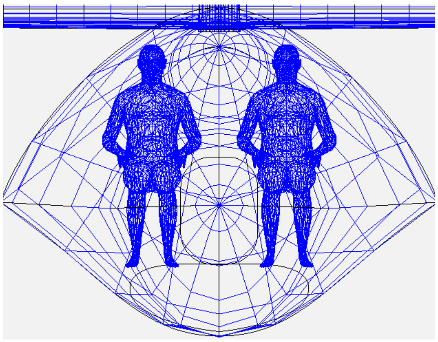

Figure 4.17: Front view of how the crew, passengers and the batteries could be placed

4.2.4 Cruise Condition For New Design Without Hydrofoil

To start, the C_L value is again found

$$C_{L_{a/c}} = \frac{Wg}{\frac{1}{2}\rho_{air} V_{cruise}^2 S^w} = \frac{5500 * g}{\frac{1}{2} * 1.225 * 80^2 * 23} = 0.6$$

From airfoil tools, the airfoil NACA 4412 seemed to give a close C_L value, as well as a good L/D. The aircraft is simulated in OpenVSP in cruise conditions to evaluate its aerodynamic characteristics.

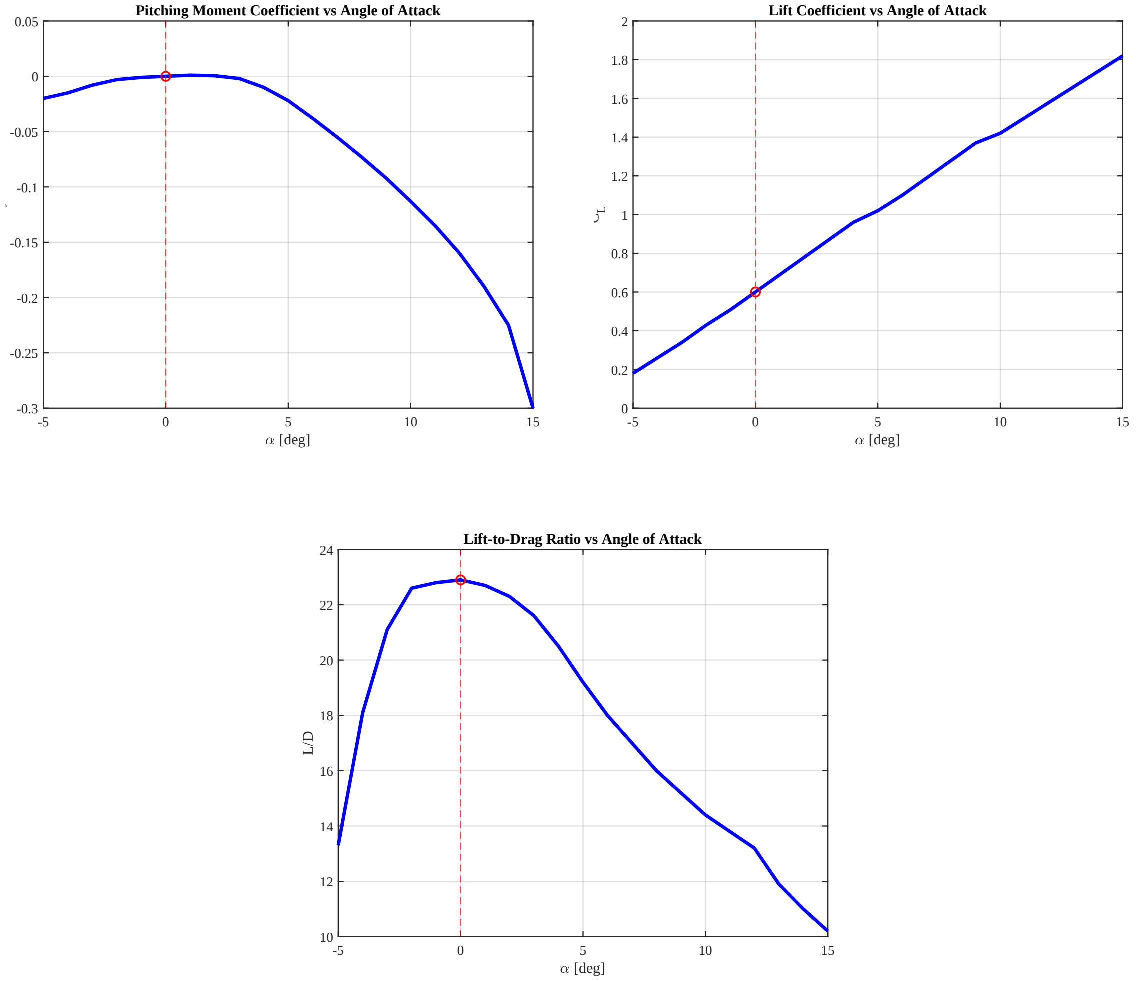

Figure 4.18: Aerodynamic coefficients for the aircraft in cruise configuration. Top left: C_m as a function of α. Top right: C_L as a function of α. Bottom: $\frac{L}{D}$ as a function of α.

The results in Fig. 4.18 show that the aircraft is trimmed at $\alpha = 0°$, where the pitching moment coefficient is zero. This shows that the aircraft maintains a stable trim in cruise. The lift coefficient reaches the target value of $C_L = 0.6$ at $\alpha = 0°$, which corresponds to the trimmed cruise condition. The lift-to-drag ratio is approximately $\frac{L}{D} = 22.5$ at $\alpha = 0°$, which is higher than the initial design estimate. This indicates that the aircraft is more efficient than initially assumed. Overall, the results show that the aircraft satisfies the required trim, lift, and efficiency conditions in cruise.

More plots can be found in appendix A.

4.2.5 Landing Condition For New Design Without Hydrofoil

To start, the $C_{L_{landing}}$ value is again found

$$C_{L_{landing_{a/c}}} = \frac{Wg}{\frac{1}{2}\rho_{air} V^2_{landing} S^w} = \frac{5500 * g}{\frac{1}{2} * 1.225 * 45^2 * 23} = 1.9$$

The aircraft was simulated in OpenVSP under landing conditions to evaluate its aerodynamic characteristics.

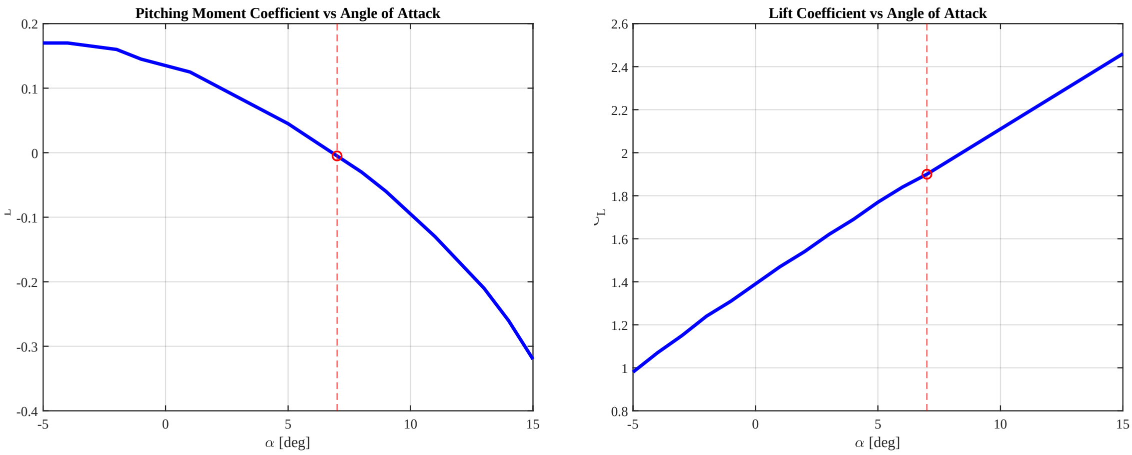

Figure 4.19: Aerodynamic coefficients for the aircraft in landing configuration. Left: C_m as a function of α. Right: C_L as a function of α.

The results in Fig. 4.19 show that the aircraft is trimmed at $\alpha = 7°$, where the pitching moment coefficient is zero. This indicates that the aircraft maintains a stable trim condition in landing configuration. The lift coefficient reaches the required value of $C_L = 1.9$ at the same angle of attack, showing that the aircraft generates enough lift during landing conditions. Overall, the results show that the aircraft satisfies both the stability and lift requirements for landing.

More plots can be found in appendix A.

4.2.6 Takeoff Condition For New Design Without Hydrofoil

To start, the takeoff velocity(V_{TO}) is found by multiplying the landing velocity by 1.1.

$$V_{TO} = V_{landing} * 1.1 = 49.5$$

Then the $C_{L_{TO}}$ value is found by

$$C_{L_{TO_{a/c}}} = \frac{Wg}{\frac{1}{2}\rho_{air}V_{landing}^2 S^w} = \frac{5500 * g}{\frac{1}{2} * 1.225 * 49.5^2 * 23} = 1.56$$

The aircraft was simulated in OpenVSP under takeoff conditions to evaluate its aerodynamic characteristics. The control surfaces were adjusted to obtain the desired coefficient values at takeoff.

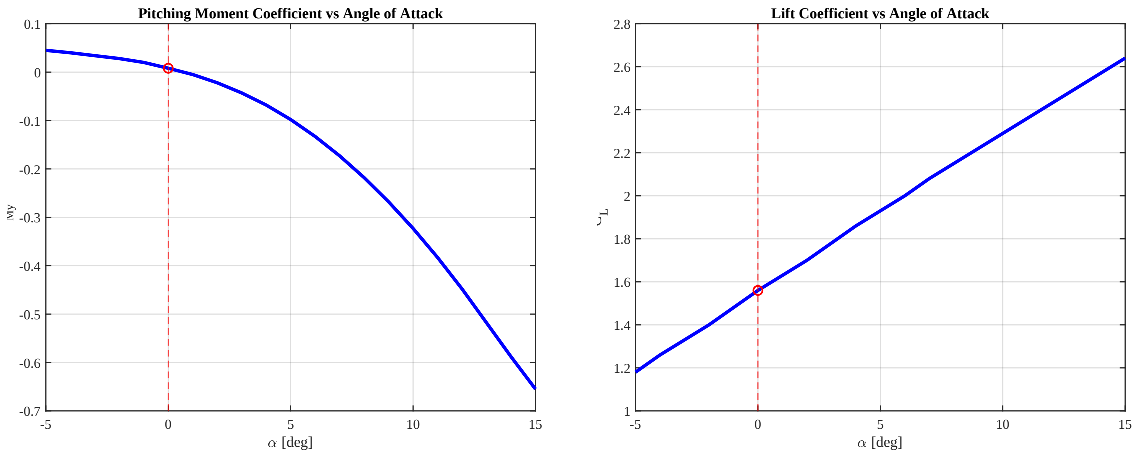

Figure 4.20: Aerodynamic coefficients for the aircraft in takeoff configuration. Left: C_m as a function of α. Right: C_L as a function of α.

The results in Fig. 4.20 show that the aircraft is trimmed at $\alpha = 0°$, where the pitching moment coefficient is zero. The lift coefficient reaches the required value of $C_L = 1.56$ at $\alpha = 0°$, indicating that the aircraft generates sufficient lift under the specified takeoff conditions. Overall, the results show that the aircraft meets the required stability and lift values for takeoff.

4.2.7 Hydrofoil Design

A lift coefficient of 0.6 is chosen and the velocity for when the aircraft enters the foiling mode is set at 15 m/s ($V_{FM} = 15$ m/s). This gives:

$$\frac{W}{S_{hf}} = 1.4 * 10^3 kg/m^2$$

From this a surface area of $S_{hf} = 0.8\ m^2$ is obtained.

Table 4.14: Hydrofoil Geometric Data

Parameter	Value
Span [m]	2.16
Area [m^2]	0.8
Aspect ratio	5.82
Tip chord [m]	0.33
Root chord [m]	0.41
Sweep [deg]	0
Incidence [deg]	5
Airfoil	NACA 4412

Looking at the pitch coefficient for the hydrofoil and its tail, we can rewrite it to find a needed aircraft tail sizing

$$C^a_{mG\alpha_{hf}} = a^{hf}(\xi_{AC^{hf}} - \xi_G) + \eta^{hft}\sigma^{hft}(a^{hft}(\xi_{AC^{hft}} - \xi_G))$$

The a/c tail is substituted in instead of the hydrofoil tail

$$C^a_{mG\alpha_{hf}} = a^{hf}(\xi_{AC^{hf}} - \xi_G) + \eta^t\sigma^t(a^t(\xi_{AC^t} - \xi_G))$$

Comparing the two equations, the tail contribution and hydrofil tail contribution must be equal

$$\eta^{hft}\sigma^{hft}(a^{hft}(\xi_{AC^{hft}} - \xi_G)) = \eta^t\sigma^t(a^t(\xi_{AC^t} - \xi_G))$$

The values of a^{hft} and a^t are assumed to be similar, so they can be canceled

$$\eta^{hft}\sigma^{hft}((\xi_{AC^{hft}} - \xi_G)) = \eta^t\sigma^t(\xi_{AC^t} - \xi_G)$$

The equation is then rewritten to find the needed a/c tail - hydrofoil surface area ratio(σ^t)

$$\sigma^t = \frac{\eta^{hft}\sigma^{hft}((\xi_{AC^{hft}} - \xi_G))}{\eta^t(\xi_{AC^t} - \xi_G)}$$

For the hydrofoil tail area, the same formula was used as for the aircraft tail, giving $S_{hft} = 0.1\ m^2$. However, this area was unable to stabilize the foil, so the hydrofoil tail area was changed to $S_{hft} = 0.2\ m^2$ instead.

Table 4.15: Hydrofoil tail Geometric Data

Parameter	Value
Span [m]	1.11
Area [m^2]	0.2
Aspect ratio	6.16
Tip chord [m]	0.16
Root chord [m]	0.2
Sweep [deg]	0
Incidence [deg]	-0.5
Airfoil	NACA 0012

While $(\xi_{AC^{hft}} - \xi_G) = 2$ m, $(\xi_{AC^t} - \xi_G) = 6.7$ m and $\eta^{hft} = 1$. Putting these into the above equation gives

$$\sigma^t = \frac{\frac{0.2}{0.8} * 2}{\frac{\rho_{air}}{\rho_{water}} * 6.7} = 60.92$$

$$\sigma^t = \frac{S^t}{S^{hf}}$$

$$S^t = 60.92 * 0.8 = 48.74m^2$$

4.2.8 Takeoff Condition For Hydrofoil

To start, the hydrofoil is designed to have a lift coefficient of $C_{L_{hf}} = 0.6$. Since the simulations are performed using the aircraft wing as the reference area, the obtained lift coefficient must be scaled to the hydrofoil reference area. This is done using the surface area ratio between the main wing and the hydrofoil:

$$C_{L_{hf}} = \frac{0.021}{\frac{0.8}{23}} = 0.6$$

The hydrofoil is simulated on its own in OpenVSP under takeoff conditions.

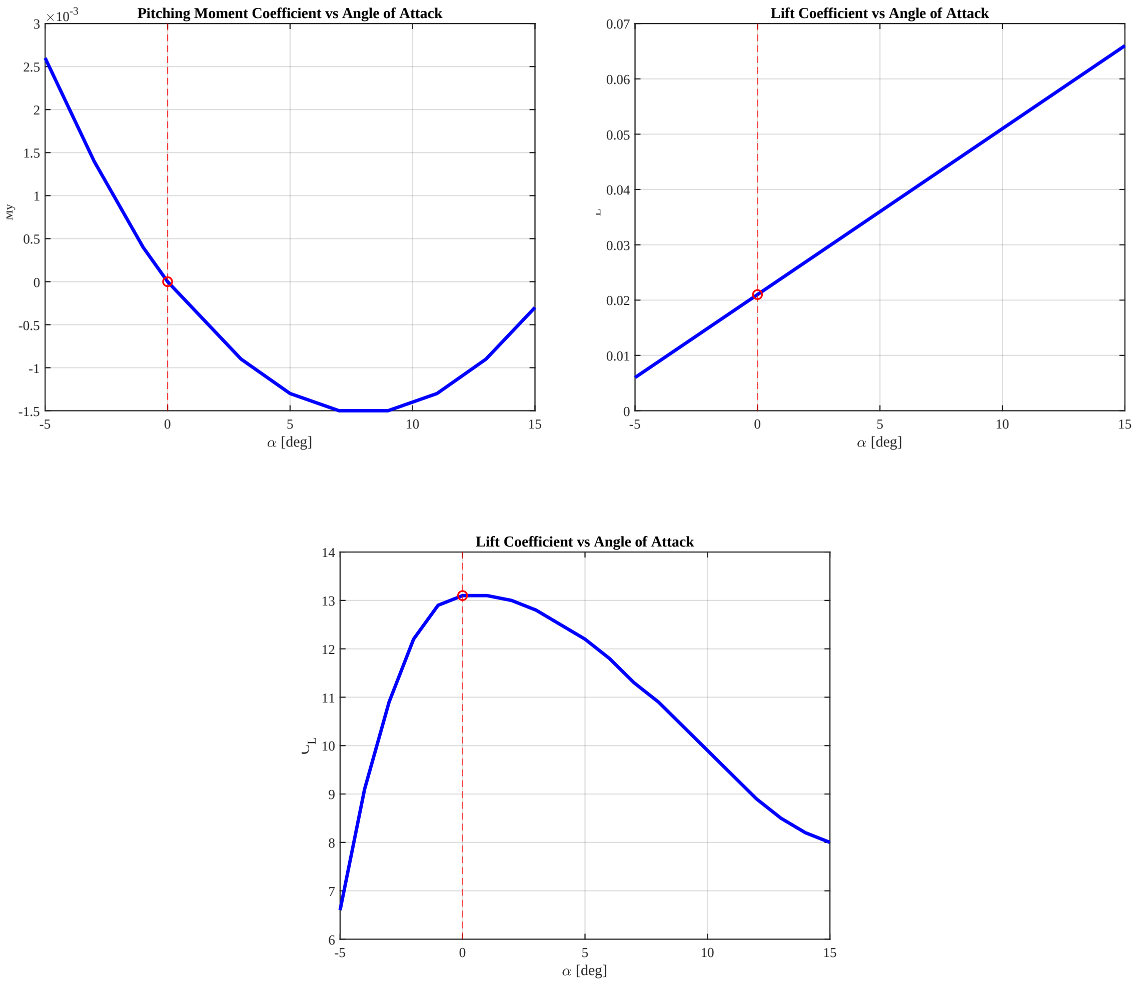

Figure 4.21: Aerodynamic characteristics of the hydrofoil in takeoff conditions. Top left: C_m as a function of α. Top right: C_L as a function of α. Bottom: $\frac{L}{D}$ as a function of α.

The results in Fig. 4.21 show that the hydrofoil is stable in takeoff conditions, with the pitching moment coefficient being zero at $\alpha = 0°$. The lift coefficient reaches the required value of $C_{L_{hf}} = 0.6$ at the expected angle of attack, indicating that the hydrofoil provides enough lift. The lift-to-drag ratio is slightly above 13, showing that the hydrofoil has a moderate aerodynamic efficiency under the given conditions. Overall, the results shows that the hydrofoil meets the lift requirement and maintains stable behavior, while having a reasonable lift-to-drag performance.

More graphs can be found in appendix A.

4.2.9 Cruise Condition

The a/c and the hydrofoils are simulated together in cruise conditions to evaluate if the hydrofoil affects the aerodynamic behavior of the aircraft. The combined aircraft and hydrofoil configuration was simulated in OpenVSP using the same setup as for the aircraft alone.

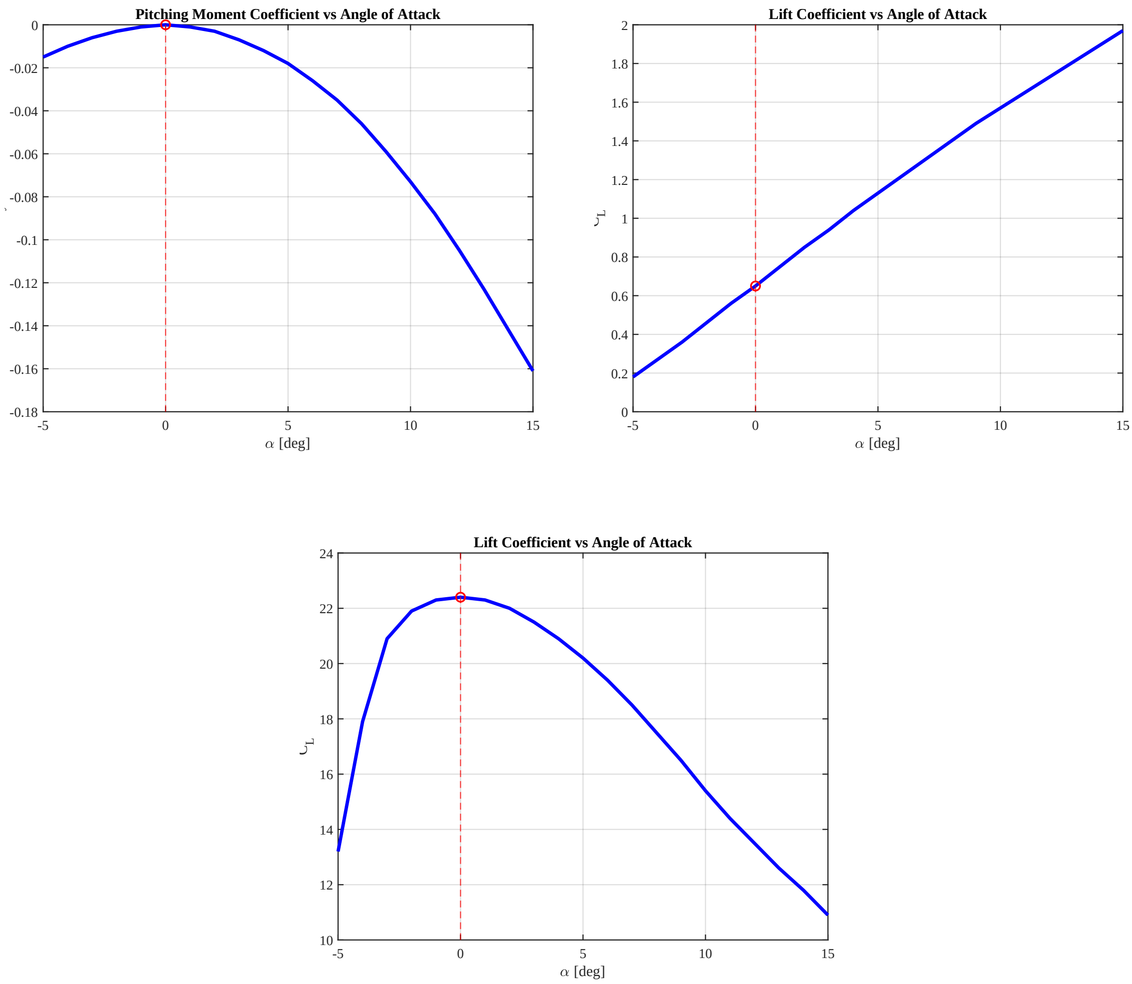

Figure 4.22: Aerodynamic coefficients in cruise configuration. Top left: C_m as a function of α. Top right: C_L as a function of α. Bottom: $\frac{L}{D}$ as a function of α.

The results in Fig. 4.22 show that the pitching moment coefficient reaches zero at $\alpha = 0°$, showing that the pitching stability is the same as for the aircraft without the hydrofoil. The lift coefficient reaches the target value of $C_L = 0.6$ at the expected angle of attack, showing that the lift coefficient is not affected by the hydrofoil. The lift-to-drag ratio remains above the initial design value of 18, indicating that the aerodynamic efficiency of the aircraft is preserved. Overall, the results show that the hydrofoil does not significantly affect the aerodynamic performance of the aircraft during cruise.

More plots can be found in appendix A.

4.2.10 Landing Condition

The a/c and the hydrofoils are simulated together in landing conditions to evaluate if the hydrofoil affects the aerodynamic behavior of the aircraft. The combined aircraft and hydrofoil configuration was simulated in OpenVSP using the same control surface settings as for the aircraft alone.

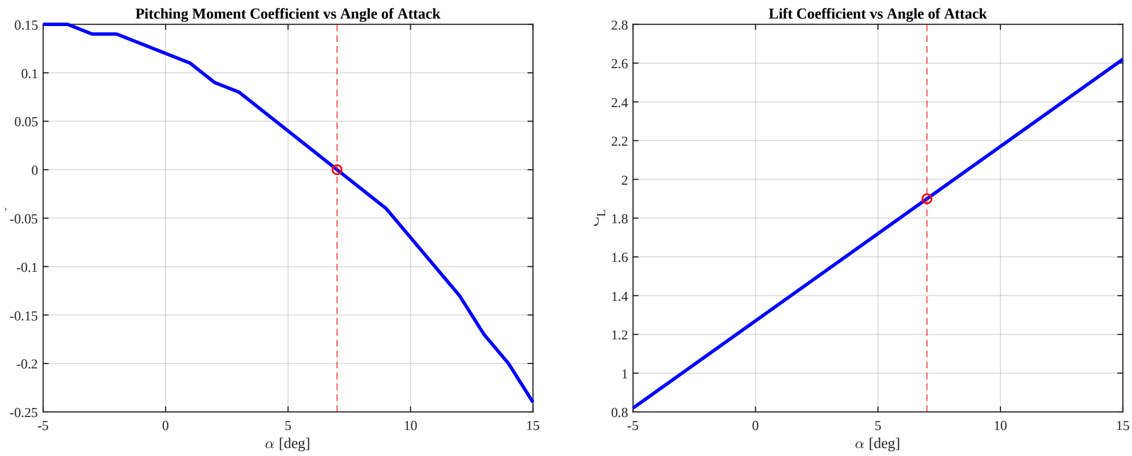

Figure 4.23: Aerodynamic coefficients in landing configuration. Left: C_m as a function of α. Right: C_L as a function of α.

The results in Fig. 4.23 show that the pitching moment coefficient reaches zero at $\alpha = 7°$, which is the same as the aircraft without the hydrofoil. This shows that the hydrofoils has no major effect on the aircrafts pitch stability. The lift coefficient reaches the required value of $C_L = 1.9$ at the expected angle of attack, showing that the lift coefficient remain unchanged. Overall, the results indicate that the hydrofoil does not change the aerodynamic behavior in any noticeable way of the aircraft during landing.

More plots can be found in appendix A.

4.2.11 Weight Estimation of Parts

4.2.11.1 Wing Weight

Table 4.16: Wing Weight Parameters

Parameter	Description and Value
W_{dg}	Design gross weight 12138 lb
N_z	Ultimate load factor 3
S_w	Wing area 247.6 ft^2
t/c	Thickness-to-chord ratio 12%
A	Aspect ratio 8.4
λ_w	Wing taper 0.85
Λ_w	Sweep angle at 25% MAC 0 deg
S_{csw}	Total aileron area 20 ft^2

$$W_{\mathrm{wing}} = 717.7lbs = 325.5kg$$

4.2.11.2 Horizontal Tail Weight

Table 4.17: Horizontal Tail Weight Parameters

Parameter	Description and Value
K_{uht}	Horizontal tail weight factor 1
W_{dg}	Design gross weight 12138 lb
N_z	Ultimate load factor 3
L_t	Distance from main wing to tail 22 ft
B_h	Horizontal tail span 10.5 ft
F_w	Fuselage width at horizontal tail 2.17 ft
S_{ht}	Horizontal tail area 39.8 ft^2
Λ_{ht}	Sweep angle 15 deg
A_{ht}	Aspect ratio 2.76
S_e/S_{ht}	Elevator control surface to tail area ratio 0.31
K_y	Pitch radius of gyration 6.6 ft

$$W_{\mathrm{ht}} = 57.4lbs = 26kg$$

4.2.11.3 Vertical Tail Weight

Table 4.18: Vertical Tail Weight Parameters

Parameter	Description and Value
H_t/H_v	Horizontal-to-vertical tail height ratio 1
W_{dg}	Design gross weight 12138 lb
N_z	Ultimate load factor 3
L_t	Distance from wing to tail 19.7 ft
S_{vt}	Vertical tail area 3.3 ft^2
K_z	Yaw radius of gyration 19.7 ft
A_v	Vertical tail aspect ratio 1.63
t/c_{root}	Thickness-to-chord ratio at root 14.6%
Λ_{vt}	Sweep angle 20 deg

$$W_{\text{vt}} = 202lbs = 91.6kg$$

4.2.11.4 Fuselage Weight

Table 4.19: Fuselage Weight Parameters

Parameter	Description and Value
W_{dg}	Design gross weight 12138 lb
N_z	Ultimate load factor 3
L_f	Fuselage length 39.37 ft
$\frac{L}{D}$	Lift-over-Drag 18
S_f	Fuselage wetted area 664.1 ft^2
K_{Lg}	Landing gear factor 1
K_{door}	Door cutout factor 1
K_{ws}	Wing step-up factor 0

$$W_{\text{fuselage}} = 4023lbs = 1825kg$$

4.2.11.5 Electric motor sizing and weight estimation

$$\frac{T}{W} = 0.16$$

Then the power in cruise is calculated

$$P = \frac{8637 \cdot 80}{0.82} = 842.6 \text{ kW}$$

From this the motor and inverter weight and volume are estimated as:

$$W_{motor} = 283.1 \text{ kg}$$

$$V_{motor} = 91.7 \text{ L}$$

and

$$W_{inverter} = 60.4 \text{ kg}$$

$$V_{inverter} = 46.4 \text{ L}$$

Since the aircraft will have two motors the weight and volume of each electric motor and inverter will be halved.

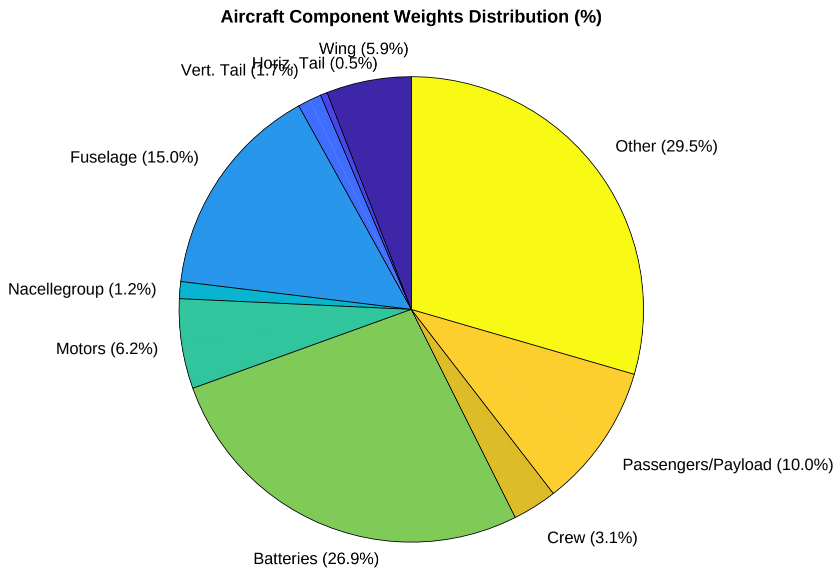

Figure 4.24: Circle diagram of main components weight

4.2.12 Initial design performance

The initial takeoff distance was first calculated using the highest obtained hydrofoil $\frac{L}{D}$ value. However, the calculated Float + FM takeoff distance became imaginary, indicating that the aircraft is unable to maintain positive acceleration throughout the takeoff run. To further investigate this behavior, the acceleration was plotted as a function of velocity for both the Float + FM and the conventional OF configuration.

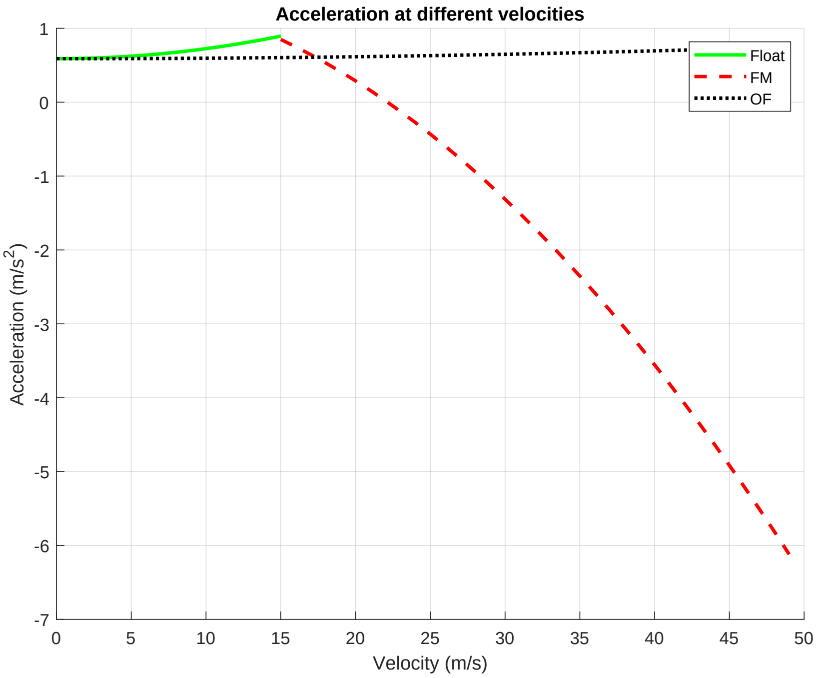

Figure 4.25: Acceleration as a function of velocity for FM at 15 m/s

As shown in Fig. 4.25, the net acceleration becomes negative after approximately $V = 22$ m/s. This shows that the total drag exceeds the available thrust at higher velocities, preventing the aircraft from reaching takeoff speed. The results suggest that the selected thrust-to-weight ratio of $\frac{T}{W} = 0.16$ is too low for the hydrofoil configuration, the hydrofoil drag is too high, or a combination of both. Since the hydrofoil drag coefficient $C_{D_{hf}}$ is directly related to the hydrofoil $\frac{L}{D}$ ratio, both the thrust-to-weight ratio and the hydrofoils $\frac{L}{D}$ become critical parameters. An analysis was done to find the required $\frac{T}{W}$ and hydrofoil $\frac{L}{D}$ values in order to determine whether the hydrofoil takeoff concept could achieve realistic performance.

4.2.12.1 $\frac{T}{W}$ Analysis

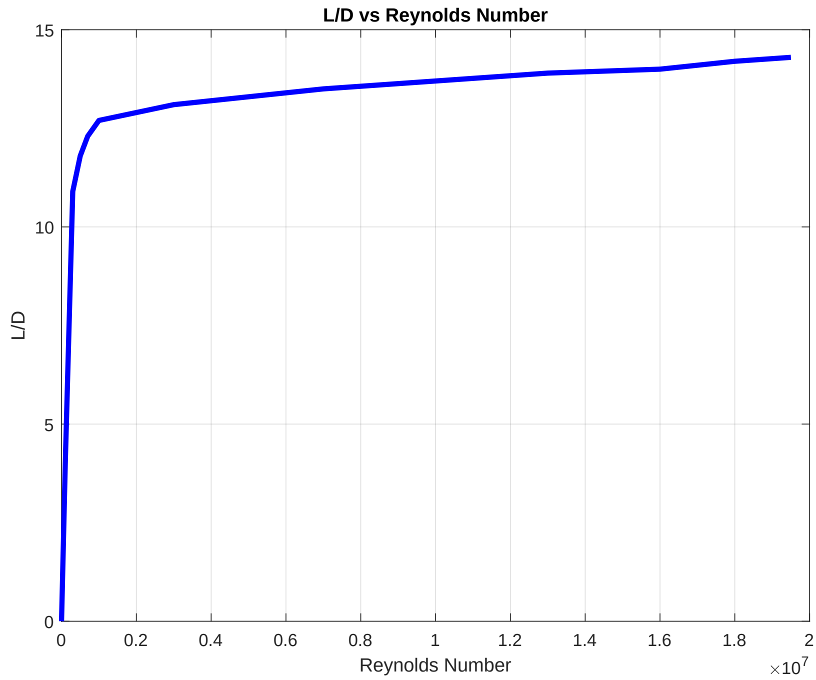

Figure 4.26: Hydrofoil $\frac{L}{D}$ ratio as a function of Reynolds number

Figure 4.26 shows the obtained hydrofoil $\frac{L}{D}$ range for different Reynolds numbers during the takeoff run. The resulting $\frac{L}{D}$ values vary between approximately 4 and 14.5, with the higher values occurring at the higher Reynolds numbers. Using the highest obtained $\frac{L}{D}$ value and the required takeoff velocity of $V = 49.5$ m/s, a required thrust-to-weight ratio is calculated.

$$\frac{T}{W}_{best} \approx 0.8$$

This results in a total takeoff distance of

$$\hat{S}_{total} = 1347 \text{ m}$$

The required $\frac{T}{W}$ is significantly higher than the initially selected value of $\frac{T}{W} = 0.16$, indicating that the original propulsion sizing is not enough for the hydrofoil configuration, or something else is off. For comparison, using the same thrust-to-weight ratio of $\frac{T}{W} = 0.8$ for the conventional OF configuration gives a takeoff distance of

$$\hat{S}_{OF} = 176 \text{ m}$$

This shows that even with the best obtained hydrofoil $\frac{L}{D}$ value, the hydrofoil configuration does not give a performance benefit compared to the conventional configuration. The additional drag generated by the hydrofoil outweighs the reduction in hydrodynamic drag, resulting in a significantly longer takeoff distance.

4.2.12.2 $\frac{L}{D}$ Analysis

Looking instead at the required hydrofoil $\frac{L}{D}$ needed to satisfy the initially selected thrust-to-weight ratio of $\frac{T}{W} = 0.16$ gives

$$K_{A,fm} = -\frac{0.16}{49.5^2} = -6.53 \cdot 10^{-5}$$

This corresponds to a required hydrofoil $\frac{L}{D}$ of approximately 135. Such a value is far above the obtained simulation results and very unrealistic to achieve. Even if a hydrofoil $\frac{L}{D}$ ratio of 135 could theoretically be achieved, the resulting takeoff performance would still be longer the conventional configuration. The calculated takeoff distances become

$$\hat{S}_{OF} = 1838 \text{ m}$$

$$\hat{S}_{total} = 5296 \text{ m}$$

The hydrofoil-assisted configuration therefore still results in a significantly longer takeoff distance compared to the conventional configuration. This indicates that improving only the hydrofoil $\frac{L}{D}$ is not sufficient to make the concept viable.

4.2.12.3 Accounting for a/c lift

25 m/s Changing the FM velocity to 25 m/s instead of 15 m/s and accounting for the added lift from the aircraft gives

$$L_{hf} = L - L_{a/c} = 53900 - 13735 = 40165N$$

$$\hat{C}_{L_{hf}} = \frac{40165}{0.5 * 1000 * 0.8 * (25^2)} = 0.16$$

Normalized with the a/c area

$$C_{L_{hf}} = 0.16 * \sigma^{hf} = 0.16 * \frac{0.8}{23} = 0.0056$$

Assuming that the $\frac{L}{D}$ is the same as for the original hydrofoil. This gives

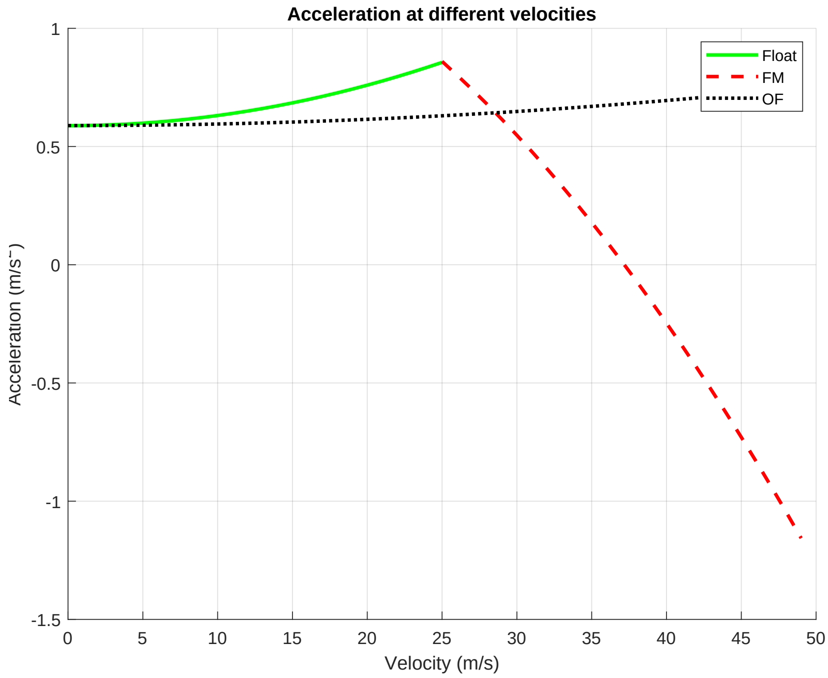

Figure 4.27: The acceleration plotted against the velocity for FM at 25 m/s

The net acceleration is still negative when the higher velocities are reached.

35 m/s Changing the FM velocity to 35 m/s and accounting for the added lift from the aircraft gives

$$L_{hf} = 26979N$$

$$C_{L_{hf}} = \frac{26979}{0.5 * 1000 * 0.8 * (35^2)} = 0.055$$

Normalized with the a/c area

$$C_{L_{hf}} = 0.055 * \sigma^{hf} = 0.0019$$

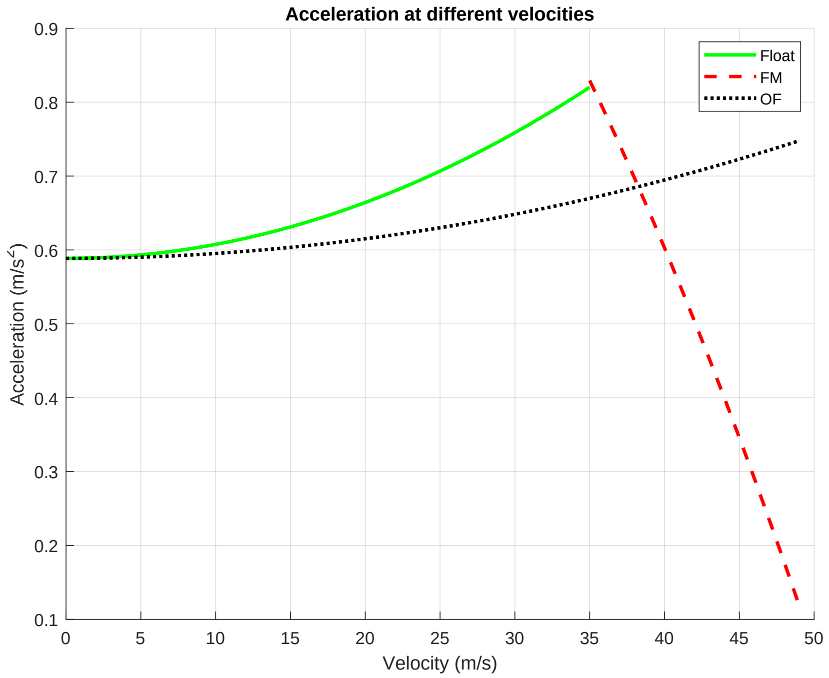

Figure 4.28: The acceleration plotted against the velocity for FM at 35 m/s

Here the net acceleration stays positive, however the calculated takeoff distance becomes $S_{35} = 2723m$ which is almost a kilometer longer than the OF mode.

45 m/s Changing the FM velocity to 45 m/s and accounting for the added lift from the aircraft gives

$$L_{hf} = 9398N$$

$$C_{L_{hf}} = \frac{9398}{0.5 * 1000 * 0.8 * (45^2)} = 0.012$$

Normalized with the a/c area

$$C_{L_{hf}} = 0.012 * \sigma^{hf} = 0.00042$$

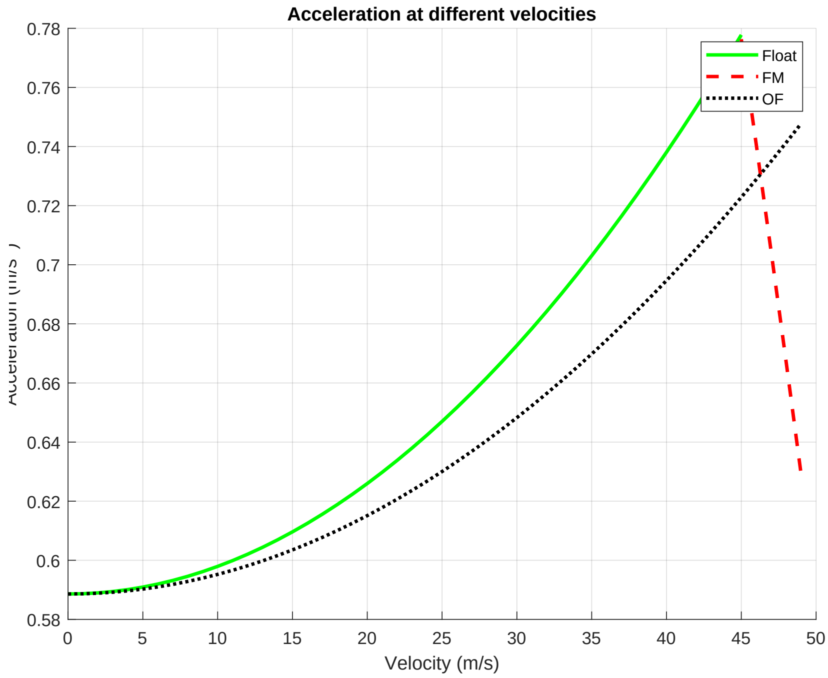

Figure 4.29: The acceleration plotted against the velocity for FM at 45 m/s

Here the takeoff distance is shorter $S_{45} = 1800m$, compared to the OF mode $S_{OF} = 1838m$. Even though the takeoff distance is marginally shorter, benefits such as smoother riding are not obtained since such a short time is spent in FM.

4.2.13 New hydrofoil design

$$\frac{T}{W} = 0.16$$

$$T = 0.16 * W = 8624N$$

Set the drag value at a reasonable number

$$D = 8000N$$

This is the wanted drag value at the takeoff velocity. From this a drag coefficient and a surface sizing can be found

$$0.5 * \rho_{air} * V_{TO}^2 * S^w * (C_{D_{a/c}} + C_{D_{hf}} * 816.33) = 8000N$$

$$C_{D_{a/c}} + C_{D_{hf}} * 816.33 = 0.2317$$

$$C_{D_{hf}} = 2.52 * 10^{-4}$$

This value might seem low, but that is because it uses the main wing area as its reference. In OpenVSP, the desired $C_{D_{hf}}$ was tried to be found by redesigning the hydrofoil and then simulating it with the airplane wing as its reference area.

4.2.14 Weight Sensitivity Study

The weight sensitivity study was performed to evaluate how the total aircraft weight changes when key design parameters are varied. The parameters included are the battery specific energy E, propulsion efficiency η, range R, empty weight fraction, crew weight, and passenger weight.

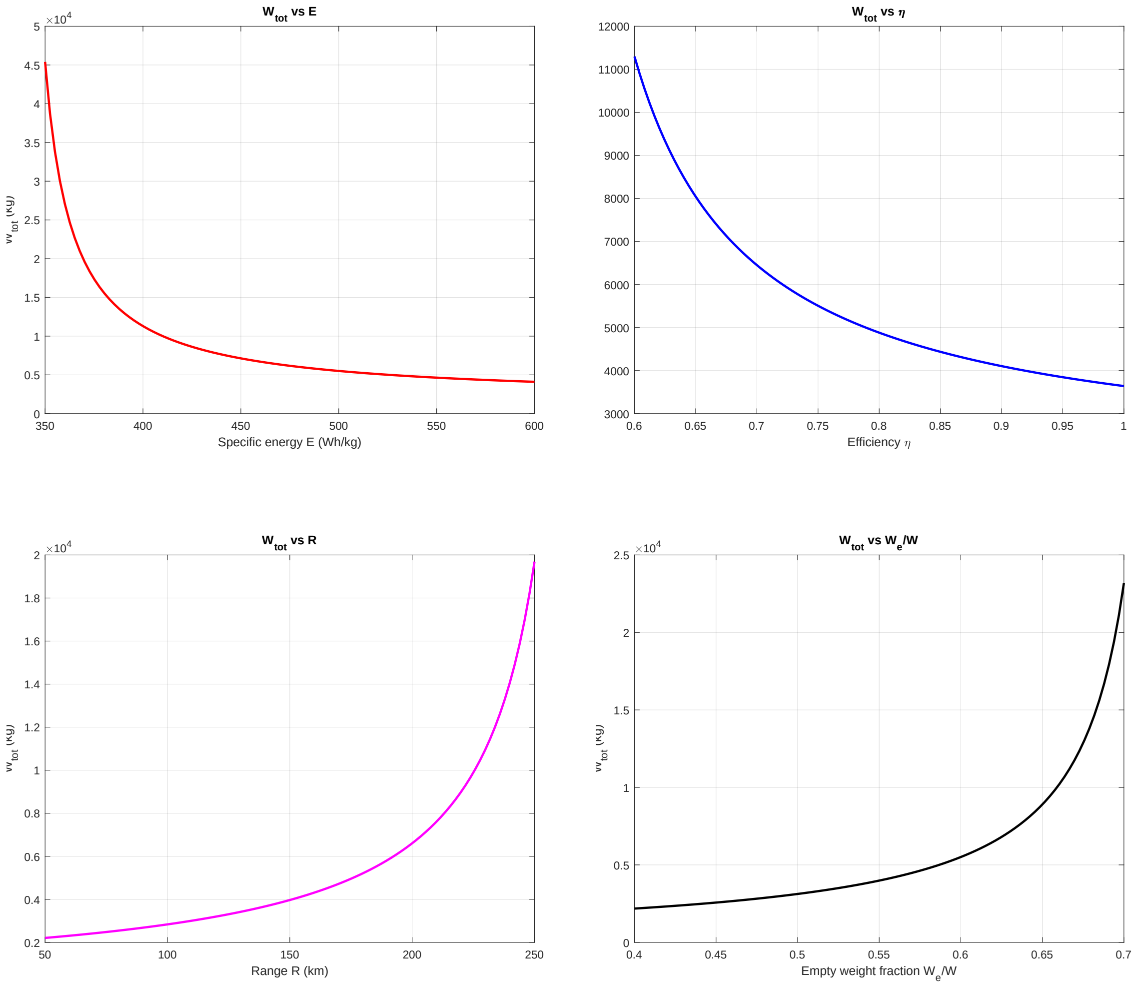

Figure 4.30: Weight sensitivity study for system-related parameters. Top left: specific energy E. Top right: efficiency η. Bottom left: range R. Bottom right: empty weight fraction.

The results show that the total aircraft weight is strongly influenced by the parameters related to the energy system and mission requirements. An increase in the specific energy E leads to a decrease in the total weight, since a lower battery mass is required to achieve the same range. A similar thing happens for the efficiency η, where higher efficiency reduces the required energy and therefore the total weight. In contrast, the total aircraft weight increases with increasing range R, as a larger amount of energy is needed, or in other words larger batteries. The empty weight fraction shows the same trend, where a higher fraction leads to an increased total weight due to a larger structural contribution.

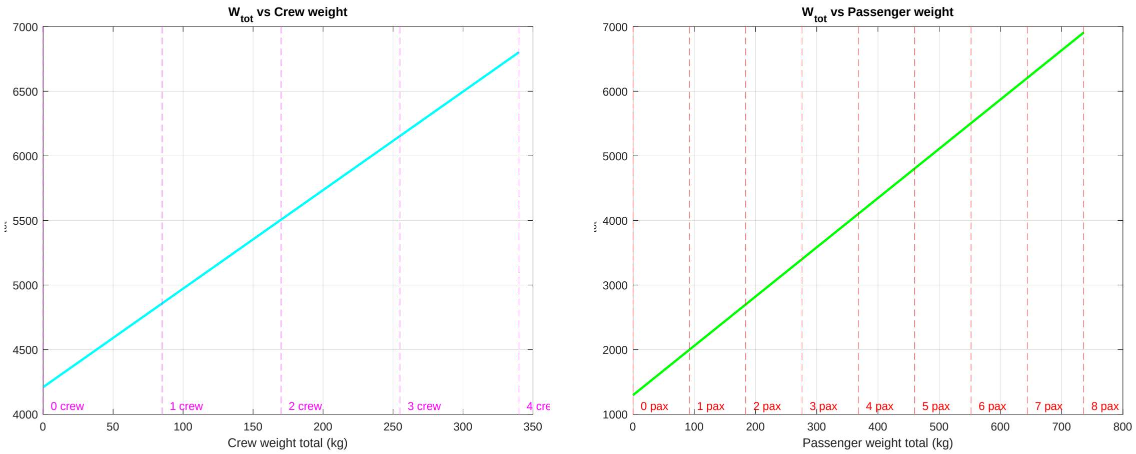

Figure 4.31: Weight sensitivity study for payload-related parameters. Left: crew weight. Right: passenger weight.

Varying the number of crew and passenger shows a direct relationship with the total weight. An increase in either crew or passenger weight results in a corresponding increase in total aircraft weight.

Weight Sensitivity Study Combined

To get an overview of all the different variables and what small changes can do for the total weight of the aircraft, the variables were all varied +- 10 %.

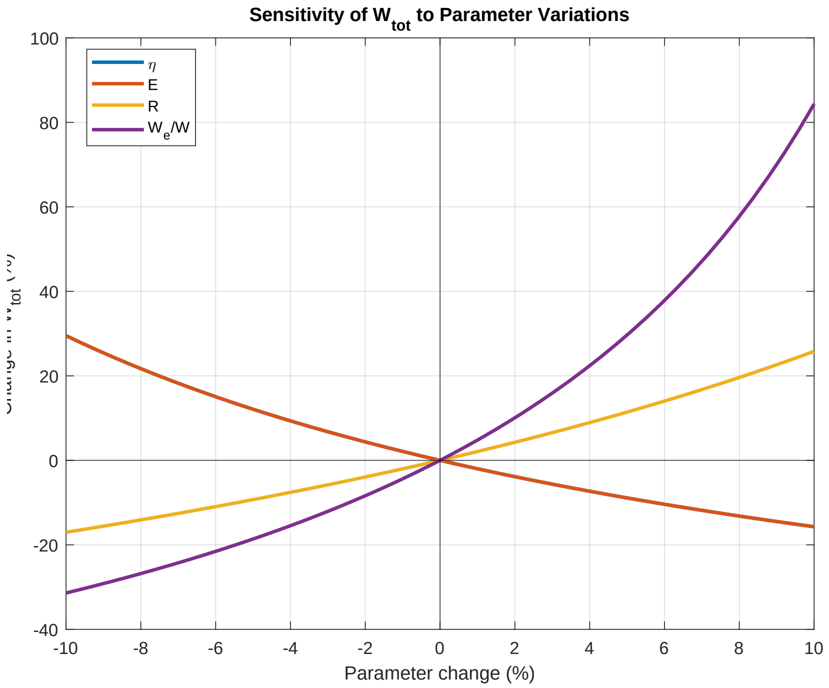

Figure 4.32: Weight Sensitivity Study +- 10%

In Fig 4.32 it is shown that the most drastic effect on the total weight would be if the empty weight changes. It can also be seen that just a 10 % increase for the specific energy could reduce the weight up to almost 20 %. On the other hand, if the specific energy isn't as good as intended and is decreased by 10 % the total weight would increase with almost 30 %. An issue here is that the graphs for the specific energy and efficiency both match which is why the graph for the efficiency is not visible. To show that their relative effects are the same, a bar chart is plotted.

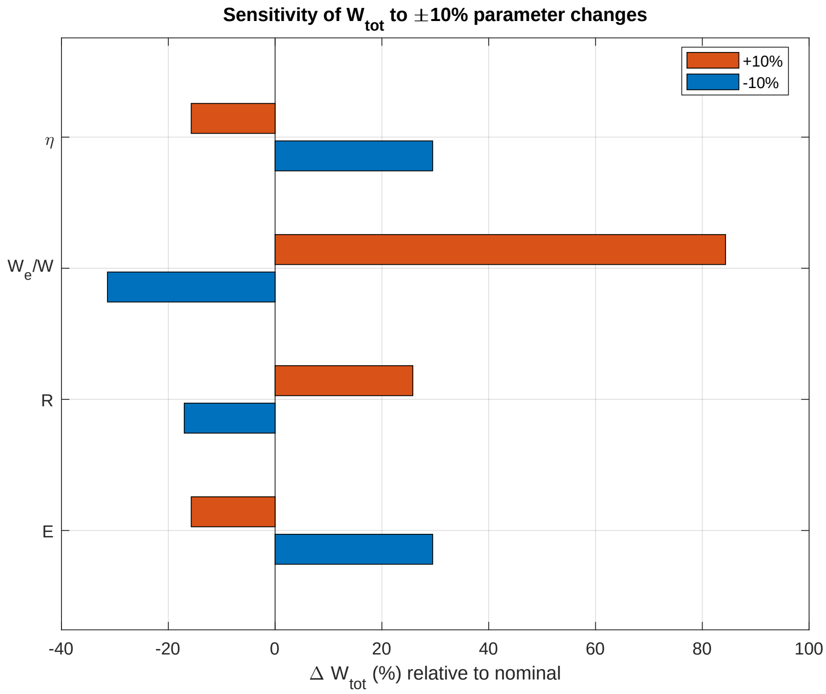

Figure 4.33: Weight Sensitivity Study Stack Diagram

In Fig 4.33 it can be seen that both the efficiency and specific energy bar are the same. It is also shown again that the variable with the highest impact is the empty weight.

4.3 Down Scaled Design for Testing

$$k_d = \sqrt{\frac{25}{5500}} = 0.067$$

Multiply the old wingloading of 49.2 psf by the scaling factor.

$$k_d * 49.2 = 3.3psf$$

From this the new wing area is calculated again.

$$S = \frac{W}{\frac{W}{S}} = 1.56m^2$$

The old wing width to fuselage length ratio is calculated, and then the drone fuselage length is calculated.

$$\frac{L_{fus}}{b_{a/c}} = \frac{L_{drone}}{b_{drone}}$$

$$L_{drone} = \frac{12}{14} * 3.6 = 3.1m$$

For the vertical and horizontal tail sizing, they are also found by multipling K_d with thier original surface areas.

$$S_{vt} = k_d * 3.3 = 0.2211$$

$$S_{ht} = k_d * 3.7 = 0.2479$$

Table 4.20: Down Scaled Main Wing Geometric and Aerodynamic Data

Parameter	**Value**
Span [m]	3.6
Area [m^2]	1.56
Aspect ratio	8.3
Tip chord [m]	0.22
Root chord [m]	0.60
Average Taper	0.915
Sweep [deg]	0
Incidence [deg]	3.5
Airfoil	NACA 4412
Dihedral [deg]	0
Mean Aerodynamic Chord (MAC) [m]	0.46
Ailerons	
Chord fraction	0.25
Span [m]	0.63
Flaps	
Chord fraction	0.25
Span [m]	0.72

Table 4.21: Down Scaled Vertical Tail Geometric Data

Parameter	**Value**
Vertical Tail Length (L_{VT}) [m]	1.5
Span [m]	0.6
Area [m^2]	0.225
Aspect ratio	1.63
Tip chord [m]	0.26
Root chord [m]	0.49
Average Taper	0.85
Sweep [deg]	20
Airfoil	NACA 0015
Mean Aerodynamic Chord (MAC) [m]	0.38
Rudder	
Area [m^2]	0.06
Fraction of Vertical Tail chord	0.46

Table 4.22: Down Scaled Horizontal Tail Geometric Data

Parameter	**Value**
Span [m]	0.83
Area [m^2]	0.25
Aspect ratio	2.76
Tip chord [m]	0.20
Root chord [m]	0.40
Sweep [deg]	15
Incidence [deg]	-3.9
Airfoil	NACA 0015
Elevator	
Elevator Area [m^2]	0.054
Fraction of Horizontal Tail chord	0.36

The needed displacement volume is again calculated.

$$V_{requierd} = \frac{W}{\rho_{water}} * 1.2 = 0.03m^3$$

The fuselage is then adjusted to obtain a close value to the desired displacement volume.

Table 4.23: Down Scaled Fuselage and Hull Geometric Data

Parameter	**Value**
Fuselage Length [m]	3.1
Maximum Diameter [m]	0.5
Hull Dimensions:	
Beam [m]	0.5
Forebody Length [m]	1.18
Afterbody Length [m]	0.315
Tail Extension [m]	0.253
Waterline Length [m]	1.495
Draft [m]	0.06
Estimated Displacement Volume [m^3]	0.04

The hydrofoils are also downscaled to match the downscaled aircrafts size.

Table 4.24: Down Scaled Hydrofoil Geometric Data

Parameter	**Value**
Span [m]	0.56
Area [m^2]	0.054
Aspect ratio	5.83
Tip chord [m]	0.086
Root chord [m]	0.1
Sweep [deg]	0
Incidence [deg]	5.5
Airfoil	NACA 4412

Table 4.25: Down Scaled Hydrofoil Tail Geometric Data

Parameter	**Value**
Span [m]	0.29
Area [m^2]	0.0135
Aspect ratio	6.1
Tip chord [m]	0.04
Root chord [m]	0.052
Sweep [deg]	0
Incidence [deg]	0
Airfoil	NACA 0012

5
Discussion and Conclusion

5.1 Summary

The aim of this thesis was to develop a conceptual design for a hydrofoiling electric seaplane and to investigate if it is a viable solution to have only a static hydrofoil to reduce the takeoff distance. The conceptual design of the hydrofoiling seaplane was developed following Raymers[6] and Riboldis[7] methodologies. The aerodynamic surfaces, their sizing, layout and performance estimations were all derived from the initial requirements and whishes for the aircraft's mission and environment. The final conceptual design features a high wing, monoplane with a conventional T-tail and two hydrofoils for use during its foiling mode.

5.1.1 Development of 1st Iteration

The initial design was developed with Hydraerospace requirements and whishes as guidelines. The final design ended up as a 9.3 ton, 12.8 meter long with a 15 meter wingspan aircraft.

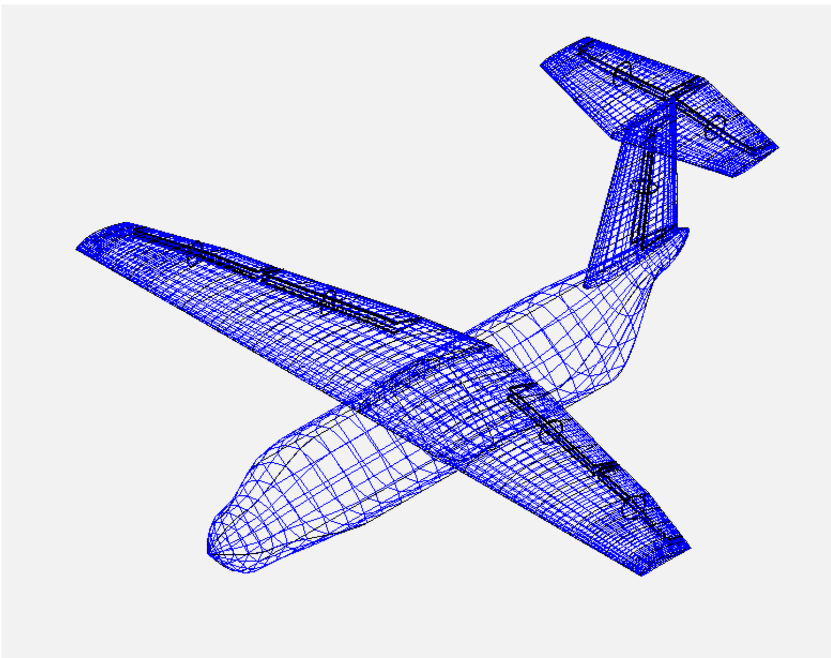

Figure 5.1: OpenVSP model of the 1st iteration of the aircraft

5.1.2 Development of 2nd Iteration

For the second iteration, the guessed $\frac{L}{D}$ was increased based on $\frac{L}{D}$ simulations from the 1st iteration, this resulted in the 2nd iteration weighing only 58.8% of the first iterations weight. The second iteration followed the same design methodology as the first iteration and its design was kept as similar to the first iteration as possible. The design for the second iteration ended up with a weight of 5.5 ton, a 12 meter long fuselage and a 14 meter wingspan.

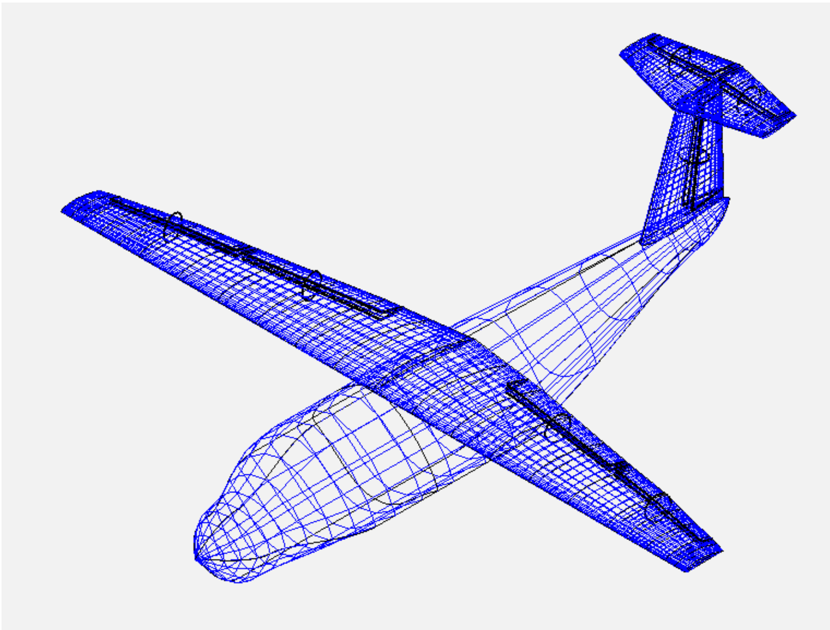

Figure 5.2: OpenVSP model of the 2nd iteration of the aircraft

5.1.3 Hydrofoil Stability and its Effect on the Aircraft in the Air

The main hydrofoil was not able to be stabilized with the aerodynamic surfaces of the aircraft. The required surface area of the aircraft tail would have needed to be almost 49 square meters, which is more than twice that of the main wing of the aircraft. Instead, a hydrofoil tail was added to obtain static stability during foil mode. The hydrofoils appeared to have little or no effect on the behavior of the aircraft in the air.

5.1.4 Takeoff Analysis

The calculated takeoff distance for the aircraft with the hydrofoil did not give a shorter takeoff distance. Instead, high values were needed for the $\frac{T}{W}$ and for the $\frac{L}{D}$ of the hydrofoil to even get the hydrofoil aircraft of the water and into the air. Even if these values could be achieved, the calculated takeoff distance for the hydrofoil aircraft was still longer than for the conventional seaplane. However, changing the velocity at which the aircraft goes into its foil mode, could at best, give a slightly shorter takeoff distance.

5.1.5 Weight Sensitivity Study

The weight sensitivity study shows that the total weight of the aircraft can change a lot from its current weight from even small changes to its dependent variables.

5.1.6 Down Scaled 25 kg Drone

The aircraft design was down scaled to 25 kg through a ratio created between the original weight and the down scaled weight. It has a wingspan of 3,6 meters and a body length of 3,1 meters.

5.2 Discussion

The final conceptual design of the aircraft is quite simple with no change of airfoil along the span of the wing or the tail, no wing twist and a very simple taper. All of these design aspects could of course be changed and improved upon, but the design still looks and gives appropriate values for its intended mission. Also, the main purpose of this project is not to design a perfect seaplane, it is to investigate if a hydrofoil seaplane is a feasible idea and give a conceptual design on how it might look. One of Hydroaerospaces questions was to see if the main hydrofoil could be stabilized with the aircraft aerodynamic surfaces alone. The main hydrofoil was initially stabilized with a hydrofoil tail, and from that the needed aircraft tail size was calculated. The needed aircraft tail size was almost 49 square meters. Remember that this value is calculated with some simplifications. However, it still shows that the a/c would need to be incredibly big to stabilize the hydrofoil alone. This is not doable, since the a/c tail would need to be more than twice as large as the a/c wing.

Another question from hydroaerospace was if using a hydrofoil for takeoff would decrease the takeoff distance when taking of from water, since seaplanes and flying boats typically have a longer takeoff distance than land based a/c. When calculating the takeoff distance using Raymers methods[6], it was found that the thrust to weight was not enough to accelerate the aircraft up to the required speed during takeoff for the foiling mode. Looking at the drag, a majority comes from the hydrofoil. To solve this issue, either the Thrust-to-weight could be increased, which would require heavier and larger batteries, or the drag from the hydrofoil could be reduced. Even if a higher thrust to weight value or a decrease in drag was possible, the hydrofoil aircraft still had a longer takeoff distance than just the aircraft as a normal seaplane taking of from water. The velocity which the aircraft entered foiling mode was also adjusted to see if it made any difference. It was found that at velocities close to the takeoff velocity of the aircraft, the hydrofoil gave a marginally shorter takeoff distance. However, from this, benefits like smoother takeoff or taxiing are not obtained since such short amount of time is spent in the foiling mode before the aircraft gets airborne.
However, after further discussion on the topic it was found that there are some errors in the way the hydrofoil case was implemented into the take off formula. It was assumed that after the aircraft reached high enough velocity for the hydrofoil to

produce enough lift, the hydrofoil would just stay underwater. This in combination with the requirement to not have any control surfaces on the hydrofoils meant that as the velocity and lift increases, the drag also increases in relation to that. This is what gave the surprising take off and acceleration results for the aircraft in foiling mode. In reality the aircraft would probably just skip of the water surface since when the hydrofoils leave the water their lift decreases which drops them back down into the water again where their lift increases, and so on... For the hydrofoil case to work, the lift coefficient for the hydrofoil would need to be reduced by either using control surfaces or decreasing the angle of attack, just like for a normal aircraft. The problem in this case is as stated earlier that hydroaerospace did not want to have any mechanisms in the hydrofoils, meaning that control surfaces or changing the angle of attack are not an option. If the lift coefficient could be reduced as the velocity increases to maintain the proper lift force, the takeoff distance would probably be shorter, which is intuitive thought. So even if the calculation was not entirely correct, it still showed that the idea of using static hydrofoils would not be possible.

The sensitivity study done on the weight on the aircraft shows clearly what the effects would be if there were changes in requirements or if the estimations for future technology would be off by a few percentage. It also shows the potential in better batteries and more efficient systems, where changes in specific energy and efficiency can have large effects on the total weight of the aircraft. If the airplane could be made lighter from changing the dependent variables, the whole aircraft size would decrease. Another possibility from for example increasing the specific energy or efficiency is to be able to increase something else, like the range or number of passengers.

Hydroaerospace wants to have the possibility to build and test the design and its takeoff performance. For this, the conceptual design was downscaled to 25 kg, which was a specification from Hydroaerospace. The downscaled aircraft was scaled through the weight, which created a ratio that gave a new wingloading and a new wing area. The rest of the aircraft was then scaled to the new wing area. However, some adjustments had to be made to the incidence angles of the wing and tail to achieve stability. Of course, the aircraft isn't exactly the same since the incidence angles are changed. However, the main reason for this downscaled design is to be able to verify the takeoff calculations. Hydroaerospace has tested this earlier with a bought rc plane which they put a hydrofoil on, which gave positive results.

5.3 Conclusion

The final design fulfilled the requirements in range, speed, payload, etc. However, the idea of using only a fixed hydrofoil and the aircraft's aerodynamic surfaces for control is not possible.

Bibliography

[1] Aeronautics Staff, Construction Department, Navy Yard, *Air Force and Trim Moments for F-5-L Seaplane*, National Advisory Committee for Aeronautics, Technical Note No. 85, Washington, D.C., 1922.

[2] R. de Vries, R. E. Wolleswinkel, M. F. M. Hoogreef, and R. Vos, "A New Perspective on Battery-Electric Aviation, Part II: Conceptual Design of a 90-Seater," in *Proc. AIAA SciTech Forum and Exposition*, Orlando, FL, USA, Jan. 2024, pp. 1–19, doi: 10.2514/6.2024-1490.

[3] F. Falkman, *Hydroaerospace Foiling Seaplane*. Hydroaerospace, [Technical Report], [Online PDF], [Accessed: Mars. 1, 2025].

[4] F. M. N. U. Khan, M. G. Rasul, A. S. M. Sayem, and N. Mandal, *Maximizing Energy Density of Lithium-Ion Batteries for Electric Vehicles: A Critical Review*, *Energy Reports*, vol. 9, no. 11, pp. 11–21, Sep. 2023. [Online]. Available: `https://www.sciencedirect.com/science/article/pii/S0306261925010864`

[5] R. E. Olson and N. S. Land, *Methods Used in the NACA Tank for the Investigation of the Longitudinal Stability Characteristics of Models of Flying Boats*, National Advisory Committee for Aeronautics, Report No. 753, Washington D.C., 1943.

[6] D. P. Raymer, *Aircraft Design: A Conceptual Approach*, 6th ed. Washington, D.C., USA: AIAA Education Series, 2018.

[7] C. E. D. Riboldi, *Flight Dynamics: Modeling, Characterization and Performance*. Bologna, Italy: Società Editrice Esculapio, 2024. ISBN: 9788893854481.

[8] C. E. D. Riboldi and S. Cacciola, *"Airplane Performance and Dynamics: Lab 14 Sizing Matrix Plot"*, Powerpoint, Department of Aerospace Science and Technology, Politecnico di Milano, Italy, AY 2024/2025.

[9] T. Pattanayak and D. Mavris, *Battery technology for sustainable aviation: A review of current trends and future prospects*, Applied Energy, Georgia Institute of Technology, Atlanta, 2022.

[10] A. G. Smith, *The Full-Scale Air Drag of Some Flying-Boat Seaplanes*, Aeronautical Research Council Reports and Memoranda No. 3082, Ministry of Supply, London: Her Majesty's Stationery Office, 1959.

[11] U.S. DRIVE Partnership, *Electrical and Electronics Technical Team Roadmap*, Oct. 2017. [Online]. Available: `https://www.vehicles.energy.gov/about/partnerships/usdrive.html`

A

Appendix A - More plots from design iterations

A.1 More Plots for 1st Iteration of only the aircraft in cruise

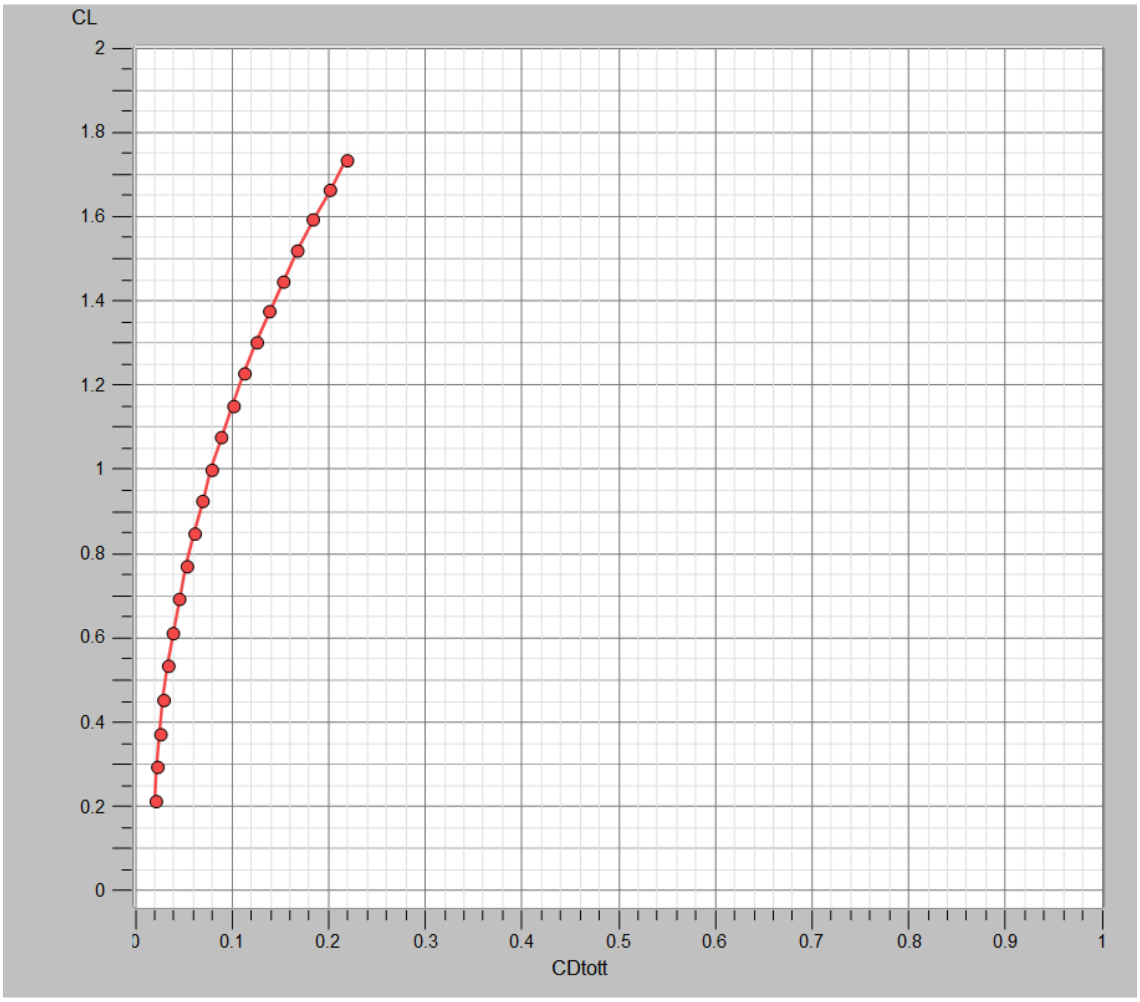

Figure A.1: C_L VS C_D curve in cruise

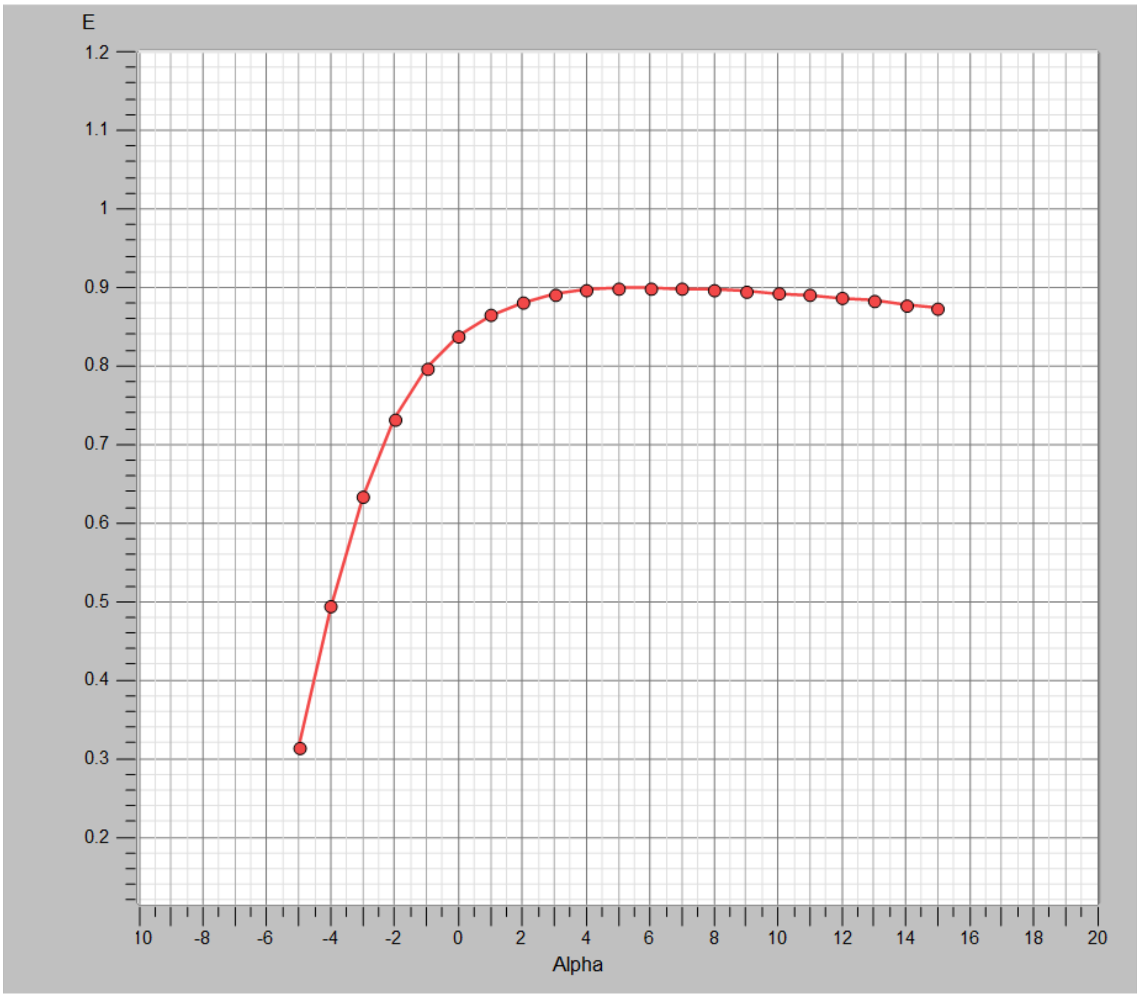

Figure A.2: Oswald factor curve

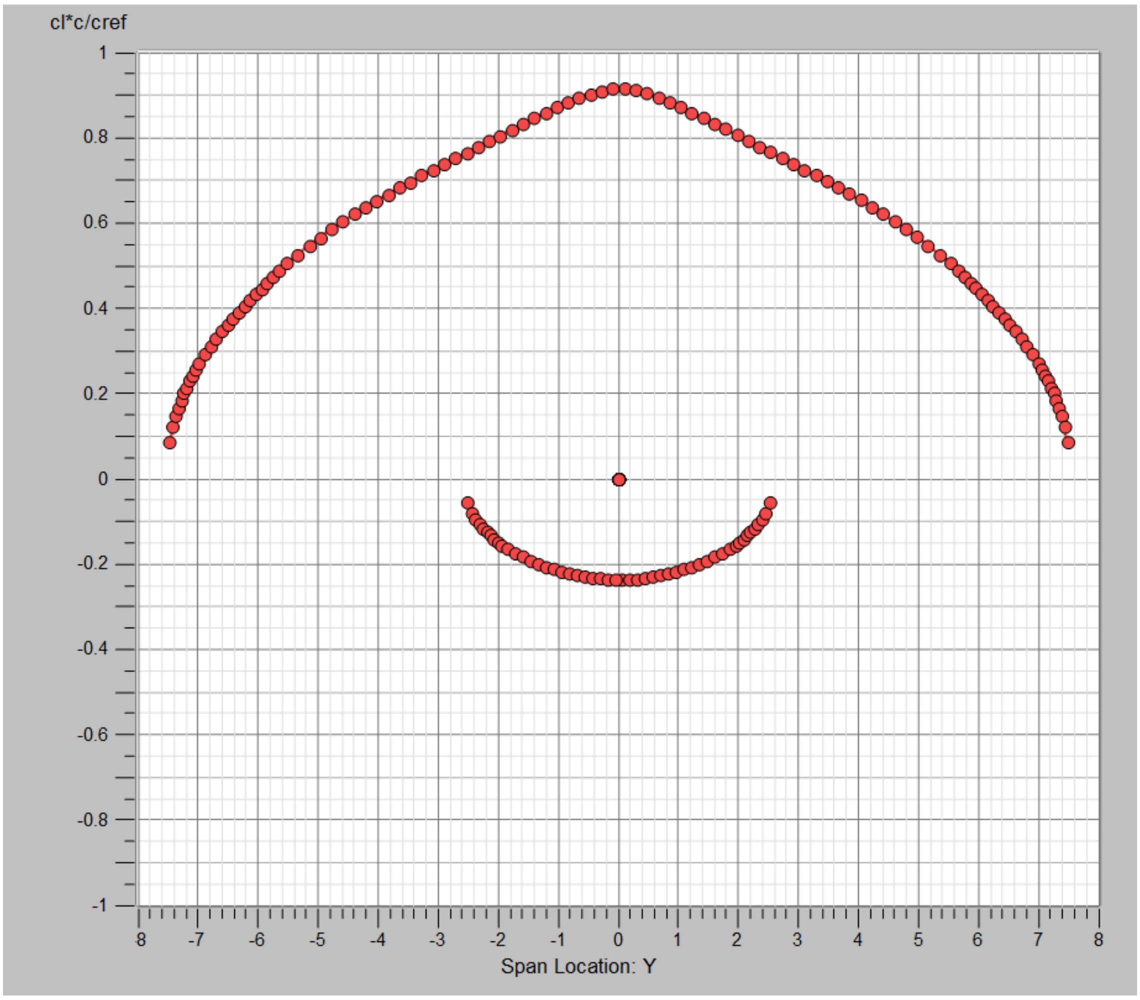

Figure A.3: Lift distribution in cruise

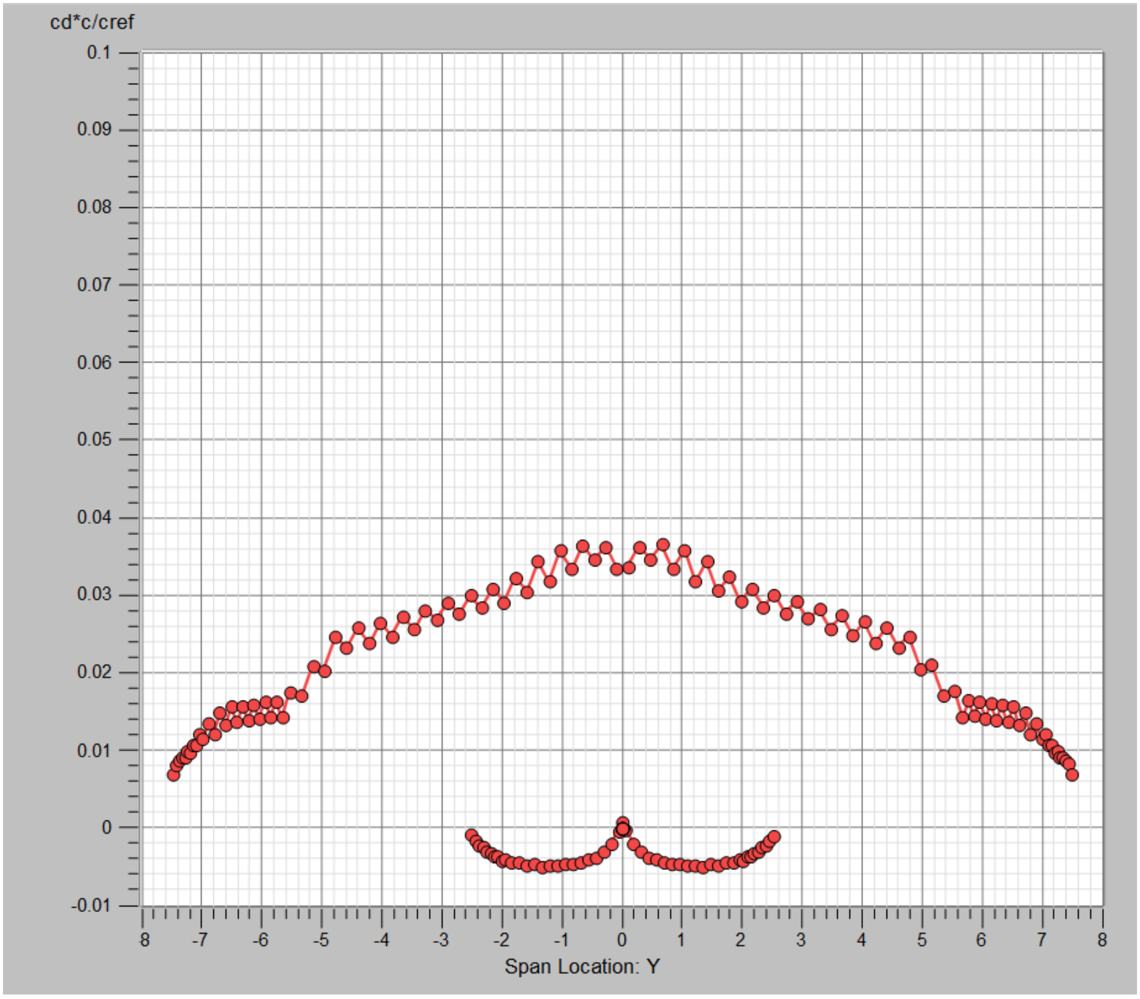

Figure A.4: Drag distribution in cruise

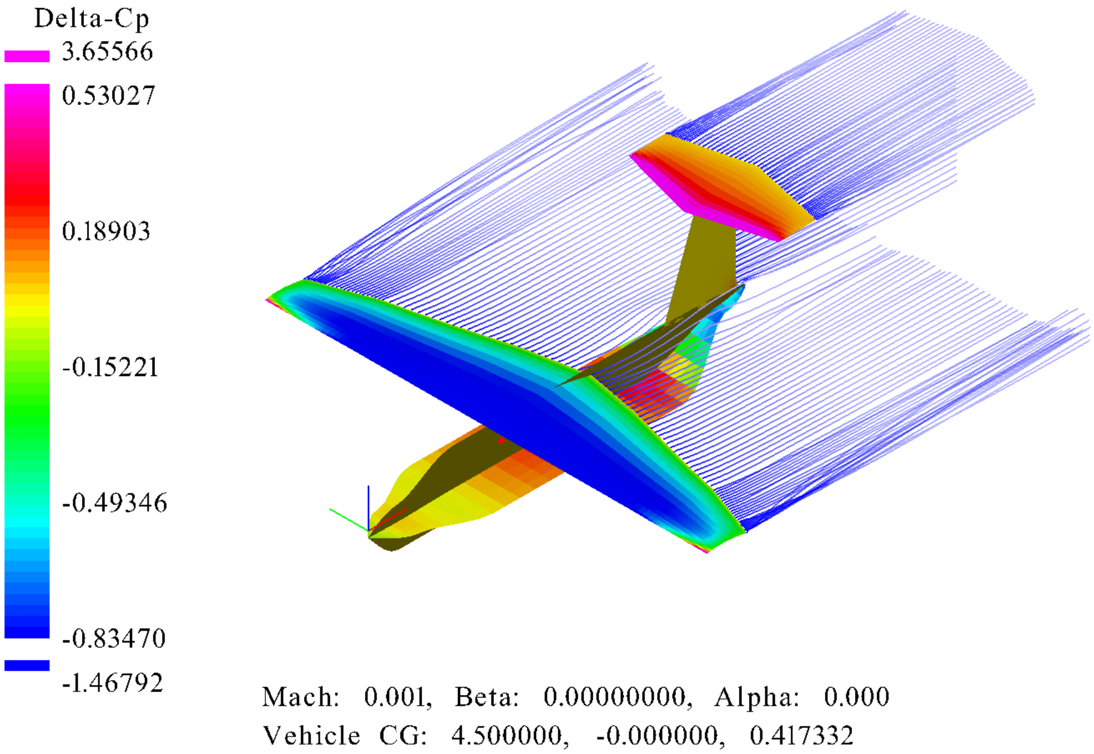

Figure A.5: Iso view pressure distribution

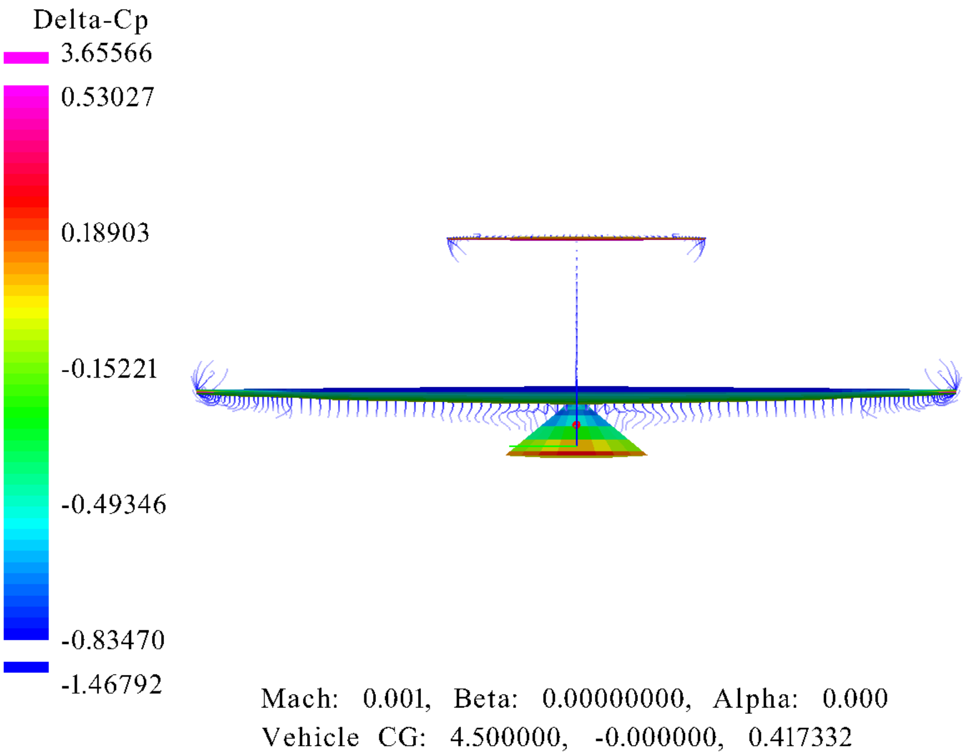

Figure A.6: Front view pressure distribution

A.2 More Plots for 2nd Iteration of only the aircraft in cruise

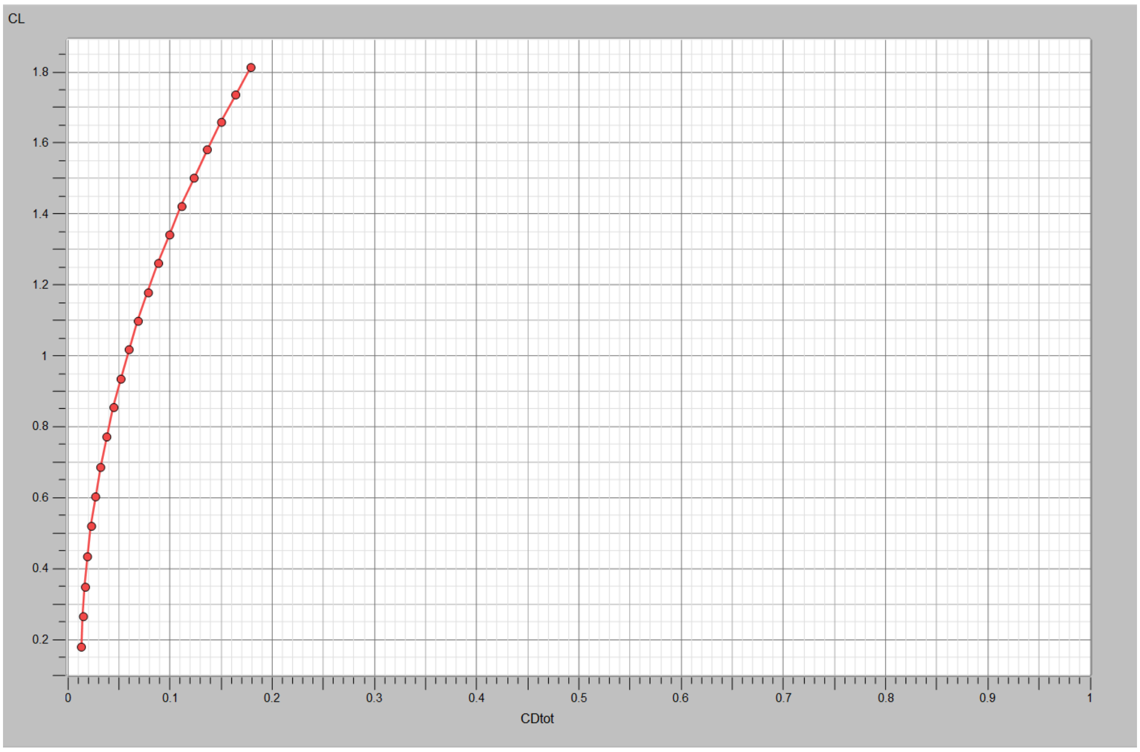

Figure A.7: C_L vs C_D curve for only the a/c in cruise conditions

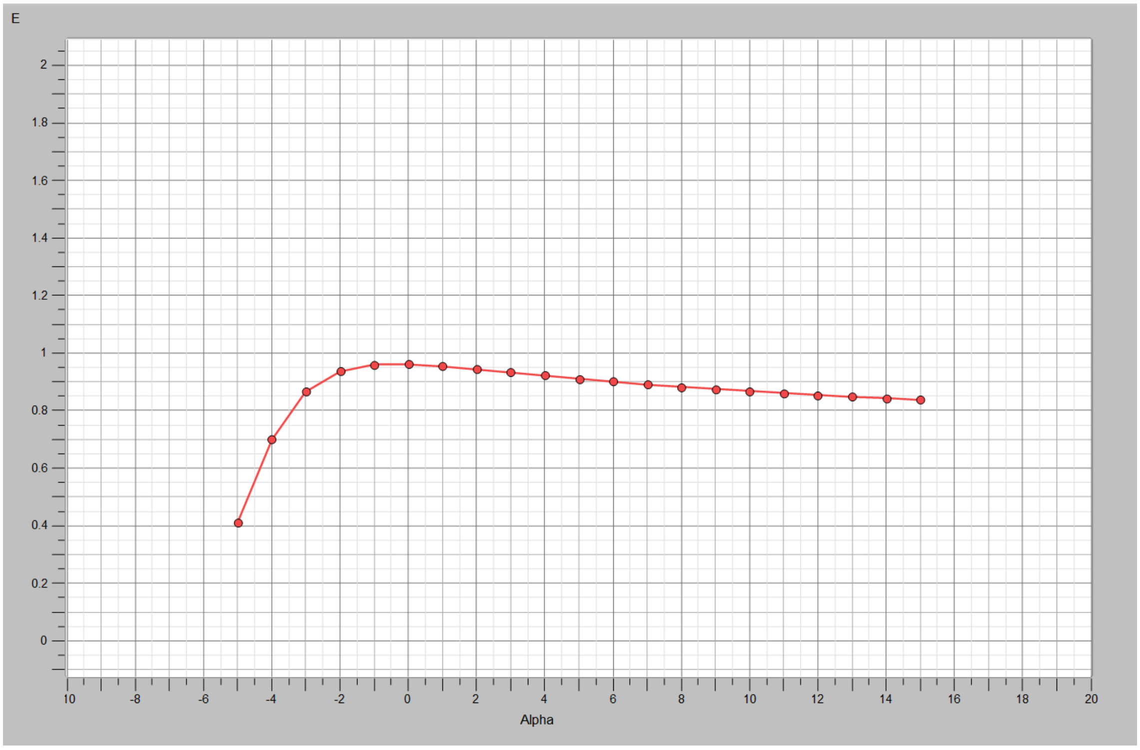

Figure A.8: Oswald Factor

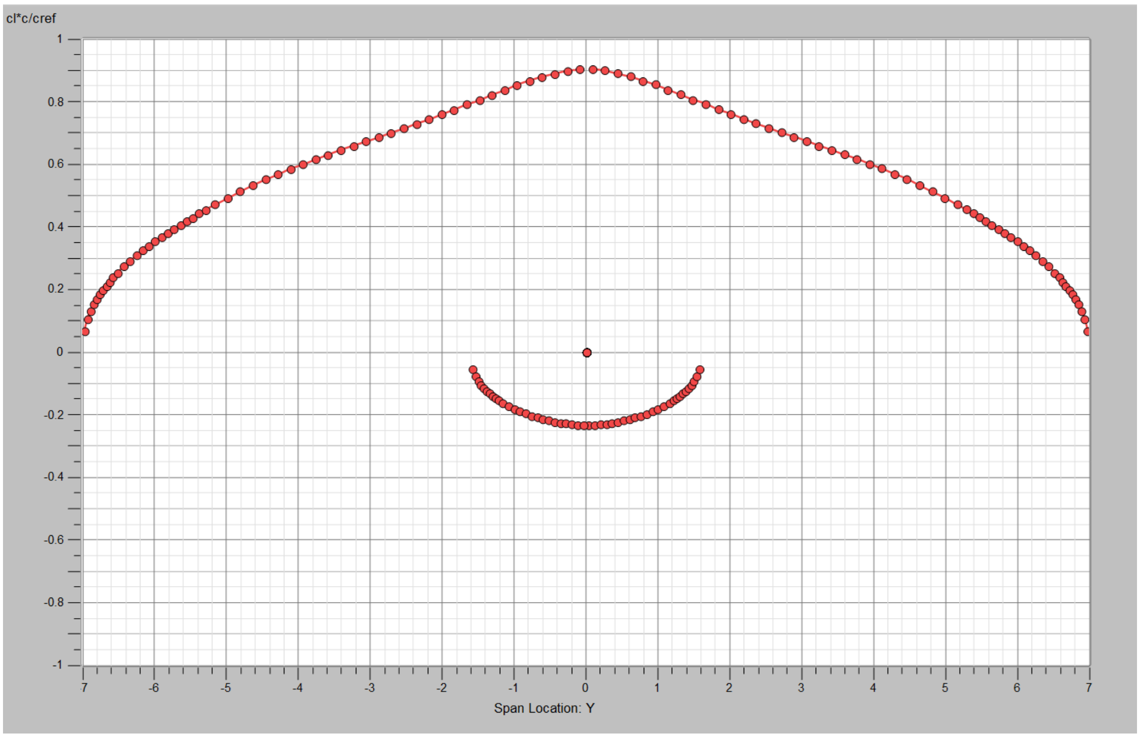

Figure A.9: Lift distribution for the a/c in cruise conditions

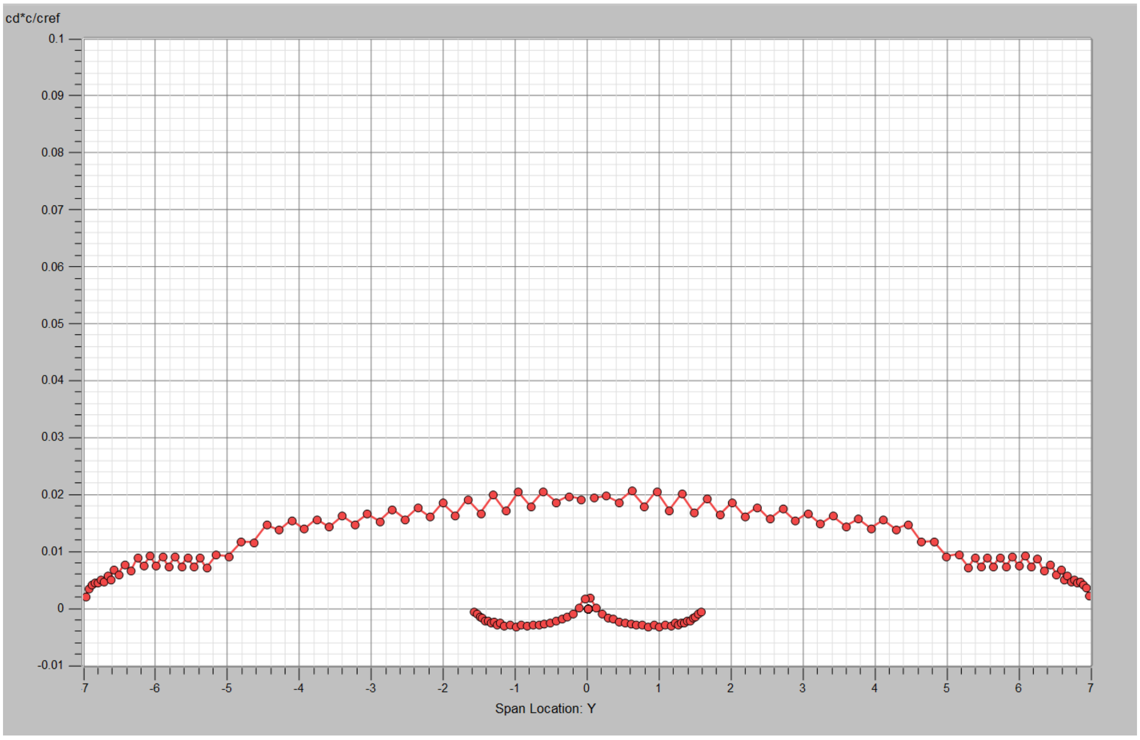

Figure A.10: Drag distribution for the a/c in cruise conditions

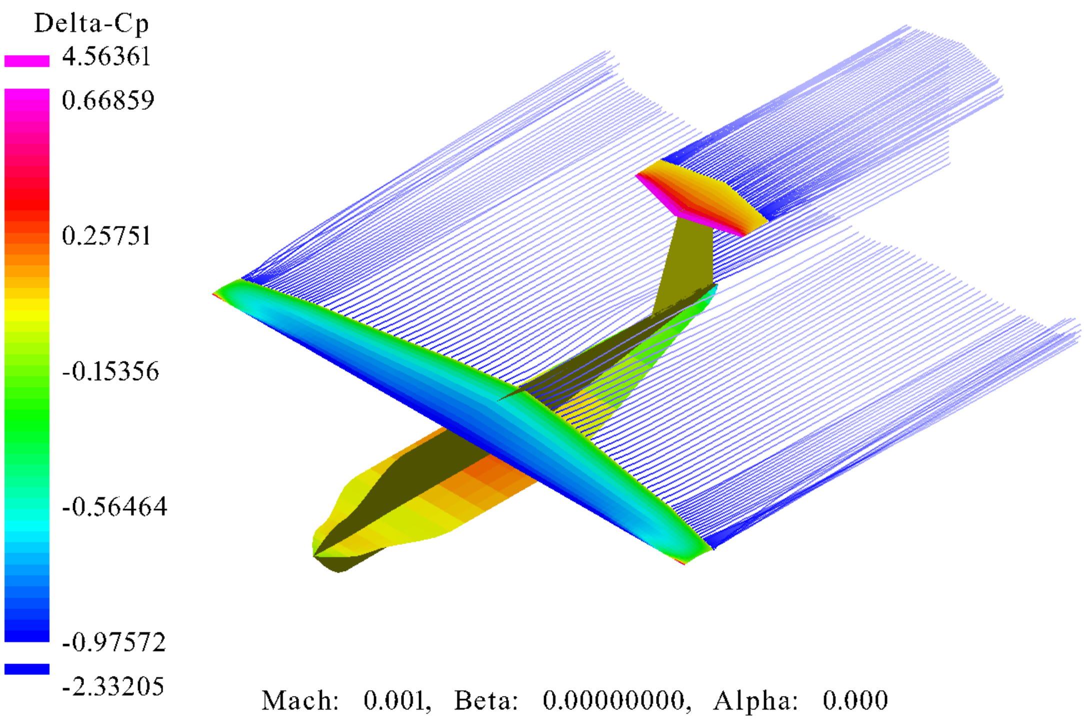

Figure A.11: Isometric view at cruise conditions with pressure distribution over the a/c

A.3 More Plots for 2nd Iteration of only the aircraft in landing

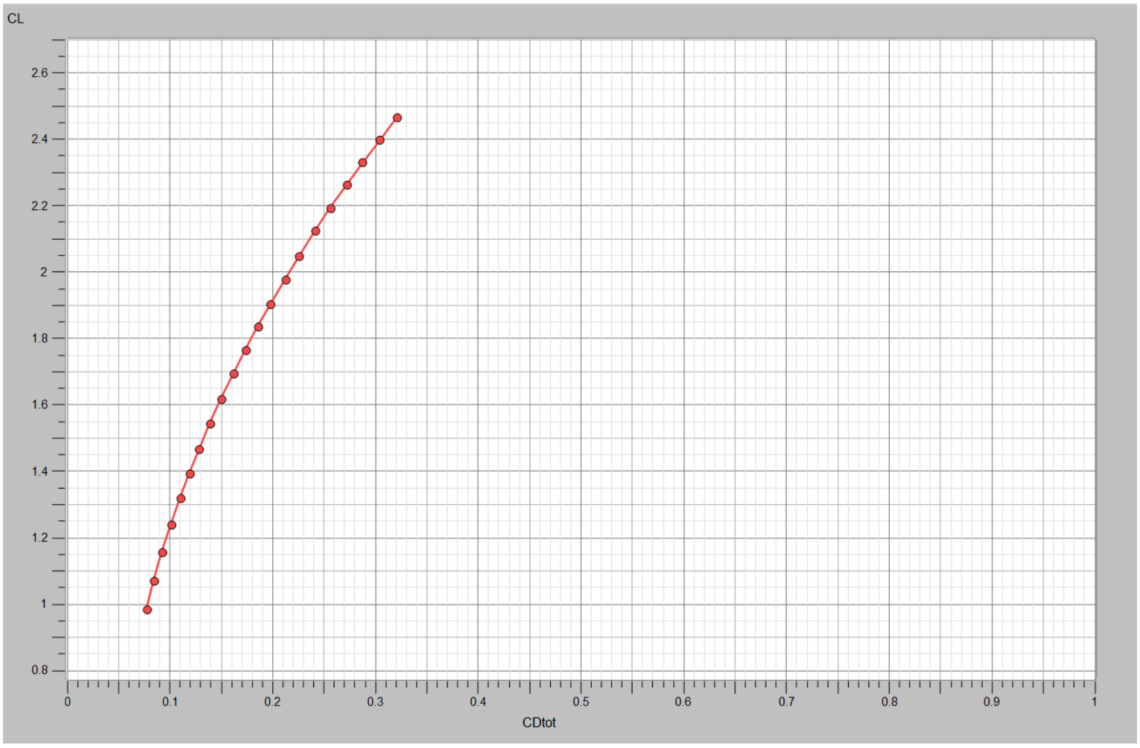

Figure A.12: C_L V C_D curve for only the a/c in landing conditions

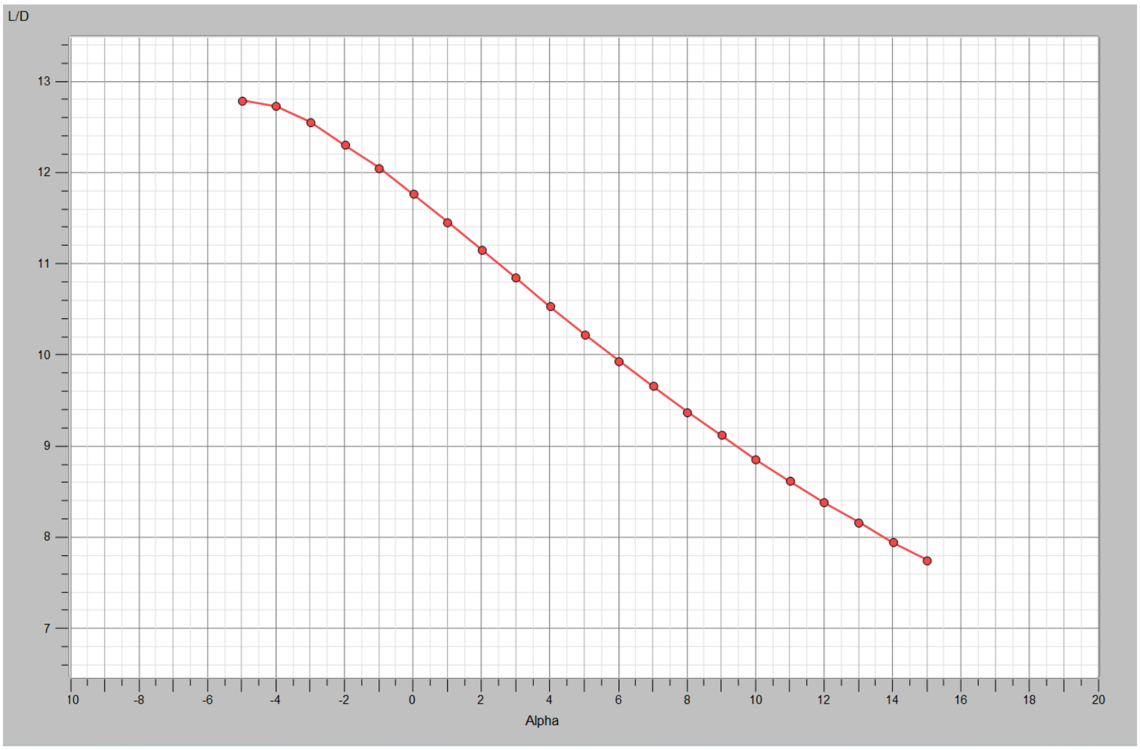

Figure A.13: Lift over Drag curve for only the a/c in landing conditions

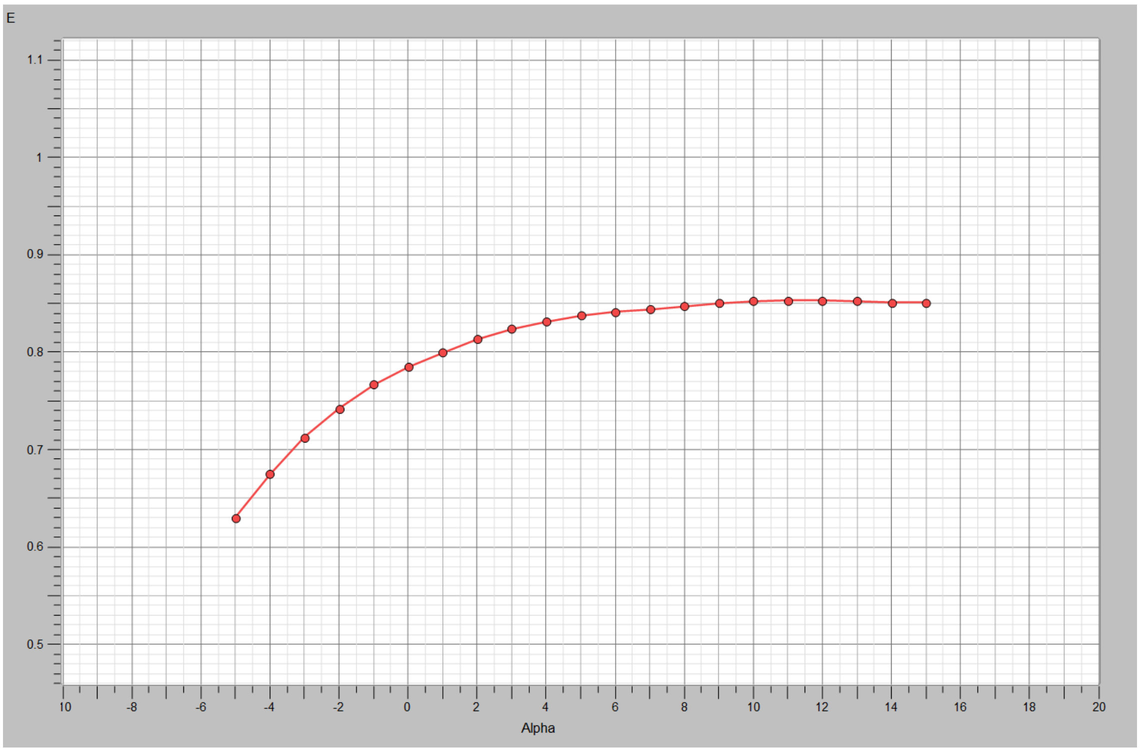

Figure A.14: Oswald Factor

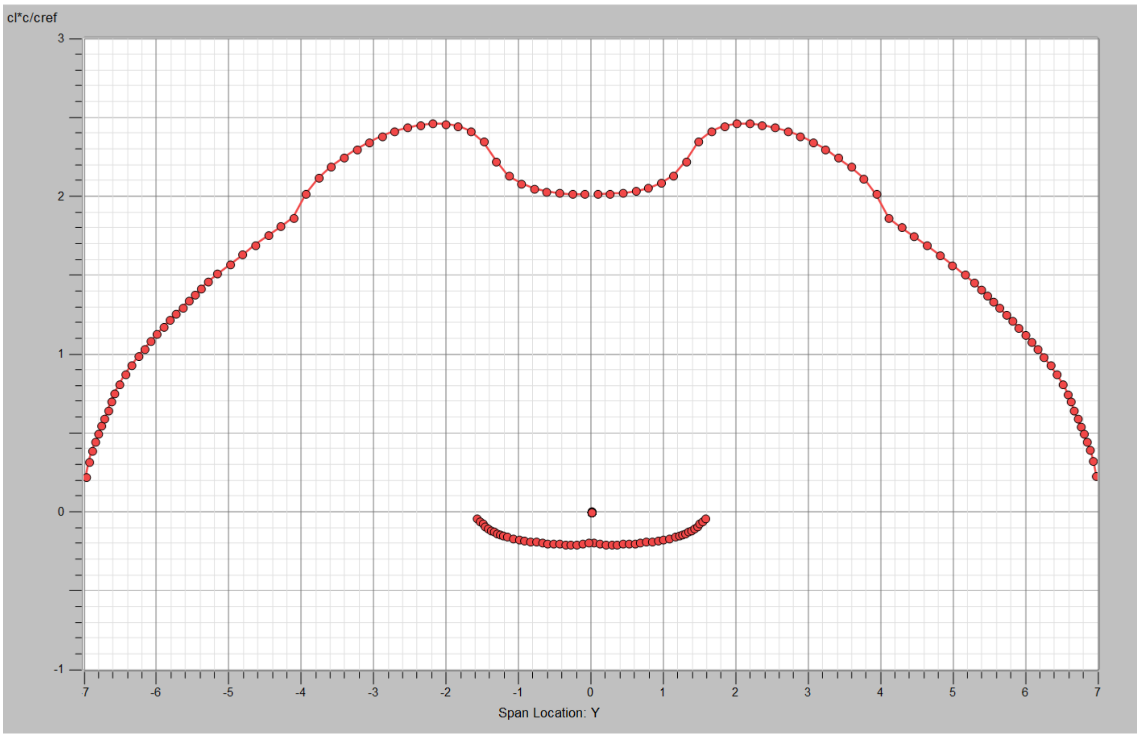

Figure A.15: Lift distribution for the a/c in landing conditions

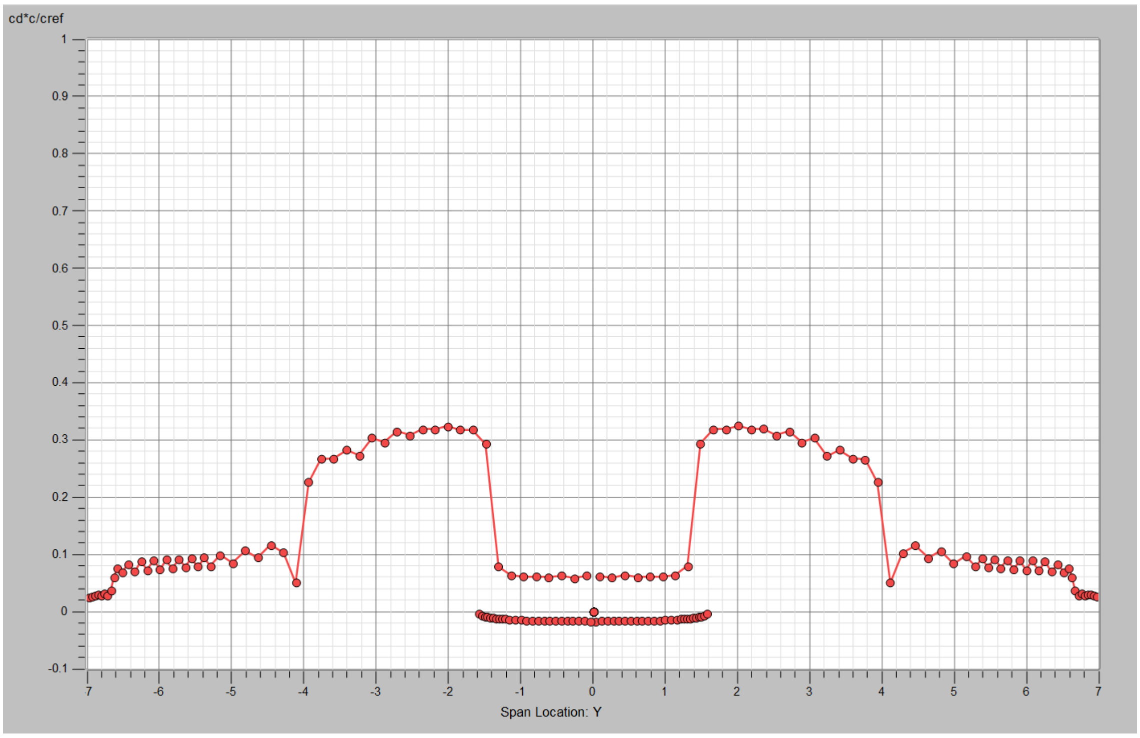

Figure A.16: Drag distribution for the a/c in landing conditions

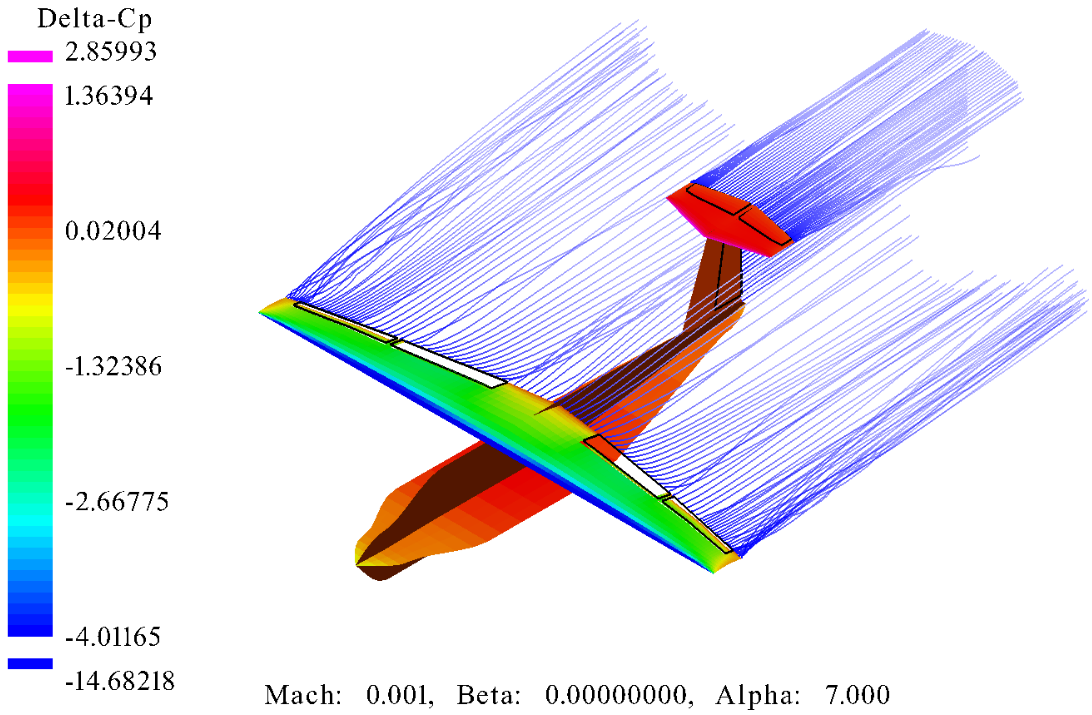

Figure A.17: Isometric view at landing conditions with pressure distribution over the a/c

A.4 More Plots for 2nd Iteration of only the aircraft in takeoff

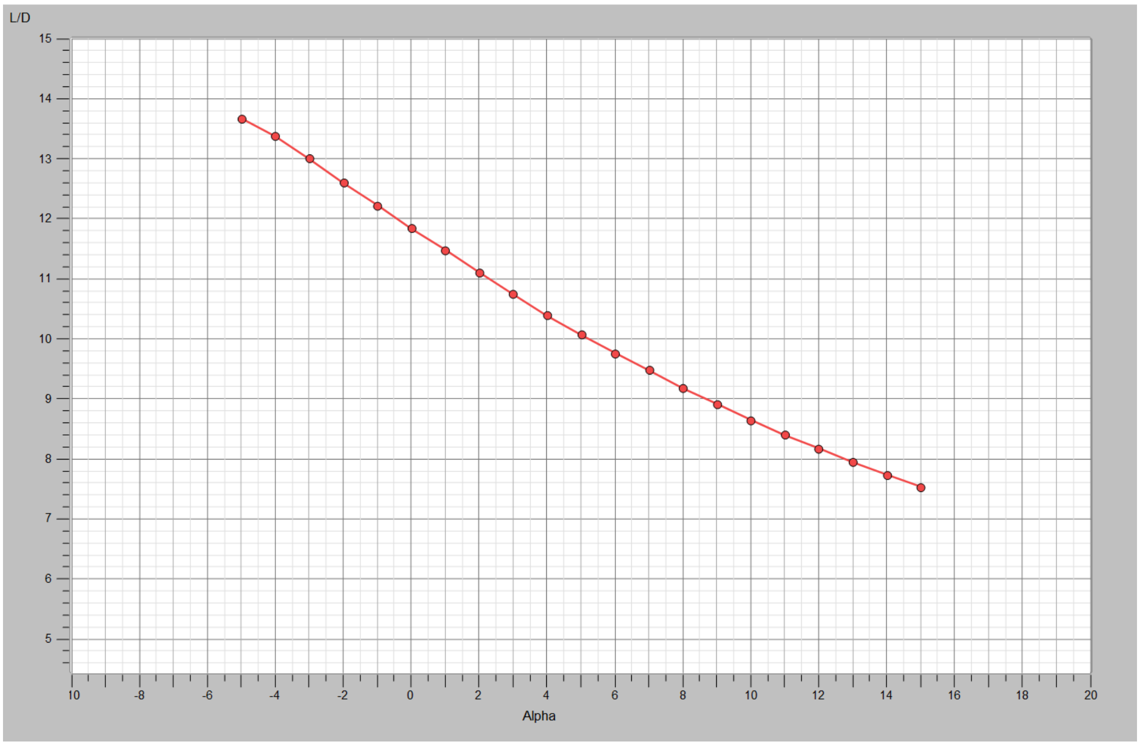

Figure A.18: Lift over Drag curve in takeoff

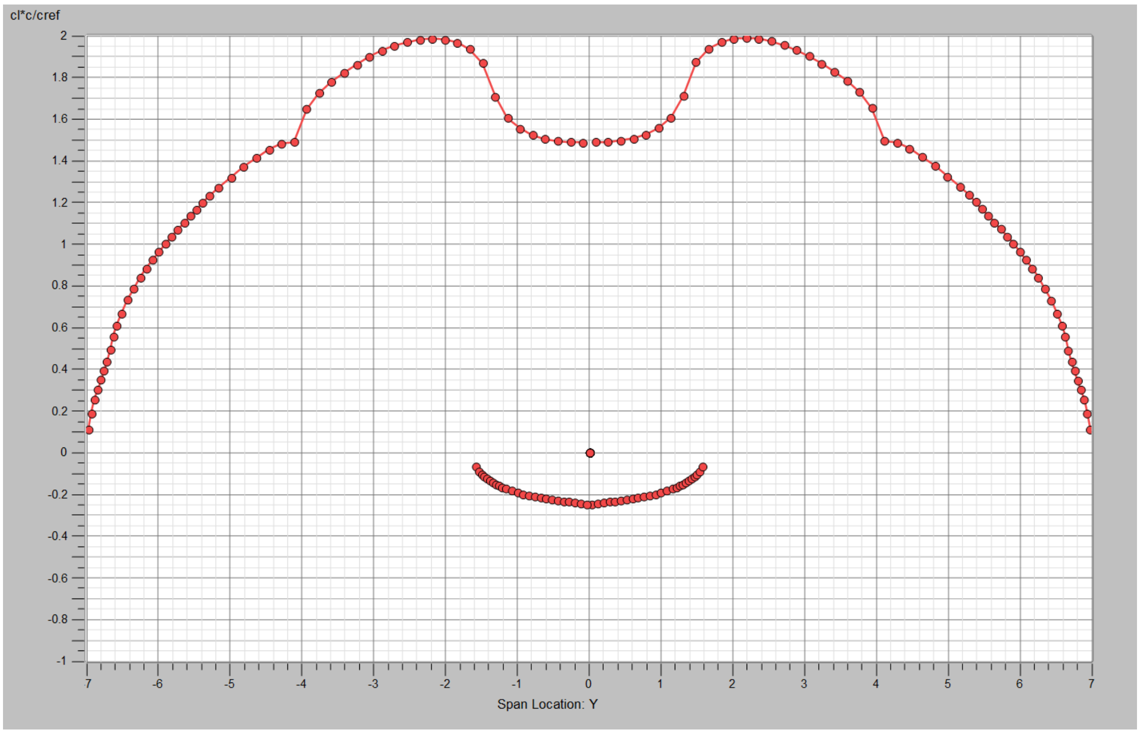

Figure A.19: Lift distribution in takeoff for a/c

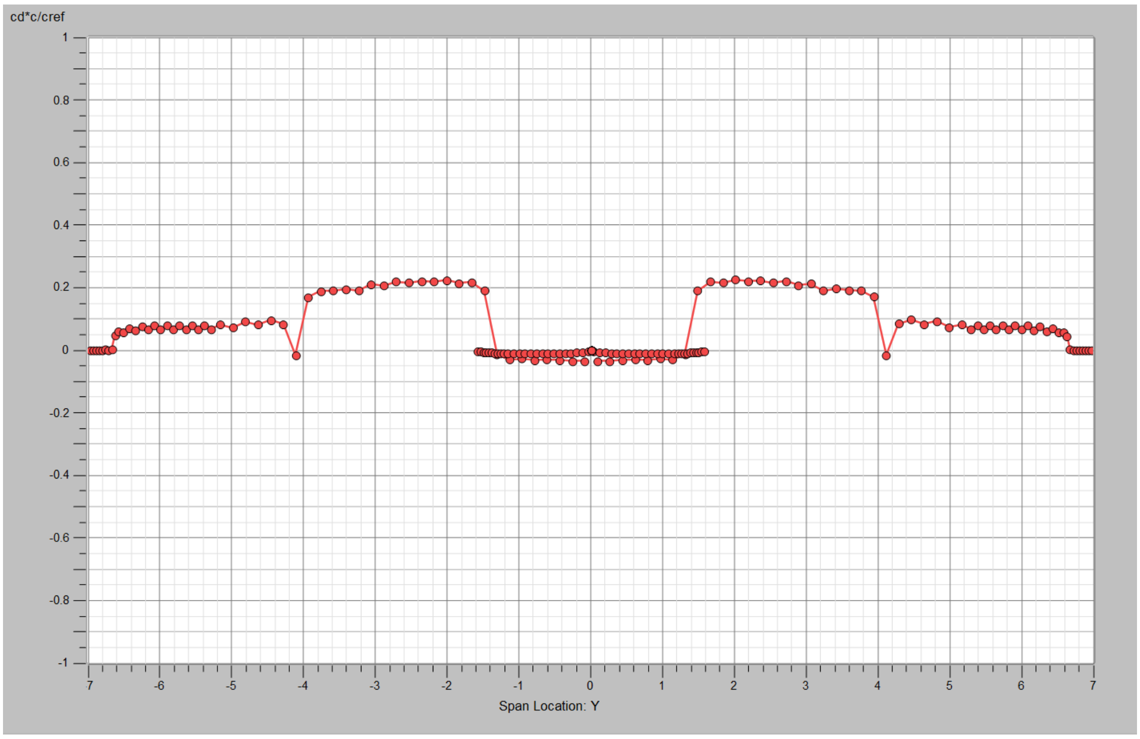

Figure A.20: Drag distribution in takeoff for a/c

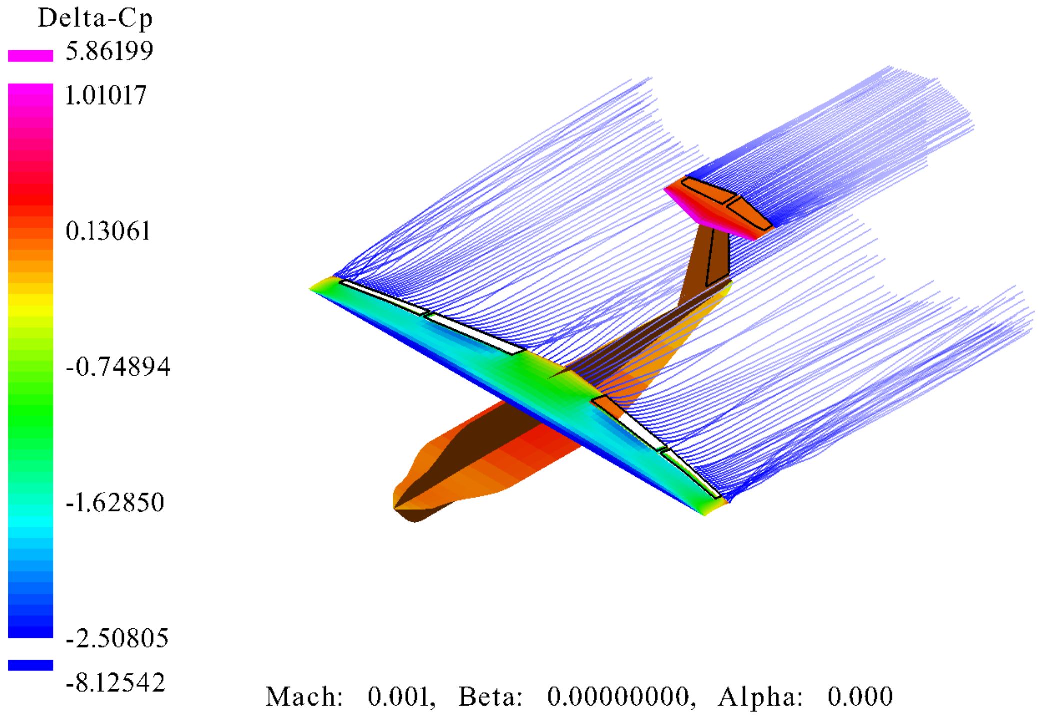

Figure A.21: Isometric view at takeoff conditions for a/c

A.5 More Plots for hydrofoil in Takeoff

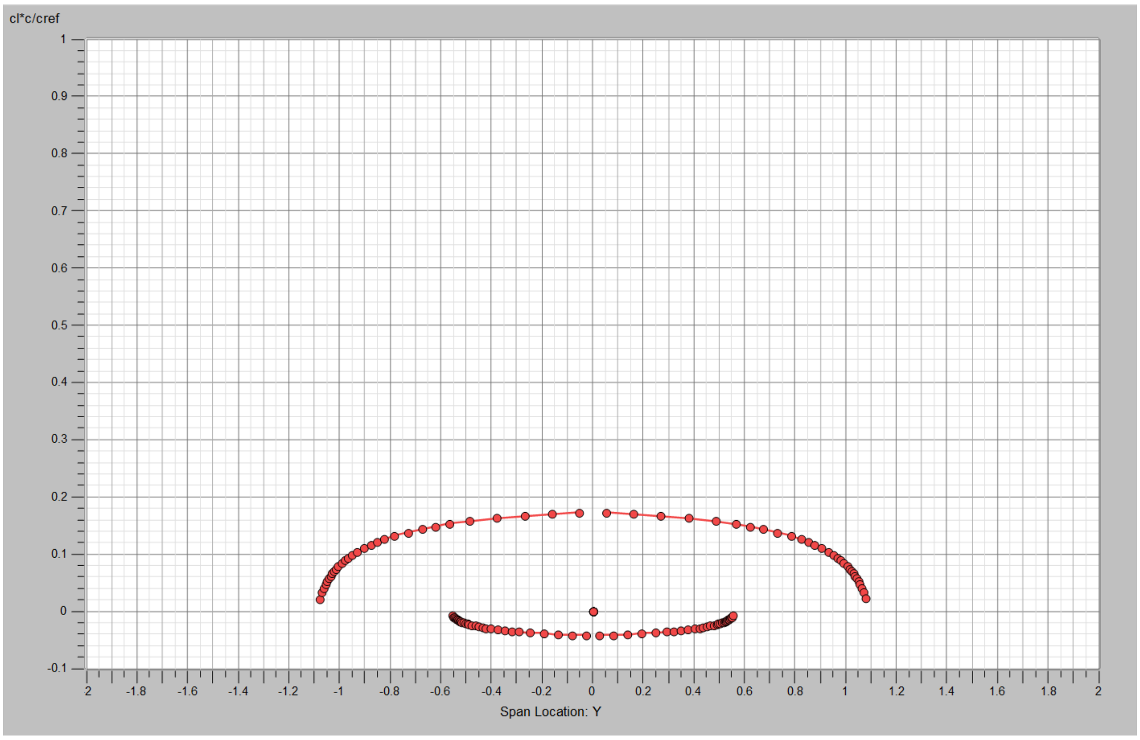

Figure A.22: Lift distribution for the hydrofoil in takeoff conditions

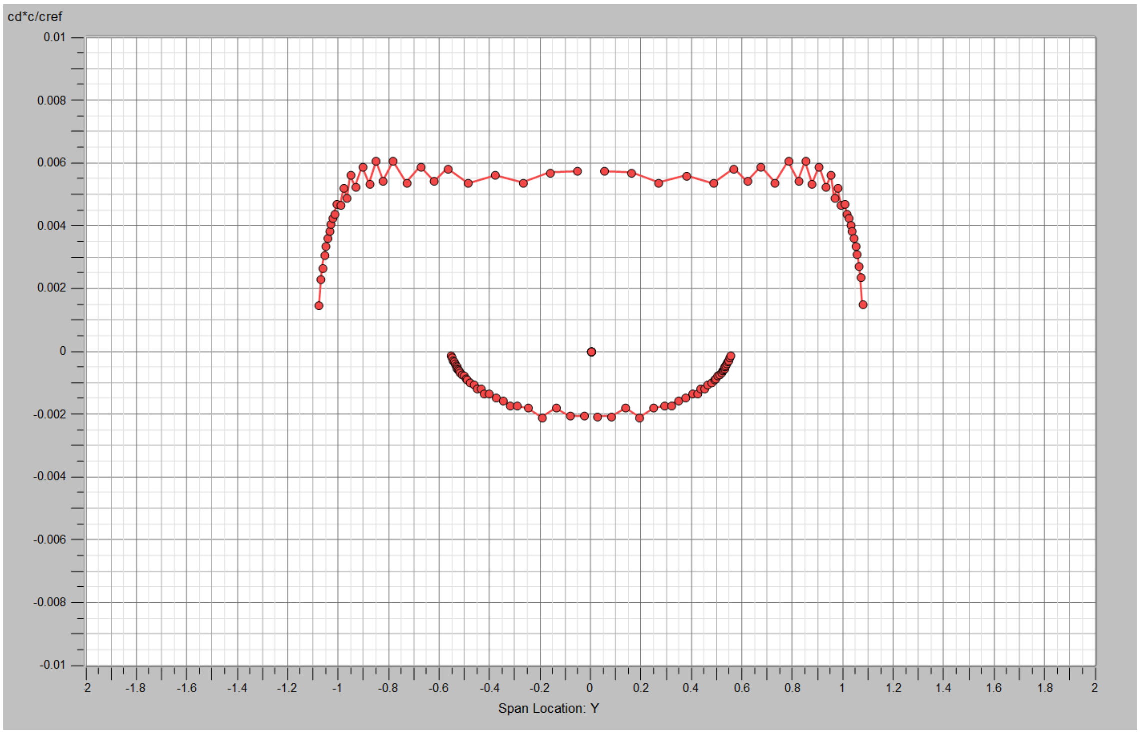

Figure A.23: Drag distribution for the hydrofoil in takeoff conditions

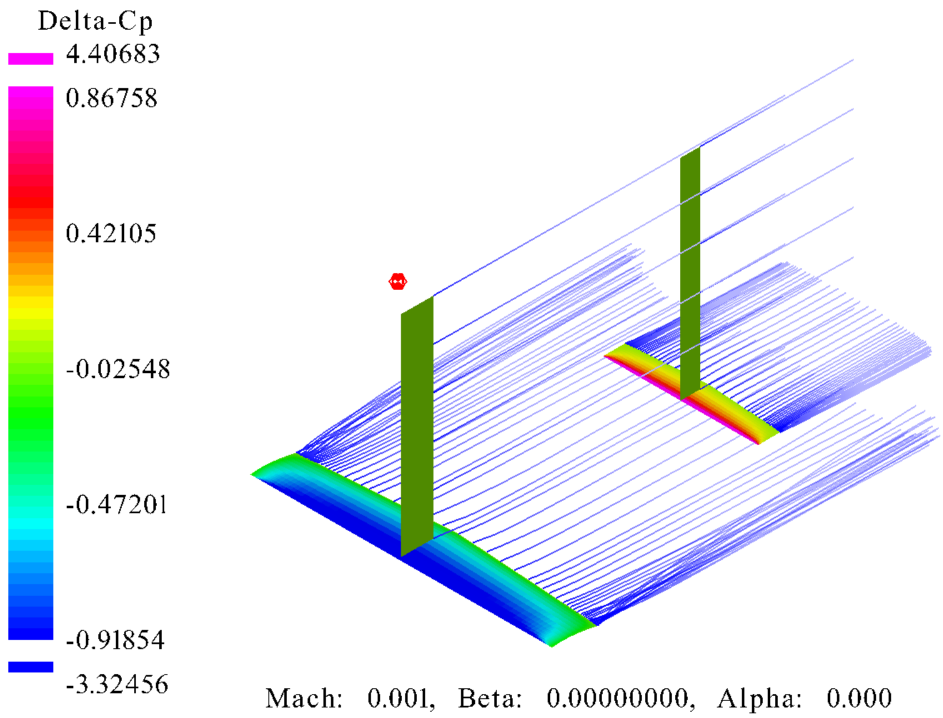

Figure A.24: Isometric view at takeoff conditions with pressure distribution over the hydrofoil

A.6 More Plots for 2nd Iteration of the aircraft and hydrofoil in cruise

Figure A.25: Lift distribution in cruise

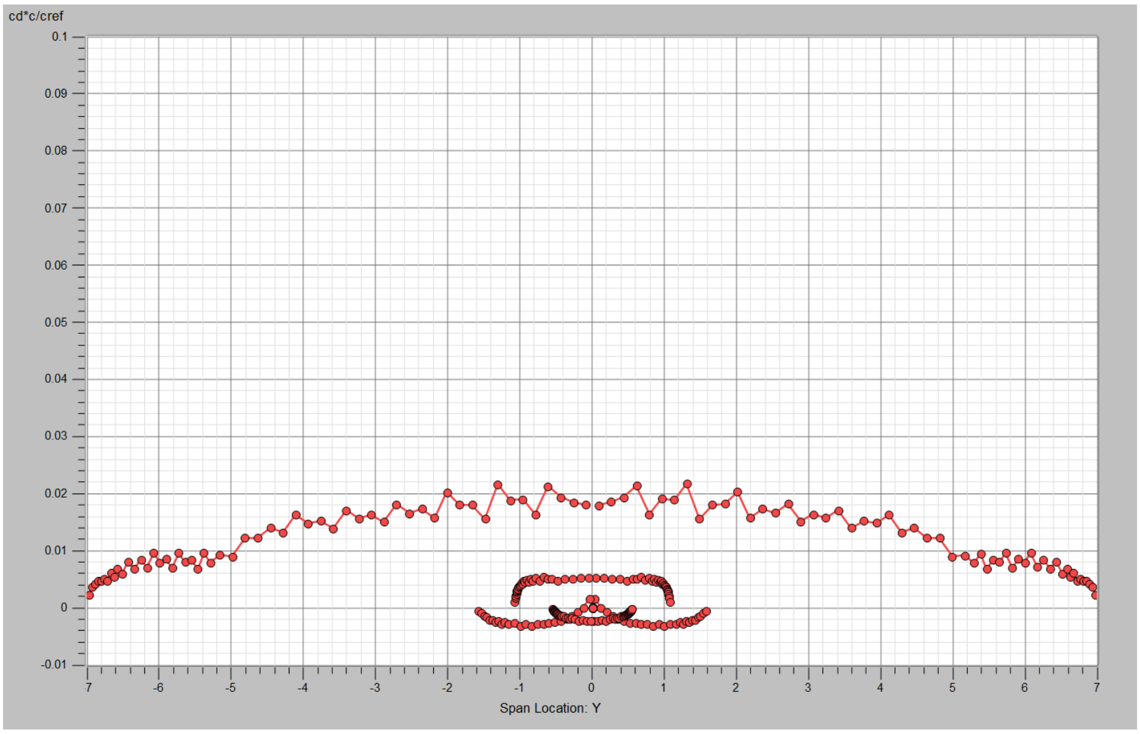

Figure A.26: Drag distribution in cruise

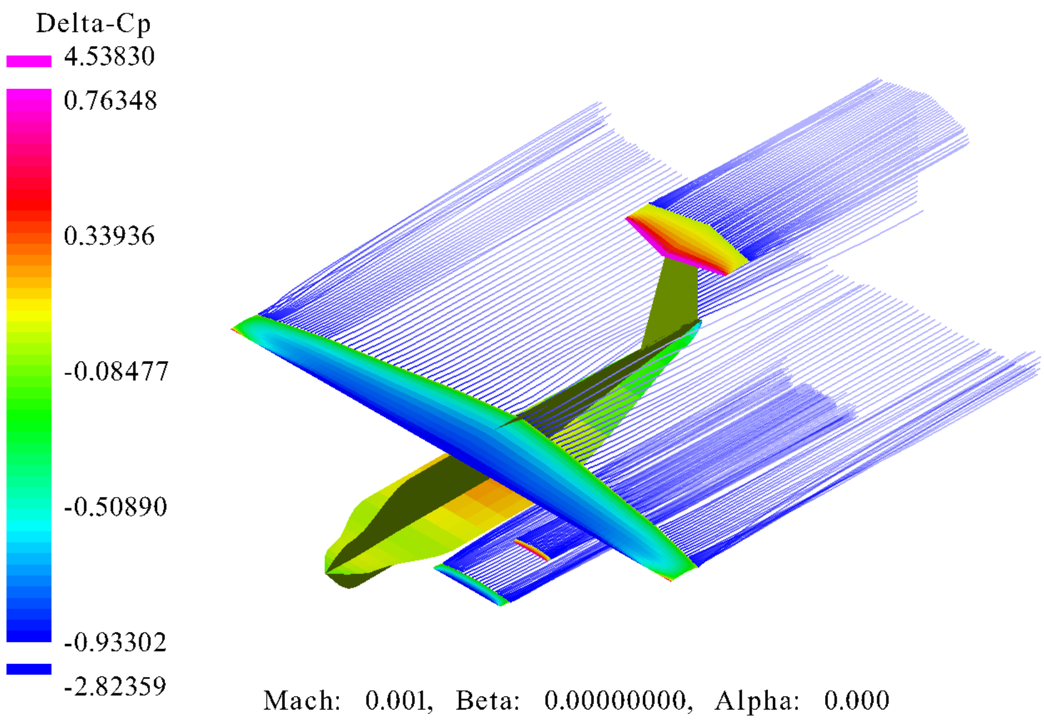

Figure A.27: Isometric view at cruise conditions

A.7 More Plots for 2nd Iteration of the aircraft and hydrofoil in landing

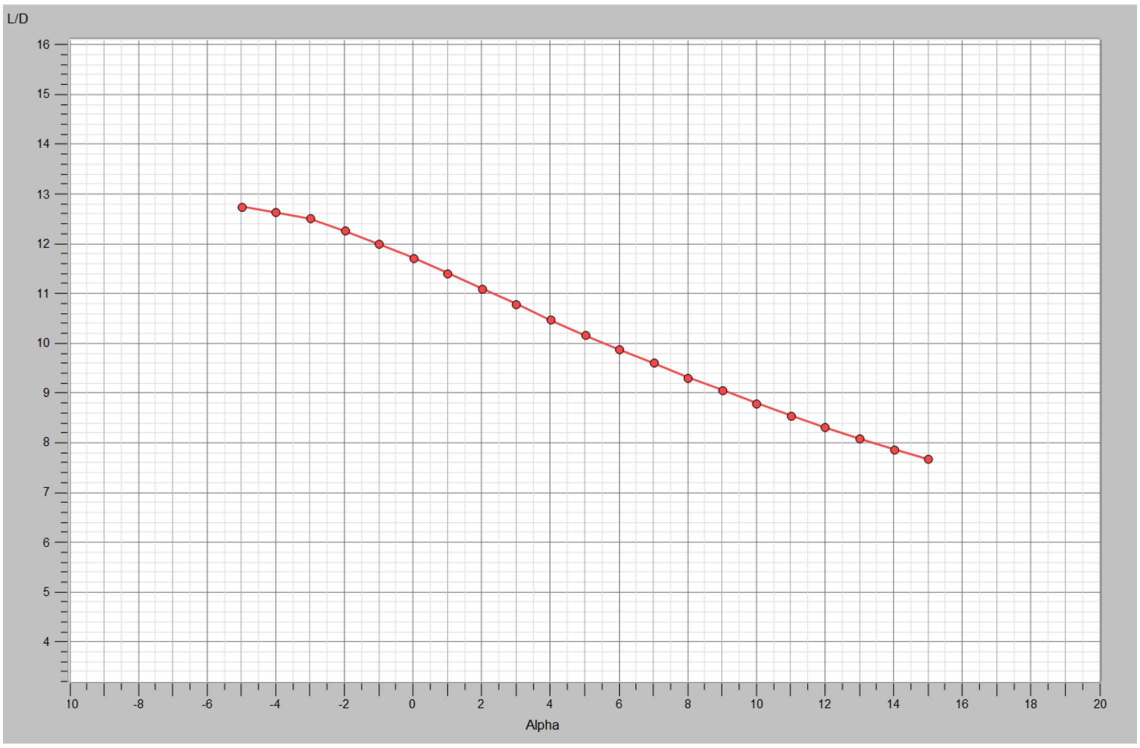

Figure A.28: Lift over Drag curve in landing

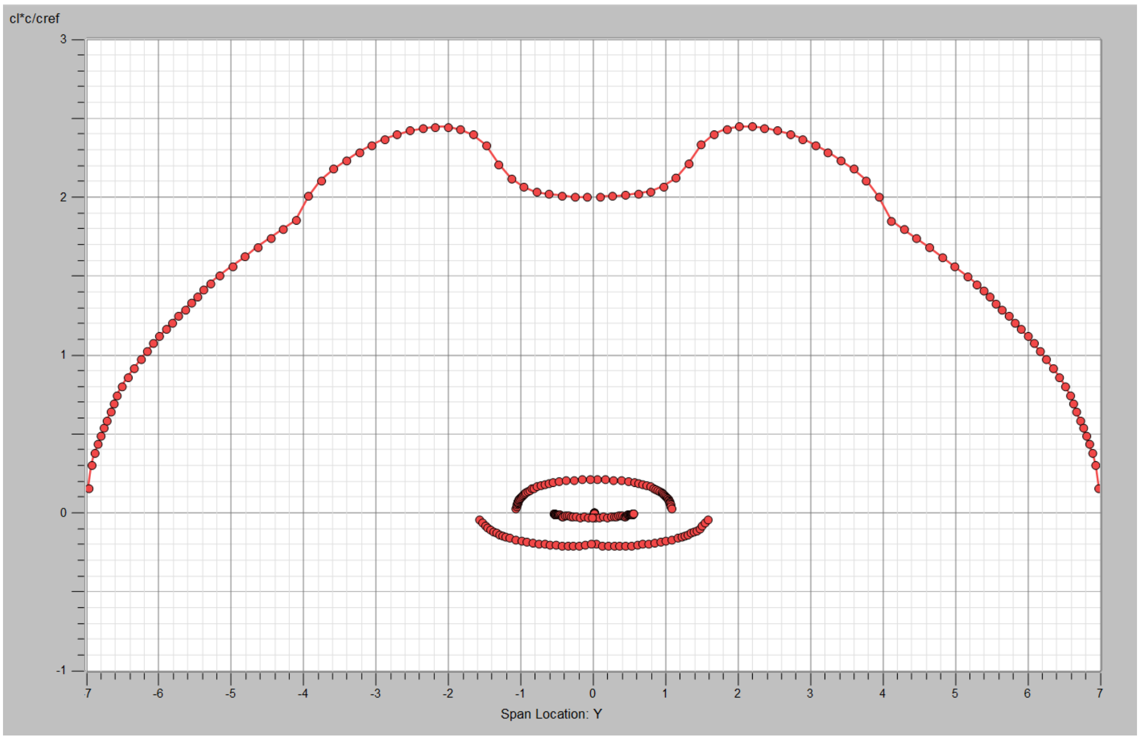

Figure A.29: Lift distribution in landing

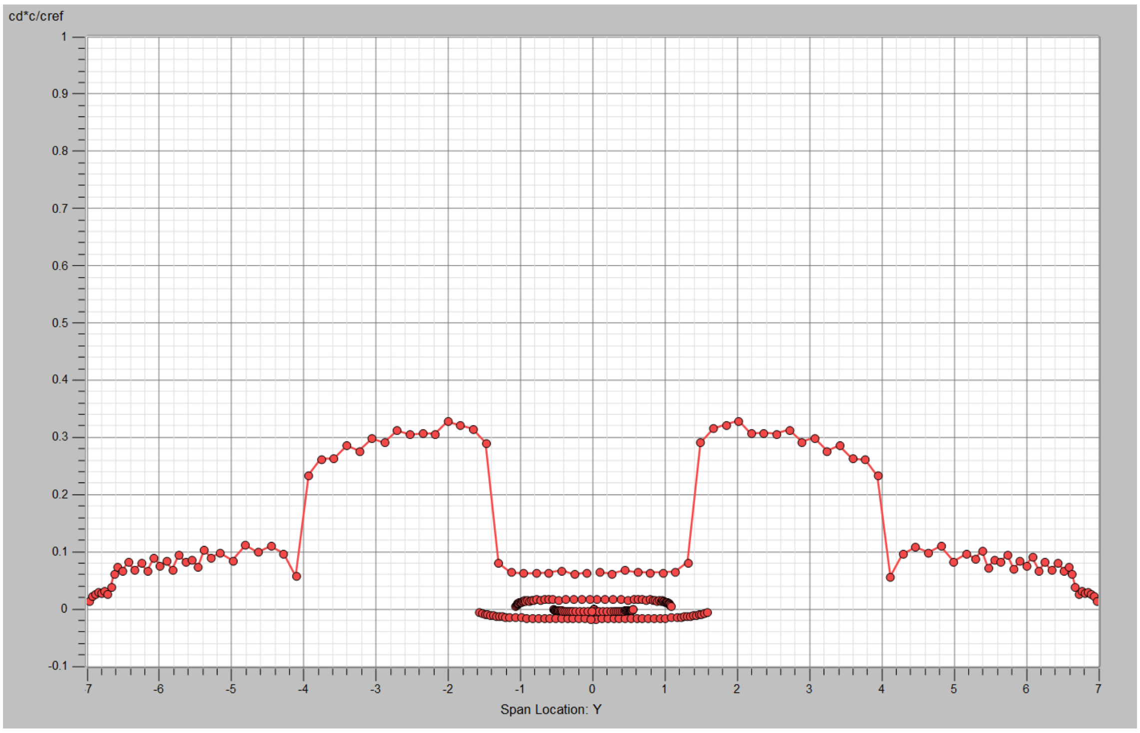

Figure A.30: Drag distribution in landing

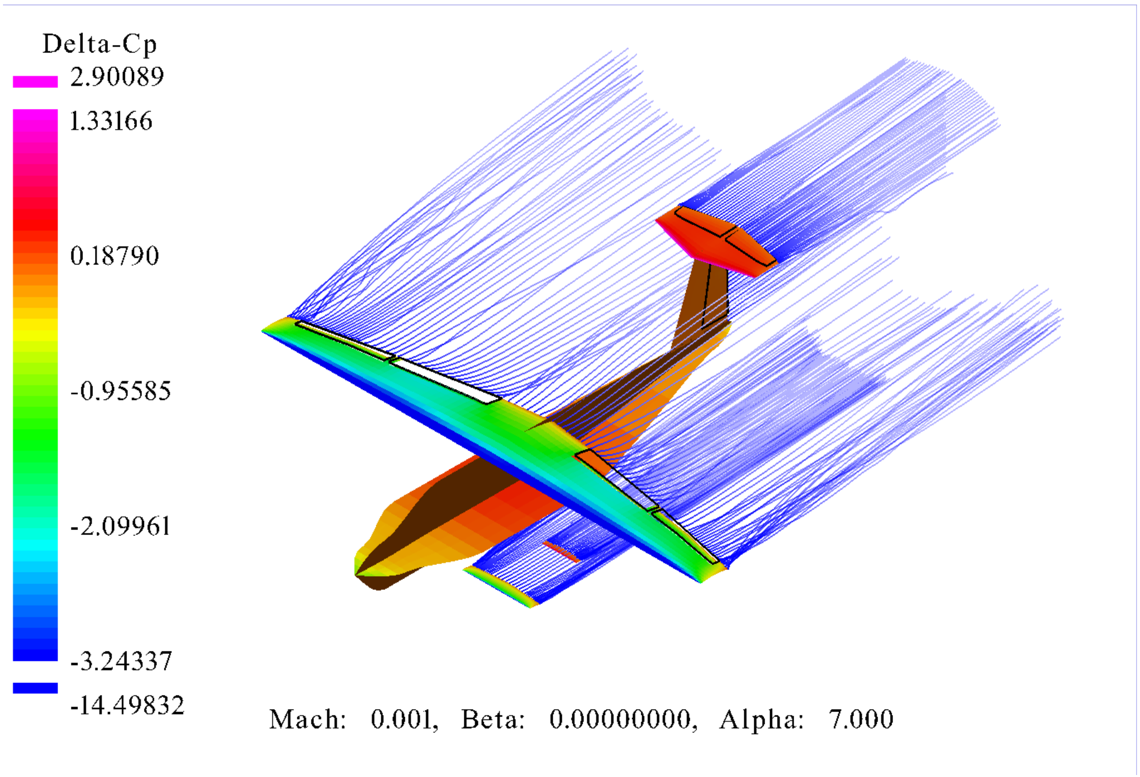

Figure A.31: Isometric view at landing conditions

DEPARTMENT OF MECHANICS AND MARITIME SCIENCES
CHALMERS UNIVERSITY OF TECHNOLOGY
Gothenburg, Sweden
www.chalmers.se

CHALMERS
UNIVERSITY OF TECHNOLOGY